WebTable 1. Biomass reductions associated with various fuel reduction treatments as prescribed at various fire-prone forests of western North America

Treatment type, forest type, and location	*Fraction of live basal area cut or killed in prescribed burn*	*Fate of logging slash*	*Δ surface fuels (estimated fraction)*	*Δ total aboveground biomass through both combustion and removal (estimated fraction)*
Prescribed fire only				
Sierran mixed conifer (Central Sierras)[a]	0.00	None	–0.70	–0.11
Sierran mixed conifer (Central Sierras)[b]	0.15	None	–0.02	–0.13
Ponderosa pine/Douglas fir (Northern Rockies)[b]	0.11	None	–0.19	–0.12
Ponderosa pine/Douglas fir (Blue Mountains)[b]	0.08	None	–0.32	–0.12
Ponderosa pine (Southwestern Plateau)[b]	0.04	None	–0.50	–0.11
Ponderosa pine/true fir (Southern Cascades)[b]	0.30	None	0.67	–0.16
Thinning only				
Sierran mixed conifer (Central Sierras)[a]	0.36	Left on site	0.96	–0.16
Sierran mixed conifer (Central Sierras)[a]	0.60	Left on site	1.60	–0.27
Ponderosa pine (Southern Rockies)[c]	0.36	Pile burned	0.01	–0.30
Ponderosa pine (Central Sierras)[d]	0.50	Pile burned	0.01	–0.42
Sierran mixed conifer (Central Sierras)[b]	0.34	Left on site	0.92	–0.15
Ponderosa pine/Douglas fir (Northern Rockies)[b]	0.54	Left on site	1.43	–0.24
Ponderosa pine/Douglas fir (Blue Mountains)[b]	0.24	Left on site	0.64	–0.11
Ponderosa pine (Southwestern Plateau)[b]	0.53	Pile burned	0.01	–0.45
Ponderosa pine/true fir (Southern Cascades)[b]	0.58	Removed	0.00	–0.49
Thinning and prescribed fire				
Sierran mixed conifer (Central Sierras)[a]	0.37	Left on site	–0.40	–0.38
Sierran mixed conifer (Central Sierras)[a]	0.66	Left on site	–0.17	–0.59
Ponderosa pine (Central Sierras)[d]	0.50	Pile burned	–0.69	–0.53
Sierran mixed conifer (Central Sierras)[b]	0.42	Left on site	–0.37	–0.41
Ponderosa pine/Douglas fir (Northern Rockies)[b]	0.78	Left on site	–0.08	–0.67
Ponderosa pine/Douglas fir (Blue Mountains)[b]	0.46	Left on site	–0.33	–0.44
Ponderosa pine (Southwestern Plateau)[b]	0.59	Pile burned	–0.68	–0.61
Ponderosa pine/true fir (Southern Cascades)[b]	0.73	Removed	–0.70	–0.72

Notes: Total biomass losses were approximated solely from basal reported area reduction according to the following assumptions: total aboveground biomass was assumed to be composed of 45% live merchantable boles (subject to removal proportional to basal area reduction), 40% live tree branch and foliage (converted to slash proportional to basal area reduction), and 15% surface fuels (both live and dead biomass and subject to combustion in prescribed fire). Prescribed fire was assumed to combust 70% of surface fuels and logging slash; pile burning was assumed to combust 99% of logging slash. [a]North *et al.* (2007); [b]Stephens *et al.* (2009); [c]Finkal and Evans (2008); [d]Campbell *et al.* (2008).

© The Ecological Society of America

WebTable 2. Burn probability for forests of Oregon, Washington, and California from 1985 to 2005

Forest type (ecoregion)	*Fraction of forest area burned annually*		*Fuel-treatment life expectancy (range in years)*	*Random probability of a treated stand being exposed to any fire*
	Any severity	*High severity*		
Cool–wet conifer (Coast Range)	0.00018	0.00002	5–15	0.0009–0.00274
Cool–mesic conifer (West Cascades, North Cascades)	0.00177	0.00046	5–15	0.00884–0.02651
Cool–dry conifer (East Cascades, North Rockies, Blue Mts)	0.00411	0.00054	10–25	0.04112–0.10279
Warm–mesic conifer (Klamath Mountains)	0.00622	0.00119	10–25	0.06217–0.15542
Warm–dry conifer (Sierra Nevada, South California Mts)	0.00780	0.00178	10–25	0.07798–0.19495

Notes: This simple prediction of wildfire-treatment occurrence by multiplying regional fire probability by fuel treatment life assumes random interaction of wildfire and treatment and does not account for strategic placement of fuel treatments. Area burned annually based on Monitoring Trends in Burn Severity fire perimeter and severity classification maps from 1985 to 2005 (http://mtbs.gov). Total forested area in each ecoregion based on 2005 National Land Cover Dataset land-cover maps (http://landcover.usgs.gov). Ecoregions correspond to Omernik Level 3 classification (Omernik 1978). Treatment life expectancies are crude estimates based on Rhodes and Baker (2008) and Agee and Skinner (2005). Being that these numbers were derived from actual region-wide land-surface-change detection, they include regional fire suppression activities. Natural burn probabilities, as well as those that may result from future management decisions or climate change, are likely to be higher.

WebReferences

Agee JK and Skinner CN. 2005. Basic principles of forest fuel reduction treatments. *Forest Ecol Manag* **211**: 83–96.

Campbell JC, Alberti G, Martin JG, and Law BE. 2008. Carbon dynamics of a ponderosa pine plantation following fuel reduction treatment in the northern Sierra Nevada. *Forest Ecol Manag* **275**: 453–63.

Finkral AJ and Evans AM. 2008. The effects of a thinning treatment on carbon stocks in a northern Arizona ponderosa pine forest. *Forest Ecol Manag* **255**: 2743–50.

Harmon ME, Moreno A, and Domingo BJ. 2009. Effects of partial harvest and site preparation on the carbon stores in Douglas-fir/western hemlock forests: a simulation study. *Ecosystems* **12**: 777–91.

North M, Innes J, and Zald H. 2007. Comparison of thinning and prescribed fire restoration treatments to Sierran mixed-conifer historic conditions. *Can J Forest Res* **37**: 331–42.

Omernik JM. 1987. Map supplement: ecoregions of the conterminous United States. *Ann Assoc Am Geogr* **77**: 118–25.

Rhodes JJ and Baker WL. 2008. Fire probability, fuel treatment effectiveness and ecological tradeoffs in western US public forests. *The Open Forest Science Journal* **1**: 1–7.

Stephens SL, Moghaddas JJ, Edminster C, *et al.* 2009. Fire treatment effects on vegetation structure, fuels, and potential fire severity in western US forests. *Ecol Appl* **19**: 305–20.

 © The Ecological Society of America

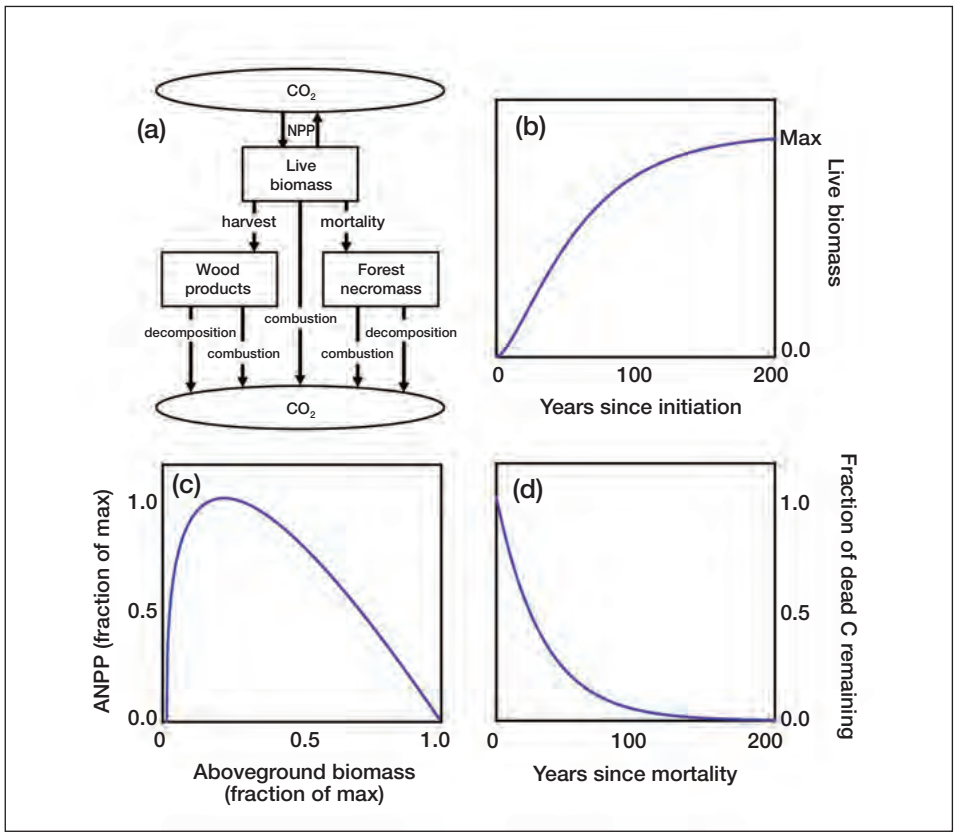

WebFigure 1. *(a) Structure and (c and d) dynamic functions behind the forest carbon model used to produce Figure 4. (b) Live biomass is assumed to aggrade over time according to a Chapman-Richards function* $y_1 = a*(1 - \exp[-b_1x_1])^c$*, the derivative of which,* $y_2 = c*b_1*y_1*(1 - \exp[\ln\{y_1/a\}/c])/\exp(\ln[y_1/a]/c)$*, allows (c) ANPP (aboveground net primary production) to be calculated annually according to current biomass;* y_1 *is aboveground live biomass in kg C* m^{-2}*,* y_2 *is ANPP in kg C* m^{-2} yr^{-1}*, a is the maximum aboveground live biomass that the site can sustain,* x_1 *is the time in years since initiation (which can be back-calculated from any assigned biomass),* b_1 *is a constant proportional to the time required to achieve maximum biomass, and c is a constant proportional to the initial growth lag. (d) Decomposition, the heterotrophic mineralization of each necromass pool including wood products, is determined according to an exponential loss function* $y_4 = M^* - k$*, where* y_4 *is loss of necromass in kg C* m^{-2} yr^{-1}*, M is the current mass of necromass in kg C* m^{-2}*, and k is a pool-specific decomposition constant. For the simulations shown in Figure 4, we used the following parameters to represent growth, harvest, combustion, and decay in a semiarid, fire-prone pine forest of western North America:* $a = 4.8$ *kg C* m^{-2}*;* $b_1 = 0.02$*;* $c = 1.6$*;* $k = 0.005$ yr^{-1} *for both forest necromass and wood products; starting* $y_1 = 4.5$ *kg C* m^{-2}*; starting* $M_{necromass} = 2.2$ *kg C* m^{-2}*; starting* $M_{products} = 0$ *Mg C* ha^{-1}*; treatment removals = 2.9 kg C* m^{-2}*; treatment related mortality (uncombusted slash) = 1% of* y_1 *at time of treatment; wildfire mortality = 95% of* y_1 *at time of fire; wildfire combustion = 10% of* y_1 *and 40% M of at time of fire.*

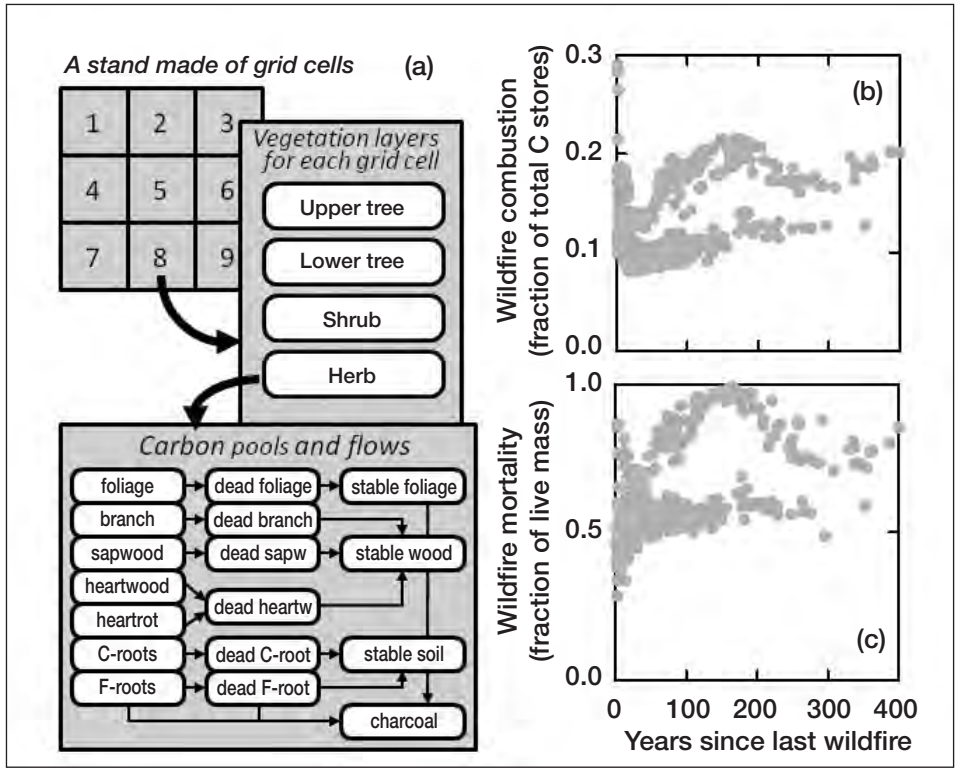

WebFigure 2. *(a) Structure and (b and c) disturbance responses behind STANDCARB, the forest carbon model used to produce Figure 5. STANDCARB simulates the accumulation of C over succession in mixed-species and mixed-age forest stands at annual time steps. The growth of vegetation and subsequent transfer of C among the various carbon pools shown in (a) are regulated by user-defined edapho-climatic inputs and species-specific responses. The imposition of wildfire in any given year results in the instantaneous transfer of C from each live pool into its corresponding dead pool (wildfire mortality) and the instantaneous loss of C from each live and dead pool to the atmosphere (wildfire combustion). The exact amount of mortality and combustion incurred in a given wildfire depends on stand-specific species composition, and the amount of biomass in each separate C pool, which at any given time may not be in equilibrium (gray circles in [b] and [c] reflect this variation). For the simulations shown in Figure 5, STANDCARB was parameterized for a semiarid ponderosa pine forest growing in eastern Oregon: max attainable biomass = 210 Mg C ha^{-1}; mean ANPP = 5.1 Mg C ha^{-1} yr^{-1}; non-fire mortality rate constants = 0.37, 0.5, 0.032, 0.017, and 0.013 yr^{-1} for foliage, fine roots, branches, coarse roots, and stems, respectively; decomposition rate constants = 0.21, 0.15, 0.08, 0.11, 0.023, and 0.017 yr^{-1} for foliage, fine roots, branches, coarse roots, stems, and soil C, respectively. It is worth noting that patterns nearly identical to those illustrated in Figure 5 result from STANDCARB parameterized for a mesic Douglas-fir forest having much larger ANPP, potential biomass, and decomposition rates. For a full description of STANDCARB structure and parameterization, see Harmon* et al. *(2009) and http://andrewsforest.oregonstate.edu/lter/pubs/webdocs/models/standcarb2.htm.*

 © The Ecological Society of America

nature climate change

LETTERS

PUBLISHED ONLINE: XX MONTH XXXX | DOI: 10.1038/NCLIMATE1264

Regional carbon dioxide implications of forest bioenergy production

Tara W. Hudiburg[1]*, Beverly E. Law[1], Christian Wirth[2] and Sebastiaan Luyssaert[3]

Mitigation strategies for reducing CO_2 emissions include substitution of fossil fuel with bioenergy from forests[1], where carbon emitted is expected to be recaptured in the growth of new biomass to achieve zero net emissions[2], and forest thinning to reduce wildfire emissions[3]. Here, we use forest inventory data to show that fire prevention measures and large-scale bioenergy harvest in US West Coast forests lead to 2–14% (46–405 Tg C) higher emissions compared to current management practices over the next 20 years. We studied 80 forest types in 19 ecoregions, and found that the current carbon sink in 16 of these ecoregions is sufficiently strong that it cannot be matched or exceeded through substitution of fossil fuels by forest bioenergy. If the sink in these ecoregions weakens below its current level by 30–60 g C m^{-2} yr^{-1} owing to insect infestations, increased fire emissions, or reduced primary production, management schemes including bioenergy production may succeed in jointly reducing fire risk and carbon emissions. In the remaining three ecoregions, immediate implementation of fire prevention and biofuel policies may yield net emission savings. Hence, forest policy should consider current forest carbon balance, local forest conditions and ecosystem sustainability in establishing how to decrease emissions.

Policies are being developed worldwide to increase bioenergy production as a substitution for fossil fuel to mitigate fossil fuel-derived carbon dioxide emissions, the main cause of anthropogenic global climate change[4,5]. However, the capacity for forest sector bioenergy production to offset carbon dioxide emissions is limited by fossil fuel emissions from this activity (harvest, transport, and manufacturing of wood products) and the lower energy output per unit carbon emitted compared with fossil fuels[6]. Furthermore, forest carbon sequestration can take from decades to centuries to return to pre-harvest levels, depending on the initial conditions and amount of wood removed[7]. The effects of changes in management on CO_2 emissions need to be evaluated against this baseline. Consequently, energy policy implemented without full carbon accounting and an understanding of the underlying processes risks increasing rather than decreasing emissions[4,8].

In North America, there is increasing interest in partially meeting energy demands through large-scale forest thinning[5], with the added benefit of preventing catastrophic wildfire and concurrent carbon loss[3]. Although forest thinning can be economically feasible, sustainable, and an effective strategy for preventing wildfire where risk is high[9,10], it remains unresolved whether this type of forest treatment can satisfy both the aims of preventing wildfire and reducing regional greenhouse gas emissions.

For both aims to be satisfied, it needs to be shown that: (1) reduction in carbon stocks due to thinning and the associated emissions are offset by avoiding fire emissions and substituting fossil fuel emissions with forest bioenergy, (2) the change in management results in less CO_2 emissions than the current or 'baseline' emissions, and (3) short-term emission changes are sustained in the long term. Determination of baseline forest sector carbon emissions can be accomplished by combining forest inventory data and life cycle assessment (LCA) that includes full carbon accounting of net biome production (NBP) on the land in addition to carbon emissions from bioenergy production and storage in wood products (LCA; ref. 6). NBP is the annual net change of land-based forest carbon (NEP; photosynthesis minus respiration) after accounting for harvest removals and fire emissions.

Our study focused on the US West Coast (Washington, Oregon and California), a diverse region due to the strong climatic gradient from the coast inland (300–2,500 mm precipitation per year) and a total of 80 associated forest types, ranging from temperate rainforests to semi-arid woodlands (Supplementary Table S1). The region is divided into 19 distinct ecoregions[11] on the basis of climate, soil, and species characteristics, and includes a broad range of productivity, age structures, fire regimes and topography. Mean net primary production (NPP) of the forest types range from 100–900 g C m^{-2} yr^{-1} (this study), falling within the global range of 100 to 1,600 g C m^{-2} yr^{-1} reported for temperate and boreal forests[12]. Forest land ownership is divided fairly evenly between public and private sectors having different management histories and objectives that affect forest carbon dynamics[13].

Carbon sequestration rates vary greatly across the region, with mean NEP ranging from -85 g C m^{-2} yr^{-1} in the dry Northern Basin to more than 400 g C m^{-2} yr^{-1} in the mesic Coast Range. After accounting for fire emissions and substantial harvest removals, regional NBP remains a significant sink of 26 ± 3 Tg C yr^{-1} or 76 ± 9 g C m^2 yr^{-1}, similar to the US average[14] and estimates for the member states of the European Union[15]. Sixteen of the 19 ecoregions, representing 98% of the forest area in the region are estimated to be carbon sinks (Fig. 1a; exceptions are drier ecoregions where annual productivity is low and fire emissions are relatively high). Thus, the observed regional sink is not solely due to the region's highly productive rainforests, which occupy 15% of the area. Within the region, California's NBP is higher than that of Oregon and Washington (107 versus 53–61 g C m^{-2} yr^{-1}), primarily owing to differences in NEP (Supplementary Table S2) and harvest between similar forest types within the same ecoregions that cross state boundaries (Supplementary Discussion and Table S3).

In addition to current management or Business-As-Usual (BAU, characterized by current preventive thinning and harvest levels), we designed three treatments (Supplementary Fig. S1a) to reflect the varying objectives of potential forest management

[1]Department of Forest Ecosystems and Society, 321 Richardson Hall, Oregon State University, Corvallis, Oregon, USA, [2]Department of Systematic Botany and Functional Biodiversity, University of Leipzig, Johannisalle 21-23, 04103 Leipzig, Germany, [3]Laboratoire des Sciences du Climat en de l'Environnement, CEA CNRS UVSQ, Centre d'Etudes Ormes des Merisiers, 91191 Gif Sur Yvette, France. *e-mail: Tara.hudiburg@oregonstate.edu.

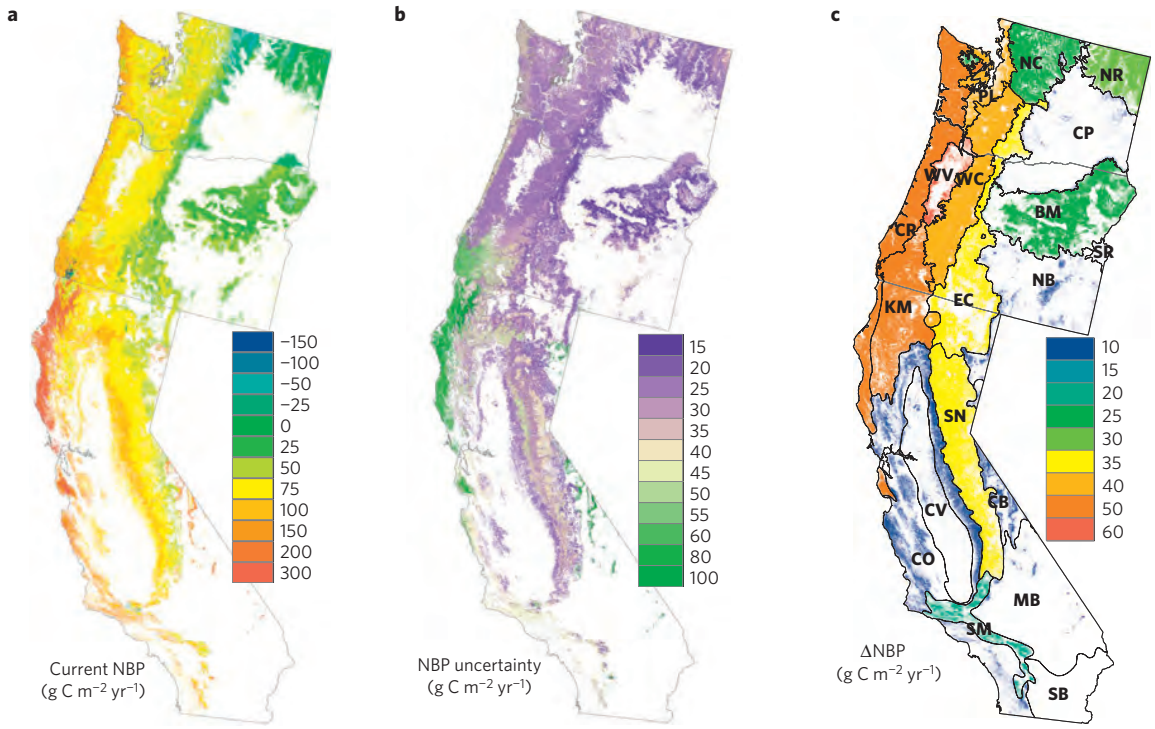

Figure 1 | Maps of US West Coast NBP and uncertainty for current and threshold conditions. Map **a** shows current NBP or BAU; positive values (warm colours) indicate forest sinks whereas negative values (cool colours) are carbon sources to the atmosphere. Map **b** shows the current NBP uncertainty estimates that were calculated using Monte Carlo simulations of mean forest type values for the components of NBP (net ecosystem productivity, fire and harvest) combined with the uncertainty associated with remote sensing land cover estimates. Map **c** represents the amount NBP would need to decrease to reach a threshold NPB where bioenergy management may result in emission decreases to the atmosphere.

systems: forest fire prevention by emphasizing removal of fuel ladders ('Fire Prevention') in fire-prone areas, making fuel ladder removal economically feasible by emphasizing removal of additional marketable wood in fire-prone areas ('Economically Feasible'), or thinning all forestland regardless of fire risk to support energy production while contributing to fire prevention ('Bioenergy Production'). Removals are in addition to current harvest levels and are performed over a 20-year period such that 5% of the landscape is treated each year. Our reliance on a data-driven approach versus model simulations strengthens our analysis in the short term, but limits our ability to make long-term predictions. Extending our study beyond a 20-year timeframe would overstretch data use because current forest growth is unlikely to represent future growth due to changes in climate, climate-related disturbance, and land use[16,17].

In our study region, we found that thinning reduced NBP under all three treatment scenarios for 13 of the 19 ecoregions, representing 90% of the region's forest area. The exceptions where NBP was not reduced were primarily due to high initial fire emissions compared to NEP (for example, Northern Basin and North Cascades; Supplementary Fig. S2). The dominant trend at the ecoregion level was mirrored at the regional level, with the Bioenergy Production scenario (highest thinning level) resulting in the region becoming a net carbon source (Supplementary Table S2 and discussion of state-level estimates). Regionally, forest biomass removals exceeded the potential losses from forest fires, reducing the *in situ* forest carbon sink even after accounting for regrowth, as found in previous studies with different approaches or areas of inference[8,18]. Because we have assumed high reductions in fire emissions for the areas treated in each scenario, it is unlikely we are underestimating the benefit of preventive thinning on NBP.

It is important to recognize that even if the land-based flux is positive (a source) or zero (carbon neutral), decreases in NBP from BAU can increase CO_2 emissions to the atmosphere. LCA was used to estimate the net emissions of carbon to the atmosphere in each treatment scenario (Supplementary Fig. S1b and Tables S4 and S5). LCA at the ecoregion level revealed that emissions are increased for 10 out of 19 of the ecoregions (Fig. 2), representing 80% of the forest area in the region. The combination of *in situ* and wood-use carbon sinks and sources emit an additional 46, 181 and 405 Tg C to the atmosphere over a 20-year period (2–14% increase) above that of the BAU forest management scenarios for the Fire Prevention, Economically Feasible, and Bioenergy Production treatments, respectively (Fig. 3).

Sensitivity analysis of our results to a range of fire emission reductions, energy conversion efficiencies, wood product decomposition rates and inclusion of wood substitution showed that carbon emissions varied by −10 to 28% from the optimum values across the scenarios, depending on the combination of assumptions (Supplementary Discussion and Table S6). The analysis revealed that an increase in estimated current fire emissions (which effectively reduces the baseline sink) may decrease total atmospheric C emissions in the Fire Prevention scenario, but only given optimum conditions for all of the other parameters (for example 100% energy efficiency). Nevertheless, if fire frequency and intensity increase in the future[19], emissions savings through forest bioenergy production may become possible, especially in ecoregions where the sink is already weak.

Previous case studies showed that harvesting an old-growth forest in the Pacific Northwest[20] or increasing the thinning removals of temperate forests is likely to deteriorate the forest and wood product carbon stock[21]. However, these studies were limited to a handful of sites, relied primarily on modelled results[3,18] and did not account for the energy requirements of forest management and wood processing nor for the potential to substitute fossil fuels with bioenergy. We build on these results by including all ecoregions,

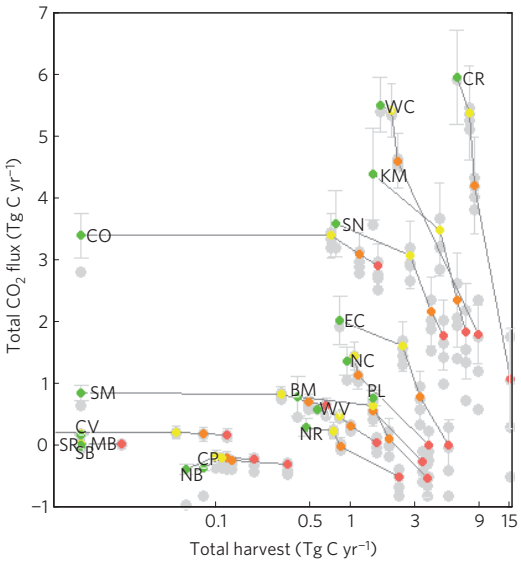

Figure 2 | Life Cycle Assessment carbon emission trends by ecoregion under various management scenarios. The *x* axis is the total harvest (BAU + treatment) and the *y* axis is the total CO_2 flux in Tg C yr^{-1} for each ecoregion. Coloured circles represent each scenario (Green = BAU, Yellow = Fire Prevention, Orange = Economically Feasible, Red = Bioenergy Production). Grey circles are the values for each sensitivity analysis set of parameters and the error bars represent the estimate uncertainty. The locations of the ecoregions indicated by labels are shown in Fig. 1a. For most ecoregions, the treatments increase emissions to the atmosphere.

all age classes (not just old-growth), three treatments including bioenergy production, and sector-based LCA. We found that even though forest sector emissions are compensated for by emission savings from bioenergy use, fewer forest fires, and wood product substitution, the end result is an increase in regional CO_2 emissions compared to BAU as long as the regional sink persists.

To determine a threshold NBP for which bioenergy management reduces atmospheric CO_2 emissions compared to BAU, we applied the same assumptions as used in the LCA. We found that if the NBP drops by 50–60 g C m^{-2} yr^{-1} in currently productive ecoregions or 15–30 g C m^{-2} yr^{-1} in currently less productive ecoregions, bioenergy management would come with CO_2 emissions savings compared to BAU (Fig 1c). Aggregating the ecoregion thresholds translates into a regional mean NBP of 45 g C m^{-2} yr^{-1} or a 41% reduction on average. Reductions in NBP may occur due to increased mortality and/or decreased growth due to climate, fire, or insect outbreaks. However, reductions in NBP from increased harvest do not qualify because harvest increases emissions; wood carbon enters the products/bioenergy chain, where subsequent losses occur. We cannot predict from the data when the threshold NBP would occur because a high resolution process-based model with the ability to incorporate future climate, nitrogen deposition, age dynamics, disturbance and management would need to be used, which is beyond the scope of this study.

Ecoregion threshold NBP is dependent on the scenario treatment removals and area because the Fire Prevention treatment targets only those areas most likely to burn. For example, to reduce emissions in the Sierra Nevada, baseline NBP would have to decrease by as much as 84 for the Bioenergy Production scenario versus only 13 g C m^{-2} yr^{-1} for the Fire Prevention scenario. In ecoregions where current sinks are marginal or weakened by climate, fire, or insect outbreaks there may be a combination of harvest intensity and bioenergy production that reduces forest sector emissions. In nine of the ecoregions where forests are carbon neutral or a source of CO_2 to the atmosphere and/or fire emissions are high for BAU, total CO_2 emissions under the Fire Prevention scenario could be reduced compared to BAU. They provide examples where management strategies for carbon emission reduction or sequestration should differ from the majority of the region; a one-size-fits-all approach will not work[22]. Finally, large areas in the Northern Rockies (for example, Colorado and Wyoming) are at present experiencing increases in forest mortality due to beetle-kill, a trend which could continue in a warmer climate[23]. These areas may already be at or below the threshold NBP; if so, they could benefit from targeted bioenergy implementation. However, simply lowering current regional harvest intensities in areas where NBP is not weakened also reduces emissions (Supplemental Discussion and Fig. S3). Also, as we have assumed large-scale implementation of these strategies in addition to BAU harvest, we may be overestimating future harvest even though harvest has declined significantly since 1990 because of restrictions placed on harvest on federal lands as part of the Northwest Forest Plan. If the strategies were used to substitute for BAU harvest, the outcome on NBP would be much different (that is, increased for the Fire Prevention scenario).

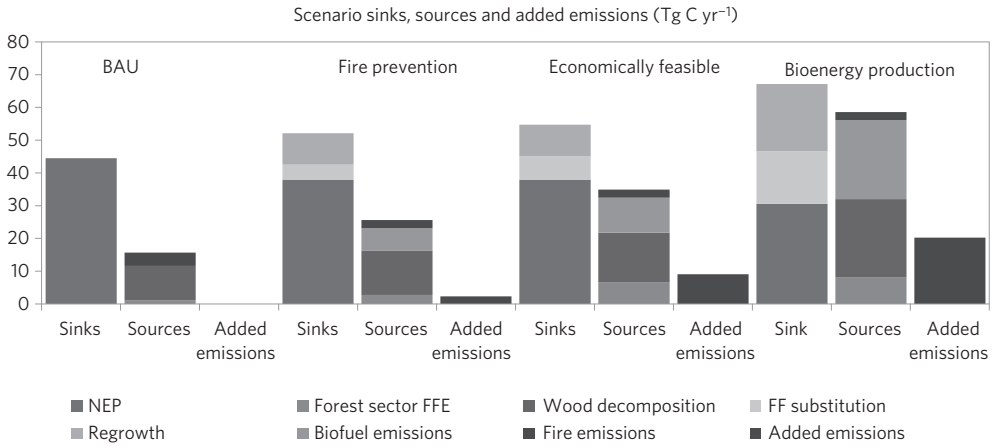

Figure 3 | Total US West Coast forest sector carbon sinks, sources, and added emissions relative to BAU under various management scenarios. Units are in Tg C yr^{-1}. Life cycle assessment estimates account for changes in carbon on land in addition to emissions associated with production, transport and usage of wood, and substitution and displacement of fossil fuel emissions associated with use and extraction. BAU results in the lowest anthropogenic emissions from the forest sector.

Our study is one of the first to provide full carbon accounting, including all of the sinks and sources of carbon emissions from the forestry sector and the current *in situ* sink, for such a large area. Given the diversity of woody ecosystems in the study region, ranging from highly productive temperate rainforests to less productive semi-arid woodlands, the trends in response probably apply to other temperate regions globally (Supplementary Table S1) where forests are at present a strong net carbon-sink (for example, Eastern US, China and Europe), although the extent of the effect remains to be established.

Greenhouse gas reduction plans call for up to 10% reductions in emissions by 2020 and forest-derived fuels are being proposed as a carbon-neutral solution to reducing energy emissions. In all of our proposed scenarios, increases in harvest volume on the US West Coast will on average result in regional emission increases above current levels, although there are a few ecoregions where the tested scenarios could result in emission savings. As long as the current *in situ* NBP persists, increasing harvest volumes in support of bioenergy production is counterproductive for reducing CO_2 emissions. In this study region, the current *in situ* NBP in tree biomass, woody detritus and soil carbon is more beneficial in contributing to reduction of anthropogenic carbon dioxide emissions than increasing harvest to substitute fossil fuels with bioenergy from forests.

Although large uncertainty remains for regional forecasts to year 2050 or 2100, it is expected that forest carbon sinks will diminish over time because of ageing of the forests, saturation of the CO_2-fertilization and N-deposition effects, and increased mortality due to climate or insects[24,25]. This would require new assessments to identify management options appropriate for each situation. Carbon-management is not the sole criteria that should be considered when planning forest management. Our findings should thus also be evaluated against other ecosystem services, such as habitat, genetic and species diversity, watershed protection, and natural adaptation to climate change.

Methods

We quantified forest sequestration rates and test forest thinning scenarios across the region using a data-intensive approach which, for the first time, takes into account the diversity of forest characteristics and management. We combined Landsat remote sensing data with inventories and ancillary data to map current forest NEP, NBP, and changes in NBP with three thinning scenarios. The approach can be applied at multiple scales of analysis in other regions.

We combined spatially representative observational data from more than 6000 FIA plots (see Supplementary Methods and Table S7) with remote sensing products on forest type, age and fire risk[26], a global data compilation of wood decomposition data and 200 supplementary plots[13] to provide new estimates of US West Coast (~34 million hectares) forest biomass carbon stocks (Supplementary Table S8), NEP (the balance of photosynthesis and respiration) and NBP (the *in situ* net forest carbon-sink accounting for removals). We included all forestland in our analysis, across all age classes (20–800 years old) and management regimes. Plot values were aggregated by climatic region (ecoregion), age class and forest type, and this look-up table was used to assign a value to each associated 30 m pixel.

We use regional combustion coefficients to determine fire emissions. Only 3–8% of live tree biomass is actually combusted and emitted in high severity fire in the Pacific Northwest[31], contrary to other studies that report much higher emissions because they assume 30% of all aboveground woody biomass is consumed[27]. Although the latter contradicts extensive field observations[28,29] and modelling studies[30] in the region, we included 30% as the upper-end combustion factor in our sensitivity analysis (Supplementary Table S9).

In addition to the spatially explicit estimates of stocks and fluxes under current management or BAU (current forest harvest), three treatments were designed (Fire Prevention, Economically Feasible, and Bioenergy Production; Supplementary Fig. S1a) to reflect the varying objectives of potential future forest management over the next 20 years; within the proposed time period for CO_2 reductions in the US Areas were prioritized for treatment by fire risk and frequency. The proposed treatments result in additional harvest removals because we assume the current harvest rate for wood products will continue in the future. We limit our specific analysis to the short term because this is the timeframe suitable for policymakers, effectiveness of fire protection treatments, and an appropriate use of the data-driven approach. However, to investigate conditions (for example, sink saturation) that could invalidate our short-term results in the long term, we also calculated the *in situ* NBP at which the atmosphere may benefit from bioenergy removals.

Last, we studied the net effects of the thinning treatments on atmospheric CO_2 by LCA of carbon sources and sinks that includes the post-thinning NBP and wood use (harvest, transport, manufacturing, decomposition, wood product substitution, conversion and use of bioenergy, and displacement of fossil fuel extraction emissions; Supplementary Fig. S1b and Table S4,S5).

Received 19 July 2011; accepted 30 September 2011; published online XX Month XXXX

References

1. Buyx, A. & Tait, J. Ethical framework for biofuels. *Science* (2011).
2. Gustavsson, L., Börjesson, P., Johansson, B. & Svenningsson, P. Reducing CO_2 emissions by substituting biomass for fossil fuels. *Energy* **20,** 1097–1113 (1995).
3. Hurteau, M. D. & North, M. Carbon recovery rates following different wildfire risk mitigation treatments. *Forest Ecol. Manag.* **260,** 930–937 (2010).
4. Fargione, J., Hill, J., Tilman, D., Polasky, S. & Hawthorne, P. Land clearing and the biofuel carbon debt. *Science* **319,** 1235–1238 (2008).
5. Richter, D. Jr *et al.* Resource policy: Wood energy in America. *Science* **323,** 1432–1433 (2009).
6. Law, B. E. & Harmon, M. E. Forest sector carbon management, measurement and verification, and discussion of policy related to climate change. *Carbon Manag.* **2,** 73–84 (2011).
7. Harmon, M. E. & Marks, B. Effects of silvicultural practices on carbon stores in Douglas-fir—western hemlock forests in the Pacific Northwest, USA: Results from a simulation model. *Can. J. Forest Res./Rev. Can. Rech. Forest* **32,** 863–877 (2002).
8. Searchinger, T. D. *et al.* Fixing a critical climate accounting error. *Science* **326,** 527–528 (2009).
9. Evans, A. & Finkral, A. From renewable energy to fire risk reduction: A synthesis of biomass harvesting and utilization case studies in US forests. *GCB Bioenergy* **1,** 211–219 (2009).
10. Huggett, R. J. Jr, Abt, K. L. & Shepperd, W. Efficacy of mechanical fuel treatments for reducing wildfire hazard. *Forest Policy Econ.* **10,** 408–414 (2008).
11. Omernik, J. M. Ecoregions of the conterminous United States. Map (scale 1:7,500,000). *Ann. Assoc. Am. Geogr.* **77,** 118–125 (1987).
12. Luyssaert, S. *et al.* Old-growth forests as global carbon sinks. *Nature* **455,** 213–215 (2008).
13. Hudiburg, T. *et al.* Carbon dynamics of Oregon and Northern California forests and potential land-based carbon storage. *Ecol. Appl.* **19,** 163–180 (2009).
14. Birdsey, R. A. in *US Climate Change Science Program and the Subcommittee on Global Change Research* (eds King, A. W. *et al.*) (2007).
15. Luyssaert, S. *et al.* The European carbon balance: part 3: Forests. *Glob. Change Biol.* **16,** 1429–1450 (2009).
16. Battles, J. *et al.* Climate change impacts on forest growth and tree mortality: A data-driven modeling study in the mixed-conifer forest of the Sierra Nevada, California. *Clim. Change* **87,** 193–213 (2008).
17. Ryan, M. G. Temperature and tree growth. *Tree Physiol.* **30,** 667–668 (2010).
18. Mitchell, S. R., Harmon, M. E. & O'Connel, K. E. B. Forest fuel reduction alters fire severity and long-term carbon storage in three Pacific Northwest ecosystems. *Ecol. Appl.* **19** (2009).
19. Rogers, B. *et al.* Impacts of climate change on fire regimes and carbon stocks of the US Pacific Northwest. *J. Geophys. Res.* http://dx.doi.org/10.1029/2011JG001695 (in the press).
20. Harmon, M. E., Ferrell, W. K. & Franklin, J. F. Effects on carbon storage of conversion of old-growth forests to young forests. *Science* **247,** 699–702 (1990).
21. Nunery, J. S. & Keeton, W. S. Forest carbon storage in the northeastern United States: Net effects of harvesting frequency, post-harvest retention, and wood products. *Forest Ecol. Manag.* **259,** 1363–1375 (2010).
22. Marland, G. & Schlamadinger, B. Forests for carbon sequestration or fossil fuel substitution? A sensitivity analysis. *Biomass Bioenergy* **13,** 389–397 (1997).
23. Evangelista, P. H., Kumar, S., Stohlgren, T. J. & Young, N. E. Assessing forest vulnerability and the potential distribution of pine beetles under current and future climate scenarios in the Interior West of the US. *Forest Ecol. Manag.* **262,** 307–316 (2011).
24. van Mantgem, P. J. *et al.* Widespread increase of tree mortality rates in the Western United States. *Science* **323,** 521–524 (2009).
25. Stinson, G. *et al.* An inventory-based analysis of Canada's managed forest carbon dynamics, 1990 to 2008. *Glob. Change Biol.* **17,** 2227–2244 (2011).
26. LANDFIRE Data Distribution Site, USGS (US Department of Interior, Geological Survey, 2009) http://gisdata.usgs.net/website/landfire/.
27. Wiedinmyer, C. & Hurteau, M. D. Prescribed fire as a means of reducing forest carbon emissions in the western United States. *Environ. Sci. Technol.* **44,** 1926–1932 (2010).
28. Campbell, J., Donato, D., Azuma, D. & Law, B. Pyrogenic carbon emission from a large wildfire in Oregon, United States. *J. Geophys. Res.* **112** (2007).
29. Meigs, G., Donato, D., Campbell, J., Martin, J. & Law, B. Forest fire impacts on carbon uptake, storage, and emission: The role of burn severity in the Eastern Cascades, Oregon. *Ecosystems* **12,** 1246–1267 (2009).

30. Ottmar, R. D., Pritchard, S. J., Vihnanek, R. E. & Sandberg, D. V. 14 Final Report JFSP Project 98-1-9-06, 2006.

Acknowledgements

This research was supported by the Office of Science (BER), US Department of Energy (DOE, Grant no. DE-FG02-07ER64361), for the North American Carbon Program study, 'Integrating Remote Sensing, Field Observations, and Models to Understand Disturbance and Climate Effects on the Carbon Balance of the West Coast US'. We further thank M. Harmon for discussions of wood product life-cycle assessment. T.W.H. is funded by a DOE global change education program PhD fellowship (GREF). S.L. is funded by ERC Starting Grant 242564.

Author contributions

T.W.H. designed and implemented the study with guidance from B.E.L. and S.L. T.W.H., S.L. and B.E.L. co-wrote the paper and S.L. contributed to parts of the analysis. C.W. provided essential data and methods for the analysis and valuable comments on the manuscript.

Additional information

The authors declare no competing financial interests. Supplementary information accompanies this paper on www.nature.com/natureclimatechange. Reprints and permissions information is available online at http://www.nature.com/reprints. Correspondence and requests for materials should be addressed to T.W.H.

Page 1

Query 1: Line no. 48
Please note that the e-mail addresses of all authors have been removed, except that of the corresponding author, as per journal style.

Query 2: Line no. 48
Please provide postcodes for first affiliation.

Query 3: Line no. 58
You define LCA again here, is this necessary?

Query 4: Line no. 61
NEP appears in brackets following a description of NBP. Please check.

Query 5: Line no. 70
NPP used only once, style guide dictates that the acronym be removed. Ok?

Page 2

Query 6: Line no. 1
Figure 1 caption, should NPB be changed to NBP?

Page 3

Query 7: Line no. 1
Dotted line present in one version of the two supplied figures. Please check the figure now processed is ok.

Query 8: Line no. 30
Is there a missing unit or a percentage value after '84'?

Page 4

Query 9: Line no. 54
Please check whether the above given '[31]' is a reference. Only 30 reference are there.

Query 10: Line no. 79
Please provide volume and page range for ref. 1.

Query 11: Line no. 79
Because of the odd symbols appearing in the authors of Ref. 2, we have checked and corrected the name of the second author.

Query 12: Line no. 116
Please provide page range/article id for refs 18, 28.

Query 13: Line no. 119
Any update for ref. 19.

Query 14: Line no. 147
Please provide publisher for ref. 30.

Page 5

Query 15: Line no. 8
As NPG do not allow unnamed individuals in the acknowledgement we have modified 'We further thank an anonymous reviewer for discussions of economic analysis of bioenergy production, an LCA specialist for helpful comments on our LCA, and M. Harmon for discussions of wood product life-cycle assessment.' to 'We further thank M. Harmon for discussions of wood product life-cycle assessment.'

Mitig Adapt Strateg Glob Change
DOI 10.1007/s11027-011-9331-9

ORIGINAL ARTICLE

Global warming potential factors and warming payback time as climate indicators of forest biomass use

Kim Pingoud · Tommi Ekholm · Ilkka Savolainen

Received: 9 June 2011 / Accepted: 14 October 2011
© Springer Science+Business Media B.V. 2011

Abstract A method is presented for estimating the global warming impact of forest biomass life cycles with respect to their functionally equivalent alternatives based on fossil fuels and non-renewable material sources. In the method, absolute global warming potentials (AGWP) of both the temporary carbon (C) debt of forest biomass stock and the C credit of the biomass use cycle displacing the fossil and non-renewable alternative are estimated as a function of the time frame of climate change mitigation. Dimensionless global warming potential (GWP) factors, GWP_{bio} and GWP_{biouse}, are derived. As numerical examples, 1) bioenergy from boreal forest harvest residues to displace fossil fuels and 2) the use of wood for material substitution are considered. The GWP-based indicator leads to longer payback times, i.e. the time frame needed for the biomass option to be superior to its fossil-based alternative, than when just the cumulative balance of biogenic and fossil C stocks is considered. The warming payback time increases substantially with the residue diameter and low displacement factor (DF) of fossil C emissions. For the 35-cm stumps, the payback time appears to be more than 100 years in the climate conditions of Southern Finland when DF is lower than 0.5 in instant use and lower than 0.6 in continuous stump use. Wood use for construction appears to be more beneficial because, in addition to displaced emissions due to by-product bioenergy and material substitution, a significant part of round wood is sequestered into wood products for a long period, and even a zero payback time would be attainable with reasonable DFs.

Keywords Forest biomass · Bioenergy · Wood products · Climate impacts · GWP factors · Biogenic C debt · Displacement of fossil GHG emissions · Material substitution · Pulse response model

1 Introduction

Biomass is basically a renewable carbon- (C) neutral source of energy and materials when emissions from biomass use are re-absorbed into the re-growth of new biomass. Thus, the C

K. Pingoud (✉) · T. Ekholm · I. Savolainen
VTT Technical Research Centre of Finland, Tekniikantie 2, Espoo, P.O. Box 1000, FI-02044 VTT, Finland
e-mail: kim.pingoud@vtt.fi

Published online: 03 November 2011

dynamics of the biomass stocks differ essentially from those of permanent fossil sources, which basically cannot be sequestered back into their original tectonic stocks. In practice, the impact of biomass use on emissions is much more complex. For example, the conversion of C-rich lands such as rainforests, peatlands, savannahs and grasslands to produce food-crop-based biofuels causes a change in land use (LUC), which may lead to a permanent loss of terrestrial C stocks. The biofuel C debt can be high compared with the fossil C emissions that can be displaced annually by biofuels (Fargione et al. 2008). Thus, compensation of the debt may take a long time and can be described by ecosystem carbon payback time (Gibbs et al. 2008), which in the worst case could be several centuries. On the other hand, biomass plantations on degraded land may have a positive impact on the terrestrial C stocks, thus providing mitigation benefits in a very short time frame.

Even more complex are the market-mediated responses that cause indirect land use change (iLUC) that cannot be analysed with conventional life-cycle techniques. Increasing biofuel demand influences crop prices. As a response to higher prices, forests and grasslands may be converted into new cropland to replace the grain (or cropland) diverted to biofuels (Searchinger et al. 2008; Hertel et al. 2010). According to a model prediction for the 21st century (Melillo et al. 2009), iLUC due to biofuel expansion could be responsible for up to twice as much carbon loss as direct LUC.

The C neutrality of bioenergy and, specifically, forest-based biomass has raised a passionate debate in the US (see, e.g., Sedjo 2011) influenced by the Manomet (2010) study and the articles by Searchinger et al. (2009) and Fargione et al. (2008). There is no change in land use category (IPCC 2006) when forests are managed sustainably. In the case of established management practices being applied, the process is usually climate neutral over the rotation, as harvested biomass is replaced by the re-growth of new biomass without any significant changes in terrestrial C stocks at landscape level. However, in conventional forestry, the rotation length of a stand typically varies from a decade to more than a century. Thus, in long rotations there is a significant temporal imbalance or C debt between removal and re-growth at stand level or compared with delayed or just stopped harvest. Furthermore, a change in forest management practices, for instance, by decreasing the rotation length or increasing the use of harvest residues, also has a long-term impact on the landscape-level terrestrial stock or the stand-level C stock time-averaged over the rotation.

In addition to the biogenic C debt, the substitution impact has to be considered; i.e., how much of the fossil C emissions could be displaced by the use of biomass when taking into account all the emissions from the biomass production chain, including those from possible fertilizer use. The two factors, the terrestrial C imbalance and the displaced fossil C emissions, together determine the net C balance of the biomass use cycle with respect to its fossil fuel-based alternative.

Ambitious climate targets such as the 2°C stabilization with global greenhouse gas (GHG) emissions peaking within one decade (IPCC 2007a, p. 15, Table SPM5) emphasize rapid reductions in emissions, which also makes the timing of emissions from biomass an issue. Thus, the GHG indicators of the biomass use cycle should take into account the mitigation time frame under consideration. Conventional GHG life cycle assessment (LCA) of the biomass use cycle by the provision of one static emission factor is misleading and unable to describe the real warming impacts of the biomass use cycle within the mitigation time frame. The upfront emission profile of energy plantations with preceding conversion of C-rich lands differs from that of the fossil fuel to be displaced and has been subject to specific attention in the literature. In some standardized LCA guidelines (PAS 2050 2008)

and the EU Renewable Energy Directive (EU 2009), this momentary emission is amortized over 20 years. A more realistic basis would be to apply dynamic LCA in which either the cumulative emissions in time are considered (Schlamadinger and Marland 1996) or metrics based on cumulative radiative forcing (CRF) / absolute global warming potential (AGWP) within a time frame T is used (Kendall et al. 2009; Levasseur et al. 2010; O'Hare et al. 2009; Kirkinen et al. 2008; Repo et al. 2010).

In sustainable forestry, the upfront emission profile is different from LUC. Final felling causes a similar C debt as that of land conversion but, in addition, the post-harvest re-growth of the new stand has to be credited. Marland and Schlamadinger (Schlamadinger and Marland 1996; Marland and Schlamadinger 1997) presented a method by which the net effects of using forests, either for carbon sequestration or as a source of bioenergy to displace fossil fuels, were described as a function of time. The measure for net climate effects is the sum of the displaced emissions and carbon sequestered into forest biomass. Note that the displaced fossil C_{eq} emissions are equal to the fossil C_{eq} emissions of the functionally equivalent fossil energy system minus the fossil C_{eq} emissions of the bioenergy system, e.g. due to harvest, transport and processing of the biomass. The method can be used to assess the mitigation benefits of different forest-use strategies in time. The essential parameter in the method is the fossil carbon displacement factor (DF) describing the reduction in fossil C_{eq} emissions in proportion to the biogenic C in the biomass feedstock. DF is a measure of the mitigation efficiency of the biomass use cycle. This method is compatible with the so-called standard methodology for the GHG balances of bioenergy systems compared with fossil energy systems (Schlamadinger et al. 1997).

As shown by Marland and Schlamadinger, there are trade-offs between alternative mitigation options of managed forests. The available alternatives are substitution (i.e. use of harvested biomass to displace fossil fuels or energy-intensive materials), C sequestration and, simply, conservation of forest biomass. The amount of the trade-offs depends on many factors, such as the time frame of mitigation, rotation length and biomass re-growth rate and DF. The use of fossil alternatives instead of biomass sometimes provides near-term net GHG benefits, especially when DF is low and the rotation is long. However, in the long term, the accumulating benefit of fossil fuel substitution (i.e. avoidance of emissions from permanent tectonic C stocks) dominates due to the saturation of the C sequestration alternative.

In place of considering the net *C balance* of the biomass system with respect to its fossil reference, as done by Schlamadinger and Marland, a more realistic measure of the GHG impacts would be net *cumulative radiative forcing* (CRF) in time due to biomass use, i.e. the decrease in cumulative thermal energy radiation from the Earth to space within a given time frame. The decrease is caused by a change in atmospheric greenhouse gas concentrations due to the emission sources and sinks of biomass use.

The objective of this article is to present metrics with which the GHG impact of the biomass life cycle can be related to that of a permanent fossil C emission. Global Warming Potential (GWP) factors are derived that describe the CRF of the forest biomass life cycle– within the time frame of interest starting at the point of harvest – in proportion to the CRF of a fossil C emission at the initial time. Cherubini et al. (2011) presented a GWP_{bio} factor for the biomass resource. In this article we widen this approach to the biomass product life cycle and displaced fossil C emissions. The GWP factors to be presented are analogous to those derived for non-CO_2 gases to convert them into CO_2-equivalent fossil emissions. As numerical examples, we use alternative forest biomass scenarios including both bioenergy and long-lived wood products.

2 Method

The method in this article is aimed at estimating the warming impact of forest biomass harvest and use with respect to its fossil C-based functionally equivalent alternatives. The perspective is forward-looking, as nothing can be done to the past. The actions and choices made from now on are relevant to climate change mitigation. The objective is to present simple *ex-ante* indicators that would estimate the warming impact of a biomass use cycle in advance, within the time frame of interest starting from the point of harvest. Biomass harvest and use is assumed to represent the action having climate impacts with respect to the no-harvest and non-use baseline. The method considers the warming impact of: 1) the debt in the terrestrial C stocks due to biomass harvest and 2) the cooling impact of the biomass use cycle due to displaced fossil C emissions and C sequestration of biomass products. The C debt evolves in time depending on the development of the terrestrial C stock in both the scenarios of a harvest and a no-harvest baseline, including re-growth of new biomass. The C stock of biomass products and the displacement of emissions also vary within the considered time frame.

To estimate the radiative forcing in time, a model for the removal of the atmospheric C is needed. For this purpose, the impulse response model based on the Bern Carbon Cycle Model 2.5CC given by the IPCC (2007b, p.213) is used (see Appendix 1 for details). The impulse response describes the time behaviour of the atmospheric CO_2 concentration due to a CO_2 pulse to the atmosphere. After the pulse, the atmospheric concentration declines due to the removal of CO_2 to the ocean and biosphere.

The warming impact of CO_2 emissions is assessed using radiative forcing (RF) as an indicator of heating power in the atmosphere-surface system. RF is calculated on the basis of increased CO_2 concentration. The unit of RF is typically Watts (W) per square metre (m^2) of the surface of the Earth. RF describes the deviation in the radiation energy balance of the atmosphere-surface system due to some considered factor such as increased greenhouse gas concentration (IPCC 2007b; Monni et al. 2003).

The time integral of radiative forcing (RF) is a measure of the global warming energy absorbed due to the additional GHG emission, also called cumulative radiative forcing (CRF) or Absolute Global Warming Potential (AGWP). This cumulative warming impact, within the time frame (0,T), can be assessed for the C emissions due to a unit fossil C emission pulse released at time zero:

$$AGWP_{fos}(T) = \int_0^T RF\left(S_{fos}(t)\right)dt \tag{1}$$

where $S_{fos}(t)$ is the atmospheric CO_2 concentration due to the fossil C emission unit pulse. After its release, the C impulse is gradually transferred to the ocean and biosphere in general (Appendix 1), but there is no C uptake back to the original tectonic stocks. Thus, the fossil C emission is often said to be permanent.

For a unit C pulse from biomass harvest at time zero (causing a temporary C debt of the biomass stock), a similar equation can be presented:

$$AGWP_{bio}(T) = \int_0^T RF(S_{bio}(t))dt \tag{2}$$

where $S_{bio}(t)$ is the atmospheric CO_2 concentration due to the biomass unit C pulse so that in addition to the normal atmospheric decay of the fossil C pulse as above, biomass re-growth

(e.g. growth of a new forest stand after the regeneration cut) also affects the concentration. The value of this is highly dependent on the biomass re-growth rate. Other emission components of biomass cultivation such as N_2O from fertilizers and other climatic forcers such as albedo effects (see, e.g., Bright et al. 2011) could basically also be included in the $AGWP_{bio}(T)$.

Analogously to Eq. (2), the net cooling impact of using a unit of biogenic C at time zero with respect to a functionally equivalent fossil-based service can be considered:

$$AGWP_{blouse}(T) = \int_0^T \left(RF\left(S_{displ}(t)\right) + RF\left(S_{seq}(t)\right)\right)dt \tag{3}$$

where $S_{displ}(t)$ is the reduced atmospheric CO_2 concentration due to displaced emissions in both energy and material substitution, and $S_{seq}(t)$ is the reduced CO_2 concentration due to C sequestration into biomass products. The functionally equivalent fossil service could be a displaced fossil fuel or non-biogenic material with embodied fossil C emissions.

Summing up, Eqs. (2) and (3) give the net warming impact of the biomass use chain compared with the functionally equivalent fossil chain. The time T when the sum is equal to zero gives the *cumulative warming payback time* of the biomass chain with respect to its fossil reference service.

The climate impact of the unit biomass C pulse (Eq. 2) and displaced emissions (Eq. 3) can also be expressed in proportion to the climate impact of the fossil C unit pulse (Eq. 1). The so-called GWP_{bio} factor is defined (Cherubini et al. 2011) as the quotient of AGWPs in Eqs. (2) and (1):

$$GWP_{bio}(T) = \frac{AGWP_{bio}(T)}{AGWP_{fos}(T)} \tag{4}$$

GWP_{bio} is dimensionless and a function of the mitigation time frame (0,T) under consideration. It is analogous to the GWP factors describing the relative warming impact of non-CO_2 gases to that of CO_2. Another GWP factor can be defined by considering, in addition to just the C pulse due to biomass harvest, the net cooling impact due to the use of harvested biomass:

$$GWP_{netbio}(T) = \frac{AGWP_{bio}(T) + AGWP_{biouse}(T)}{AGWP_{fos}(T)} \tag{5}$$

$$= GWP_{bio}(T) + GWP_{biouse}(T) \tag{6}$$

The first term in Eq. (6) is GWP_{bio}. The second term, GWP_{biouse} , is the relative cooling impact compared with the warming impact of the fossil pulse (Eq. 1). In the case that the displacement of fossil C emission takes place immediately after biomass harvest:

$$GWP_{biouse}(T) = -DF \tag{7}$$

where DF is the displacement factor (Schlamadinger and Marland 1996). GWP_{biouse} in Eq. (7) is constant, as the displaced fossil C emissions have the same dynamics as the unit fossil C emission. In this article, however, GWP_{biouse} covers a wider range of options than just the displacement of fossil fuels, such as cascading use of biomass including material substitution, temporal C stock of the biomass product and recycling into bioenergy. In

this latter case, GWP_{biouse} is a non-constant function of the time frame (0,T). The two GWP terms in Eq. (6) are simple dimensionless indicators of the biomass use in climate change mitigation within the given time frame related to the climate impacts of a fossil C pulse. As GWP_{netbio} depends on T, the time T when $GWP_{netbio}(T) = 0$ is the cumulative-warming payback time defined above.

In defining the GWP factors, an instant emission pulse at time zero is usually considered. However, the approach could also be generalized to other cases such as step emissions where a continuing biomass harvesting activity is started at time zero. Here a fossil C step pulse must be used as the reference.

3 Results

3.1 Bioenergy from forest residues

The numerical example of bioenergy production from forest harvest residues is based on the results of the study by Repo et al. (2010) in which the decay of Norway spruce (*Picea abies*) branches and stumps of various diameters in time were estimated with the Yasso07 model (Yasso07 2011). The emission rates and decomposition dynamics of residues are related to the climate conditions and the type of residues. The residue diameters considered were 1, 2 and 5 cm for branches and 10, 20, 26 and 35 cm for stumps, and the assumed climate conditions correspond to those of Southern Finland.

When calculating the indicators, it is assumed that in the baseline case the residues are left on site and decomposed slowly to the atmosphere. In the bioenergy case, the residues are combusted and emitted to the atmosphere in the year of harvest. The biogenic C debt is the difference in C balance between the bioenergy and the baseline case. Two options are considered: a pulse and a step use of residues. In the pulse option, residues containing 1 Mg (=megagram or metric ton) of biomass C were harvested and used in 2010, causing a pulse emission of bioenergy. In the step option, an activity was started in 2010 using annual residues containing 1 Mg of biomass C, causing a step emission from bioenergy.

The net biogenic C emission due to the pulse use of residues, i.e. the emission due to the bioenergy pulse *minus* the terrestrial C emission in the no-use baseline (shown for the 5 cm branches in Fig. 1a), was 1 Mg C in 2010 but just negative after that because of the decomposition of residues in the no-use baseline. The reference fossil C pulse is simply the 1 Mg C emission in 2010, also shown in Fig. 1a. The atmospheric concentration $S_{bio}(t)$ due to the net biogenic C emission is then estimated using the pulse response model (Appendix 1) and the cumulative warming impact $AGWP_{bio}(T)$ calculated by Eq. (2). Similarly, the fossil C concentration $S_{fos}(t)$ due to the fossil C pulse in Fig. 1a is estimated and $AGWP_{fos}(T)$ is calculated by Eq. (1). The AGWP curves are shown in Appendix 1. The dimensionless GWP_{bio} (T) factor calculated by Eq. (4) is shown in Fig. 1b as a function of the time frame T.

The climate benefits of the biomass use cycle, characterized by the displacement factor DF, are dependent on the biomass combustion efficiency and the fossil fuel displaced by bioenergy. The magnitude of DF for a modern biomass boiler displacing coal combustion could be 0.9 or even higher. For natural gas displacement, it would be in the order of 0.5. For illustrative purposes in Fig. 1, it is simply assumed that DF = 0.6, which means that with 1 Mg biomass C in harvest residues, 0.6 Mg C from fossil fuel is displaced. In the case that energy displacement takes place immediately after the biomass harvest, $GWP_{biouse}(T)$ is constant in time and equal to $-DF = -0.6$. (The $AGWP_{biouse}$ is shown in Fig. 8 of Appendix 1.) Accordingly, GWP_{netbio} decreases to zero in 2028 so that the climate benefit

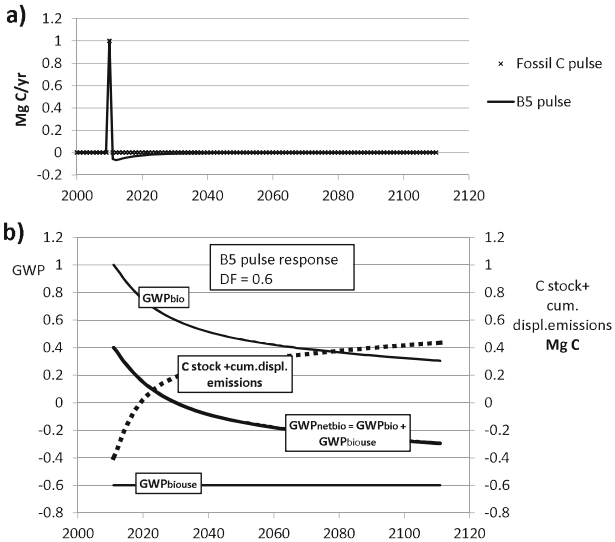

Fig. 1 **a** Fossil C and biomass C (forest residue branches of *Picea abies*, 5 cm in diameter = B5) net emissions to the atmosphere due to the energy production pulse. After the positive value in 2010, the biogmass curve is negative. The biomass net curve is the remainder of the bioenergy emission pulse and slow decay of forest residues on the cutting site. **b** Relative warming impacts described by GWP_{bio}, GWP_{biouse} and GWP_{netbio} calculated on the basis of the B5 net emission curve due to the energy production pulse. The relative warming impact of the B5 net emission curve is about 0.4 over a 50-year time horizon (in 2060) compared with a fossil emission pulse, if no displacement of fossil carbon is accounted for. If the displacement factor is 0.6, a cooling benefit of 0.2 can be reached in 50 years (in 2060). The role of displacement is crucial to the total net impact. The sum of terrestrial C stock and cumulative displaced emissions is shown as the *dashed line*

in terms of cooling (i.e. a negative value) with respect to the fossil energy alternative is obtained in a time frame longer than 18 years (Fig. 1b).

The climate benefit criterion in the original method of Schlamadinger and Marland — the sum of the biogenic C balance and cumulative displaced fossil emissions–is positive already in 2019, after which there are climate benefits in terms of a positive (terrestrial + tectonic) C stock with respect to the fossil fuel alternative (Fig. 1b). Thus, the C balance payback time (9 years) is essentially shorter than the cumulative warming payback time (18 years) of the present method. The results for other residue diameters are similar.

Figure 2a illustrates how the biogenic C emissions from a step use of harvest residues are related to branch and stump diameters. Estimating the concentrations $S_{bio}(t)$ and $S_{fos}(t)$ due to the biomass C emission of the 5 cm branches and the fossil C step emission in Fig. 2a and performing similar calculations to those in Fig. 1 with DF = 0.6 results in $stepGWP_{bio}(T)$, $stepGWP_{biouse}(T)$ and $stepGWP_{netbio}$ in Fig. 2b. For comparison purposes, the sum of the biomass C balance and cumulative displaced fossil emissions are presented. Both the C balance payback time (21 years) and the warming payback time (32 years) are higher in this step case than in the pulse case in Fig. 1.

One hundred years is a regularly applied time frame in climate policy, and the GWP (100 years) factors a simplified way of describing the relative warming impact of non-CO_2 GHGs in proportion to CO_2 in emissions reporting. Applying this analogy to the biomass C emissions from the use of harvest residues (Fig. 3) shows, for example, that the climate

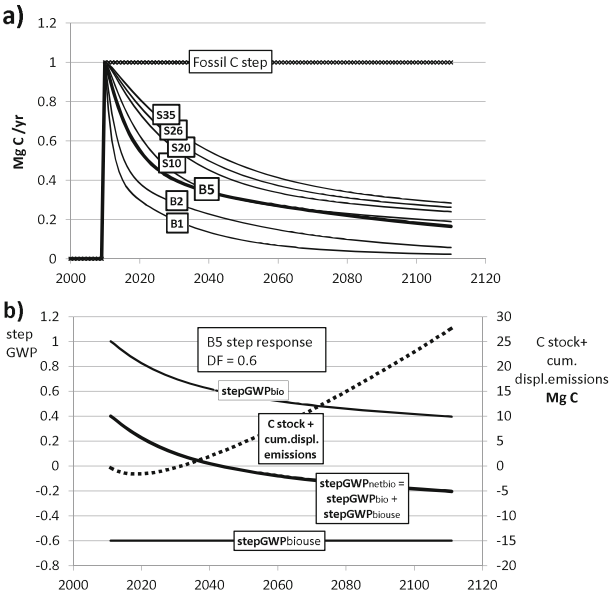

Fig. 2 **a** Fossil C and biomass C (forest residue branches and stumps of various diameters) net emissions to the atmosphere due to continuous energy production starting in 2010 (step function). **b** Relative warming impacts described by $stepGWP_{bio}$, $stepGWP_{biouse}$ and $stepGWP_{bionet}$ calculated on the basis of the B5 net emission curve due to continuous energy production starting in 2010 (step function). The relative warming impact of the B5 net emission curve is about 0.5 over a 50-year time horizon compared with fossil energy emission if no displacement of fossil carbon is accounted for. If the displacement factor is 0.6, a cooling effect of 0.08 can be reached in 50 years. The sum of ecosystem carbon stock and cumulative displaced emissions is shown as the *dashed line*

impact of the use of 1 Mg C of 20 cm stumps corresponds to an instant fossil C emission of approximately 0.4 Mg C and continuous 1 Mg C annual stump use to a 0.5 Mg C annual fossil emission – excluding here the substitution benefits of bioenergy.

Energy substitution is taken into account in Fig. 4, which estimates the warming payback time as a function of the displacement factor DF. The results illustrate the sensitiveness of the climate benefit on the displacement factor DF. For example, energy use of the largest stump fraction (35 cm) in the Repo et al. (2010) study only creates less cumulative warming than the fossil fuel alternative after 100 years if DF is less than 0.5 in instant use (Fig. 4a) or 0.6 in continuous use (Fig. 4b).

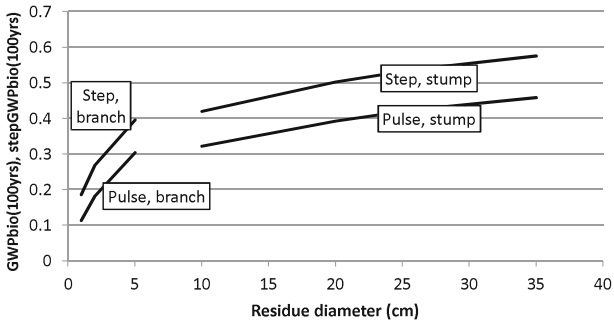

Fig. 3 GWP_{bio}(100 year) for different residues as a function of their diameter calculated for pulse and stepwise energy production

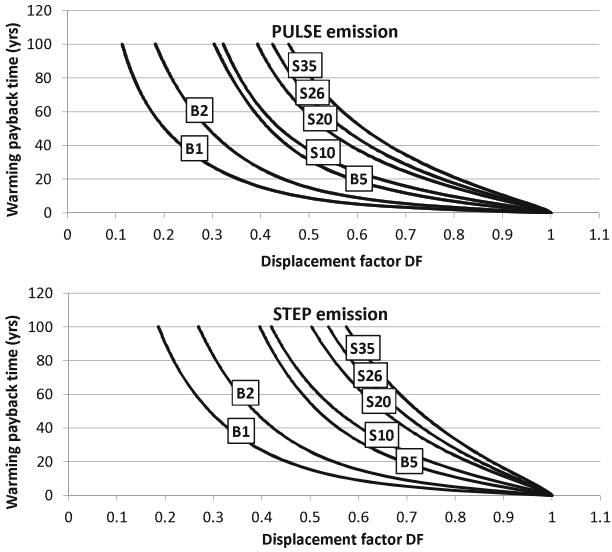

Fig. 4 Cumulative warming payback time as a function of displacement factor DF for different residue diameters (branches 1, 2 and 5 cm; stumps 10, 20, 26 and 35 cm) when the use is instant (pulse energy production) vs. continuous (stepwise energy production)

3.2 Stem biomass for long-lived wood products

In addition to energy use, climate benefits can potentially be obtained by material use of forest biomass. Here, a modern wooden office building displacing a conventional concrete one is considered. The details of the calculation of the DF factors and C stock of wood products are given in Appendix 2 based on the LCA study by Häkkinen and Wirtanen (2006). The main building material is assumed to be Scots pine (*Pinus sylvestris*) grown in Southern Finland. The parts of the stem not applicable to long-lived materials are assumed to be used for bioenergy. The growth curve for the stemwood of the pine stand (Fig. 5) is estimated by the MOTTI simulator (Hynynen et al. 2005) whose data are based on test areas in Finland comprising all age classes (Hynynen et al. 2002), though the representativeness of data for stands older than 140 years is weak. The soil C balance is excluded and only stemwood growth is considered. For simplicity, the thinning of forest stands is also excluded. Applying the growth curve in Fig. 5, it is assumed that the point of final felling can be varied. After felling, we assume that the re-growth follows the same growth curve starting from time zero and that the C debt at felling is equal to the biogenic C in stemwood.

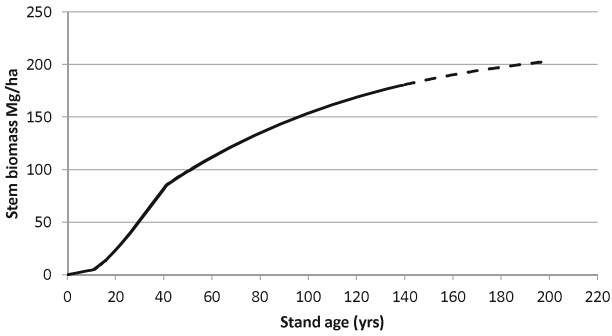

Fig. 5 Development of the stem biomass of a Scots pine (*Pinus sylvestris*) stand without thinnings estimated by the MOTTI simulator (Hynynen et al. 2002, 2005). The *dashed line* marks uncertain numbers beyond a 140-year stand age

The pulse from the final felling of 1 Mg of biogenic C at stand age 80 (Fig. 6a) is slightly positive within a decade of felling — a C debt with respect to the baseline of no-felling – because the re-growth of the new stand is slower at the beginning than the growth of the old stand after 80 years (cf. Fig. 5). Thereafter, the development of the new stand is faster, thus forming a net C sink in proportion to no use. However, according to the estimates by the MOTTI simulator, there does not appear to be a clear saturation point within the 200-year time frame that is considered – but the data beyond 140 years should be assessed with caution. As a consequence of the shape of the growth curve, the GWP_{bio} factor (Fig. 6b) is even greater than 1 in the beginning, after which it decreases due to the declining C debt caused by the re-growth. The uncertainty of the growth curve is reflected in GWP_{bio} after 2070.

In the material substitution case, GWP_{biouse} (Fig. 6b) includes both the displacement of fossil C emissions – due to the bioenergy use of by-products and recycled wood products – and the temporary C stock of wood products (Eq. 3). It is not constant in time, such as in the case of harvest residues used immediately for bioenergy. For illustrative purposes, we use an underestimate of 50 years of the building use life. After decommissioning, wood materials are recycled for bioenergy with a 50-year delay and the biomass C sequestered in wood products displaces fossil C emissions with DF = 0.6. The GWP_{biouse} is close to −1 in the first 50 years despite the moderate DF. This reflects the benefits of combined material and energy substitution in climate change mitigation compared with the pure energy substitution. The overall climate performance with respect to the concrete building is described by the indicator GWP_{netbio}. Similarly to the forest residue case, the GWP-based metrics gives a longer payback time (36 years) than the sum of the C stock and cumulative displaced emissions (23 years). However, with a slightly higher DF for by-product bioenergy, in the order of 0.8, the GWP_{netbio} would be negative already at the year of construction and the warming payback time would be zero.

Another factor contributing negatively to climate benefits is the slow growth of the Scots pine stand. In addition, there does not appear to be any clear saturation point for the growth

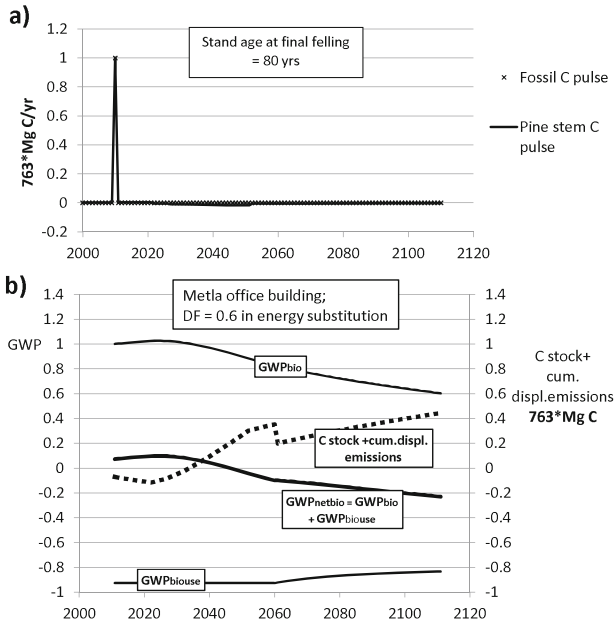

Fig. 6 **a** Net carbon emissions due to biomass use pulse for wooden building and energy (see details in the main text). The net emissions are the remainder of the biomass carbon emissions in the use case and the reference case. **b** Relative warming impacts described by GWP_{bio}, GWP_{biouse} and GWP_{netbio} for the material displacement calculated based on the net emission curve given in **a**) and the LCA data given in the Appendix 2. The sum of ecosystem carbon stock and cumulative displaced emissions is shown as the *dashed line*

beyond the commercial rotation length. Consequently, GWP_{bio} calculated as a function of the stand age at final felling appears relatively insensitive to the felling age (Fig. 7). In the shortest time frame, the cumulative warming impact is similar to the fossil C emission because, within 20 years, the re-growth does not fill the C debt with respect to the no-felling alternative.

4 Discussion and conclusions

The GWP metrics applied to the biogenic C debt was recently introduced by Cherubini et al. (2011). It results in GWP_{bio} factors that are analogous to the GWP factors derived for non-CO_2 GHGs. They are aimed at providing simple but realistic climate indicators in an LCA of bioenergy systems. In this article, the metrics is extended by considering GWP_{bio}– in addition to *pulse* emission – for the biomass *step* emission and introducing the GWP factor for the relative cooling impact of biomass-displacing fossil fuels or emission-intensive materials, called GWP_{biouse}, the sum of GWP_{bio} and GWP_{biouse} (= GWP_{netbio}) being an indicator of the net climate benefits with respect to the fossil alternative. The consideration of the net GHG benefits of biomass use is similar to the metrics of Schlamadinger and Marland (1996) in which the cumulative displaced fossil C emissions due to biomass use are added to the biomass C balance in time, forming an indicator of the overall C benefits in proportion to the fossil alternative.

The GWP_{bio} factor takes into account the dynamics of the biomass C due to the re-growth of biomass credited *ex-ante*. The analysis is forward-looking. No climate credits are given for past C sequestration. The starting point of the estimated climate impacts is when the biomass C stock is harvested and taken into use either as energy or materials. By the net GWP factor, the climate impact of an instant biomass harvest and use cycle can be converted into a fossil C pulse emission (or removal) whose cumulative warming impact is the same or, alternatively, the continuous biomass harvest and use of an equivalent fossil C step emission. The analysis is based on a presumed development of the terrestrial C stock following harvest and thus involves uncertainties. It could be performed in a similar way at landscape level as at stand level. The GWP_{bio} and GWP_{biouse} are estimated as a function of the time frame T, but the appropriate time frame T to be used is open to question. As a comparison, the 100-year time period is used in national emission inventories when converting non-CO_2 gas emissions to CO_2 equivalents, but the urgency of climate change mitigation may justify the use of even shorter periods in the future.

By fixing the time frame T, two simple emission-related indicators are provided: one for the biomass resource and the other for the biomass use cycle replacing fossil carbon,

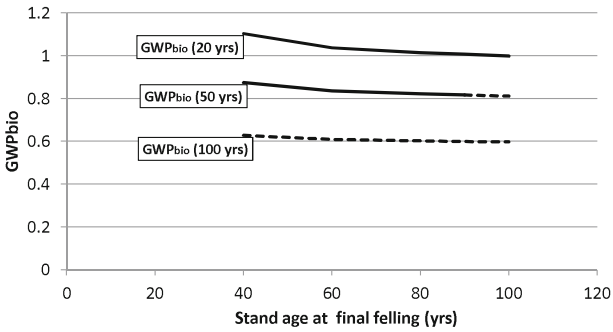

Fig. 7 GWP_{bio} for final felling when the rotation length is altered, based on the growth curve of the Scots pine (*Pinus sylvestris*) stand in Fig. 5. The *dashed line* marks uncertain numbers

relating them to the warming impact of a permanent fossil C pulse emission at time zero (or to an emission step starting at time zero). One limitation of this approach is that pure C sequestration without biomass use cannot be valued, but it could be described by the AGWP (Eqs. 2 and 3). The advantage of using radiative forcing-based metrics, such as GWP or AGWP metrics, instead of a cumulative net C balance is that non-CO_2 gases and non-GHG-based warming impacts such as albedo and particles could be included and that the cumulative radiative forcing within a given time frame is likely to be a more realistic warming indicator than just the net C balance. The GWP index would also provide a physically-based discounting factor by which the cumulative warming impact of the estimated future emissions in a fixed time horizon could be related to a permanent fossil emission at initial time. Basically, the GWP approach could be applied generally in life cycle assessment (LCA) to convert the emissions along the product life cycle to C (or CO_2) equivalent emissions or a C footprint. In the LCA application, no displaced emissions could be included, however, only those from the product life cycle.

The numerical values in the figures of the article are relatively sensitive to the biomass decay curves used in the calculations. The values employed in this article are based on Repo et al. (2010). However, as a set of decay curves are used, they also give some range for the results that can be used to describe their variability. Empirical results based on measurement should be used in the future to estimate the appropriate values of the decay curves as well their uncertainty ranges. Many of the results of this article are based on the functional methodological formulation of the impacting processes and they are valid even without exact numerical values of the biomass decay curves.

The results show that the warming payback time of the method presented is longer than for the cumulative net C balance. This is due to the fact that during the C debt – emitted to the atmosphere — a cumulative warming impact is built up that has not yet been compensated for along with the zero net C balance. When fossil C displacement takes place immediately after biomass harvest, GWP_{biouse} is constant and equal to -DF, where DF is the displacement factor of the method of Schlamadinger and Marland (Schlamadinger and Marland 1996; Marland and Schlamadinger 1997). In this case, the warming payback time can easily be estimated as a function of DF.

Ideally, DF can be high even in pure energy use of wood, e.g. in the order of 0.9 when wood displaces coal in a modern combined heat and power plant also designed for biomass or even more if peat is displaced. The energy substitution is not as efficient when, for instance, wood-based biodiesel displaces fossil diesel with DF estimates from 0.3 to 0.5 (Pingoud 2010; Soimakallio et al. 2009). However, in reality, the situation may be more complex: the increased bioenergy supply may influence the whole energy system due to market impacts, causing leakage when an additional 1 MJ of bioenergy does not fully displace a 1 MJ of fossil fuels (Stoft 2010; Rajagopal et al. 2011). Along with the tightening climate policy, the energy system will also presumably develop towards a lower C intensity, which may decrease the future displacement benefits of additional biomass. When DF is low, the warming payback time for a continuous bioenergy harvest of stumps appears to be significantly high, more than 100 years when DF is less than 0.45. Thus a high DF, or equivalently GWP_{biouse} close to -1, is a prerequisite of benefits in climate change mitigation within the short or medium term. The material use of wood appears to provide beneficial GWP_{biouse} factors when realistic model parameters are used because the advantage can be taken from many substitution components simultaneously: C sequestration into long-lived materials, the displacement of emission-intensive materials such as concrete and displacement of fossil fuels due to bioenergy from by-product flows.

The dynamics of forest biomass and terrestrial C stocks, especially in boreal and temperate regions, is relatively slow, leading to long rotation times and a slow decay of harvest residues. The numerical results presented in this study could mainly be generalized to forestry in boreal regions. The continuous activity of using forest harvest residues causes a slow reduction in dead wood and soil C pools until a new regional scale equilibrium is attained in the future. On the other hand, when the lower equilibrium is obtained, stopping the activity of using forest harvest residues would create a new C sink.

Observations indicate that very old forests can also be net carbon sinks (Luyssaert et al. 2008). The Finnish data on which the MOTTI stand simulator is based (Hynynen et al. 2002) reveal that the growth of the Scots pine stand could continue for a very long time, far beyond the rotation length in present forest management practices. The growth estimate of the old stand beyond 140 years is uncertain due to limited statistics and in reality there is also a risk of losing the big biomass stocks due to natural disturbances.

Thus, there are obvious paradoxes in the use of boreal forest biomass in climate change mitigation that are less relevant in regions with short forest rotations, fast growth and a rapid decay of forest harvest residues. Although biomass use can be C neutral over the long rotation life cycle, it is still not climate neutral. Biomass use can be sustainable in the sense that its use at landscape level is in balance with re-growth, but it is still worse for the climate in the short and medium term than just conservation and the use of fossil-based resources. The results question any rapid climate benefits when increasing the use of boreal forest biomass. However, pure conservation would lead to the loss of the renewable resource of energy and materials in the long run and a substitute for emission-intensive and non-renewable natural resources, and it could be considered unsustainable, at least from the economic viewpoint.

An open question is the optimal timing of using the C sink capacity of the boreal forests at the expense of biomass production, which should also be considered from an economic viewpoint. One long-term option would be to target win-win steady-state strategies that would have better substitution benefits and higher equilibrium biogenic C stocks (Pingoud et al. 2010) than in the prevailing baseline or business as usual. The above study indicated that the highest substitution benefits are not necessarily obtained just by maximizing biomass production but that the quality of biomass and its usability in the displacement of fossil emissions are of the essence.

What conclusions could be drawn from the use of long-rotation biomass as a measure in climate change mitigation? The appropriate baseline or reference case of forest use can be discussed and questioned. However, any change in forest use has an impact on the C balance in time. For instance, if forests at the landscape level functioned as a C sink, increased use of biomass would decrease the sink in the short run with respect to the baseline, which must be taken into account in any emission scenarios. The use of forest biomass as a renewable resource must be defended, but it is not climate neutral or C neutral in a shorter time frame, which means that fossil emissions must be cut even further to obtain the set emission targets.

To summarize:

1) The urgent time frame of climate change mitigation makes the timing of emissions an issue, including biogenic C emissions from land use change and even the C balance of sustainable forestry. The mitigation time frame is of the same magnitude as the rotation length of slow-growing boreal forests. Harvesting a stand causes a substantial C debt, at least in the short run, with respect to a no-harvest baseline, the climate impact of which should be taken into account within the mitigation time frame of interest. With a

limited forest land area, the trade-offs between increasing wood use vs. increasing C sequestration into forest biomass need to be noted. There is a potential dilemma between short-term climate benefits and long-term sustainable forestry.

2) The dynamics of tectonic fossil C stocks and renewable biogenic C stocks differ from each other. By the GWP metrics, the estimated C emissions and future removals due to the biomass C cycle can be converted into an equivalent fossil C emission in terms of the same cumulative warming impact within the time frame of interest. The emission-related indicator aims to provide a simpler and more illustrative measure than just the cumulative radiative forcing applicable as, e.g., a C footprint indicator.
3) The overall climate impacts of the forest biomass cycle are determined by the C dynamics of forestry and those of the wood use cycle. In this article, separate GWP factors were derived for both parts. The climate benefits of wood use can be valued based on the amount of fossil C emissions that can be displaced. Thus, the focus is on relative climate impact due to the wood use cycle with respect to fossil C-based alternatives. Wood use typically increases the net warming impact in the short run with the benefits coming later. The results emphasize the importance of efficient wood use – in terms of high fossil C displacement and C sequestration into long-lived wood products – as a prerequisite to short warming payback times and thus high climate benefits, which may even reduce the time to zero.

Acknowledgements The authors wish to thank Dr Jari Hynynen from the Finnish Forest Research Institute (Metla) and Professor Lauri Valsta from the University of Helsinki for their assistance with the simulations with the MOTTI model. Funding from the Sustainable Energy Programme (SusEn) of the Academy of Finland is also gratefully acknowledged.

Appendix 1. The REFUGE3 model

This appendix describes the REFUGE 3 model that was used to calculate the atmospheric concentrations and radiative forcing. The model calculates atmospheric concentrations and radiative forcing for CO_2, CH_4 and N_2O. The emissions discussed in the study are added to a background of global emission pathways that correspond to emission levels that would reach a 450 ppm-eq concentration target by 2100. The relative shares of CO_2, CH_4 and N_2O in this background pathway have been approximated from a number of emission-reduction scenarios.

After its release into the atmosphere, a CO_2 emission impulse is assumed to decay according to the impulse response function reported by IPCC (2007b, page 213), an approximation based on the Bern2.5CC carbon cycle model (Joos et al. 2001). An emission pulse, regardless of its origin, is mixed in the atmosphere and, gradually, the increase in atmospheric concentration is transferred partially to the ocean and the biosphere. The resulting increase in atmospheric CO_2 concentration $S(t)$ is then defined by

$$S(t) = \int_{t_0}^{t} E(\tau)\left(a_0 + \sum_{i=1}^{3} a_i e^{(t-\tau)/b_i}\right) d\tau \qquad \text{(A1)}$$

where $E(t)$ is the annual emission level and the parameters of the impulse response function are a_0=0.217, a_1=0.259, a_2=0.338, a_3=0.186; and b_1=172.9 years, b_2=18.51 years and b_3= 1.186 years. To improve the computability of the convolution in (A1), a recursion formula of Pingoud and Wagner (2006) has been used.

In the calculations, the biogenic C emission pulse was followed by a sink due to the re-growth of biomass. This sink reduces the level of global emissions in the REFUGE3 model and, in principle, it is accounted for simply as a series of gradually declining negative emission impulses in (A1). Therefore, the total concentration impact of biomass use as energy is a combination of the emission and subsequent sinks, and the atmospheric CO_2 dynamics for both the emissions and sinks.

The atmospheric CO_2 concentration $C(t)$ then induces radiative forcing (RF), with the expression Ramaswamy et al. (2001, p. 358)

$$RF(t) = \alpha \ln(C(t)/C_0), \tag{A2}$$

where C_0 corresponds to the atmospheric CO_2 concentration before 1850 (278 ppm assumed) and α=5.35 W/m^2. An additional concentration pulse $S(t)$ adds to the background concentration $C_{bg}(t)$ so that $C(t)=C_{bg}(t)+S(t)$, where $C_{bg}(t)$ is an generic estimate for a global 450 ppm-eq concentration pathway. As the formula for RF is non-linear, the marginal increase in RF from a marginal emission impulse depends on when the emission is released, as the global background CO_2 concentration varies over time. However, this effect is only minor and the change in RF for an emission impulse released in 2000 (i.e. when the atmospheric concentration is the lowest) is roughly 10% higher than when the impulse is released during the latter part of the century when the concentration is highest. Therefore, our illustrative emission impulse, released in 2010, should be applicable throughout the time frame used with reasonable accuracy.

As an example, the cumulative radiative forcing (CRF) or AGWP calculations of the energy use of 5 cm diameter branches (related to Fig. 1) are shown in Fig. 8. Note that when the displacement factor DF = 0.6 and there are no fossil C emissions of the bioenergy system then

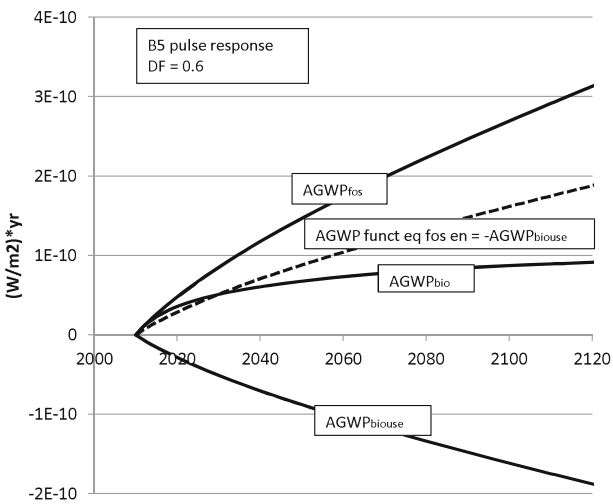

Fig. 8 Cumulative radiative forcing (CRF), i.e. AGWP, as a function of the timeframe (2010, t) for the unit pulse emission of 1 Mg fossil C at 2010 ($AGWP_{fos}$), 1 Mg of biomass C debt due to harvest of 5 cm branches at 2010 ($AGWP_{bio}$) and the displaced fossil C emissions at 2010 ($AGWP_{biouse}$) when DF = 0.6. Note that $AGWP_{biouse}$ / $AGWP_{fos}$ = −0.6. In the simple case when fossil C emissions of the bioenergy system are zero, the AGWP of the functionally equivalent fossil energy system is the *dashed line* and equal to -$AGWP_{biouse}$. The warming payback time is the time when the AGWPbio curve cuts the AGWP curve of the functionally equivalent fossil energy system

the C pulse from the fossil fuel energy system, functionally equivalent to the bioenergy system, is 0.6 Mg C.

Appendix 2. Estimation of GWP_{biouse} in combined material and energy substitution

The estimation of the GWP_{biouse} of material substitution in this study is based on the data of the life cycle assessment (LCA) of Häkkinen and Wirtanen (2006) in which a modern wood office building, the research centre of the Finnish Forest Research Institute in Joensuu, was compared with a functionally equivalent (fictional) concrete building of a conventional design (Table 1). The numbers are thus case-specific but characterize the factors involved in material substitution.

The GWP_{biouse} is estimated as follows: assuming a C content of 0.5, 305 Mg C is sequestered in long-lived wood structures. By using wood as a construction material instead of concrete, 597 Mg CO_2eq emissions or 163 Mg C were saved. Assuming that 40% of the stem biomass is used in the long-lived structures and the rest, 60%, — the by-product flow – is used as bioenergy, it implies that the total stemwood consumption is equal to 763 Mg C, and the by-product flow 458 Mg C. Part of the latter goes to the energy required for processing the wood materials and the rest can be used to displace fossil fuels elsewhere. By assuming that all the renewable primary energy consumed in wood building is wood-based and that the average moisture content of the by-products (bark, chips, sawdust) is 50% with a specific heat value of 16.6 GJ/(Mg dry matter), 114 Mg dry matter wood or 57 Mg biomass C of by-products is consumed as the internal process energy of wood materials. Thus, 401 Mg biomass C can be used to displace fossil energy elsewhere. Assuming DF = 0.6 for this energy substitution, 240 Mg C fossil emissions could be displaced. Thus, the total reduction in C emissions at the year of harvest/construction would be equal to 708 Mg C of which 43% consists of biomass C sequestered into long-lived material, 23% of material substitution and 34% of energy substitution. The reduction would represent 93% of the biogenic C stock of the stemwood consumed.

For illustrative purposes it is assumed that the lifetime of the building would be (just) 50 years after which the demolished wood structures would be recycled into bioenergy. If DF at 2060 were equal to 0.6, 183 Mg C could be displaced so that the net emission would be 122 Mg C, or 16% of the biomass C of the stemwood.

Table 1 LCA data of the wood office building of the Finnish Forest Research Institute (Metla) and of its functionally equivalent concrete alternative (Häkkinen and Wirtanen 2006)

	Wood building	Concrete building
Total weight (Mg)	1920	4710
Weight of wood structures (Mg)	610	0
Non-renewable primary energy (GJ)	3460	7430
Renewable primary energy (GJ)	1880	540
Total (GJ)	5340	7970
Emissions (Mg):		
Mg CO_2	320	804
Mg CH_4	0.63	1.27
Mg N_2O	0.01	0.33
Total (Mg CO_2eq)	336	933

References

Bright RM, Strømman AH, Peters GP (2011) Radiative forcing impacts of boreal forest biofuels: a scenario study for Norway in light of albedo. Environ Sci Technol 45(17):7570–7580

Cherubini F, Peters GP, Berntsen T et al (2011) CO_2 emissions from biomass combustion for bioenergy: atmospheric decay and contribution to global warming. GCB Bioenergy. doi:10.1111/j.1757-1707.2011.01102.x

EU (2009) 'Directive 2009/28/EC of the european parliament and of the council of 23 April 2009 on the promotion of the use of energy from renewable sources and amending and subsequently repealing Directives 2001/77/EC and 2003/30/EC', Official Journal of the European Union L140/16-62

Fargione J, Hill J, Tilman D, Polasky S et al (2008) Land clearing and the biofuel carbon debt. Science 319 (5867):1235–1238

Gibbs HK, Johnston M, Foley JA, Holloway T et al (2008) Carbon payback times for crop-based biofuel expansion in the tropics: the effects of changing yield and technology. Environ Res Lett 3(3). doi:10.1088/1748-9326/3/3/034001

Häkkinen T, Wirtanen L (2006) Metlan Joensuun tutkimuskeskuksen ympäristö- ja elinkaarinäkökohtien arviointi [environmental and life cycle assessment of the Finnish Forest Research Institute's (Metla) research centre in Joensuu]. Espoo 2006. VTT Tiedotteita–Research Notes 2342. 29 p

Hertel TW, Golub AA, Jones AD et al (2010) Effects of US maize ethanol on global land use and greenhouse gas emissions: estimating market mediated responses. BioScience 60(3):223–231

Hynynen J, Ojansuu R, Hökkä H, et al. (2002) Models for predicting stand development in MELA system. The Finnish Forest Research Institute. Research Papers 835, ISBN 951-40-1815-X, ISSN 0358–4283

Hynynen J, Ahtikoski A, Siitonen J et al (2005) Applying the MOTTI simulator to analyse the effects of alternative management schedules on timber and non-timber production. Forest Ecol Manag 207:5–18

IPCC (2006) 2006 IPCC Guidelines for National Greenhouse Gas Inventories, vol. 4, agriculture, forestry and other land use. Prepared by the National Greenhouse Gas Inventories Programme. Eggleston HS, et al (eds). IGES, Japan

IPCC (2007a) In: Pachauri RK, Reisinger A (eds) Climate change 2007: synthesis report. Contribution of working groups I, II and III to the Fourth Assessment Report of the Intergovernmental Panel on climate change. Core writing team. IPCC, Geneva

IPCC (2007b) In: Solomon S et al (eds) Climate change 2007: the physical science basis. Contribution of working group I to the Fourth Assessment Report of the Intergovernmental Panel on climate change. Cambridge University Press, Cambridge, United Kingdom and New York

Joos F, Prentice IC, Sitch S et al (2001) Global warming feedbacks on terrestrial carbon uptake under the Intergovernmental Panel on Climate Change (IPCC) emission scenarios. Global Biogeochem Cycles 15 (4):891–907

Kendall A, Chang B, Sharpe B (2009) Accounting for time-dependent effects in biofuel life cycle greenhouse gas emissions calculations. Environ Sci Technol 43(18):7142–7147

Kirkinen J, Palosuo T, Holmgren K, Savolainen I (2008) Greenhouse impact due to the use of combustible fuels: life cycle viewpoint and relative radiative forcing commitment. Environ Manag 42:458–469

Levasseur A, Lesage P, Margni M et al (2010) Considering time in LCA: dynamic LCA and its application to global warming impact assessments. Environ Sci Technol 44(8):3169–3174

Luyssaert S, Schulze ED, Börner A et al (2008) Old-growth forests as global carbon sinks. Nature 455 (7210):213–215

Manomet (2010) Massachusetts biomass sustainability and carbon policy study: report to the Commonwealth of Massachusetts Department of Energy Resources. Natural Capital Initiative Report NCI-2010-03. 182 p. http://www.manomet.org/sites/manomet.org/files/Manomet_Biomass_Report_Full_LoRez.pdf. Cited 2 June 2011

Marland G, Schlamadinger B (1997) Forests for carbon sequestration or fossil fuel substitution? a sensitivity analysis. Biomass Bioenergy 13(6):389–397

Melillo JM, Reilly JM, Kicklighter DW et al (2009) Indirect emissions from biofuels: how important? Science 326(5958):1397–1399

Monni S, Korhonen R, Savolainen I (2003) Radiative forcing due to anthropogenic greenhouse gas emissions from Finland: methods for estimating forcing of a country or an activity. Environ Manag 31 (3):401–411

O'Hare M, Plevin RJ, Martin JI et al (2009) Proper accounting for time increases crop-based biofuels' greenhouse gas deficit versus petroleum. Environ Res Lett 4(2). doi:10.1088/1748-9326/4/2/024001

PAS 2050 (2008) Specification for the assessment of the life cycle greenhouse gas emissions of goods and services. BSI

Pingoud K (2010) Greenhouse gas benefits of wooden building materials. In: Harlin A, Vikman M (eds) 2009 wood and fiber product seminar, VTT and USDA joint activity, VTT symposium 263, VTT, Espoo, 97–104. http://www.vtt.fi/inf/pdf/symposiums/2010/S263.pdf. Cited 26 May 2011

Pingoud K, Wagner F (2006) Methane emissions from landfills and carbon dynamics of harvested wood products: the first-order decay revisited. Mitig Adapt Strateg Glob Chang 11:961–978

Pingoud K, Pohjola J, Valsta L (2010) Assessing the integrated climatic impacts of forestry and wood products. Silva Fenn 44(1):155–175

Rajagopal D, Hochman G, Zilberman D (2011) Indirect fuel use change (IFUC) and the lifecycle environmental impact of biofuel policies. Energ Pol 39(1):228–233

Ramaswamy V et al (2001) Radiative forcing of climate change. In: Houghton JT et al (eds) Climate Change 2001: The Scientific Basis. Contribution of Working Group I to the Third Assessment Report of the Intergovernmental Panel on Climate Change. Cambridge University Press, Cambridge, United Kingdom and New York, NY, USA, pp 349–416

Repo A, Tuomi M, Liski J (2010) Indirect carbon dioxide emissions from producing bioenergy from forest harvest residues. GCB Bioenergy 3(2):107–115

Sedjo RA (2011) Carbon neutrality and bioenergy. A zero-sum game? Resources for the future. RFF DP 11–15. 9 p + Appx

Schlamadinger B, Marland G (1996) The role of forest and bioenergy strategies in the global carbon cycle. Biomass Bioenergy 10(5/6):275–300

Schlamadinger B, Bohlin F, Gustavsson L et al (1997) Towards a standard methodology for greenhouse gas balances of bioenergy systems in comparison with fossil energy systems. Biomass Bioenergy 13(6):359–375

Searchinger TD, Hamburg SP, Melillo J et al (2009) Fixing a critical climate accounting error. Science 326:527–528

Searchinger T, Heimlich R, Houghton RA et al (2008) Use of U.S. croplands for biofuels increases greenhouse gases through emissions from land-use change. Science 319:1238–1240

Soimakallio S, Mäkinen T, Ekholm T et al (2009) Greenhouse gas balances of transportation biofuels, electricity and heat generation in Finland–dealing with the uncertainties. Energ Pol 37(1):80–90

Stoft S (2010) Renewable fuel and the global rebound effect. Global Energy Policy Center Research Paper No. 10–06, http://papers.ssrn.com/sol3/papers.cfm?abstract_id=1636911. Cited 26 May 2011

Yasso07 (2011) Yasso07 model. Document 5/20/2011. Finnish Environment Institute. http://www.ymparisto.fi/print.asp?contentid=377996&lan=en&clan=en. Cited 26 May 2011

GLOBAL CHANGE BIOLOGY
BIOENERGY

GCB Bioenergy (2010), doi: 10.1111/j.1757-1707.2010.01065.x

Indirect carbon dioxide emissions from producing bioenergy from forest harvest residues

ANNA REPO*, MIKKO TUOMI*† and JARI LISKI*

*Finnish Environment Institute, PO Box 140, FI-00251 Helsinki, Finland, †Department of Mathematics and Statistics, University of Helsinki, PO Box 68, FI-00014 Helsinki, Finland

Abstract

Forest harvest residues are important raw materials for bioenergy in regions practicing forestry. Removing these residues from a harvest site reduces the carbon stock of the forest compared with conventional stem-only harvest because less litter in left on the site. The indirect carbon dioxide (CO_2) emission from producing bioenergy occur when carbon in the logging residues is emitted into the atmosphere at once through combustion, instead of being released little by little as a result of decomposition at the harvest sites. In this study (1) we introduce an approach to calculate this indirect emission from using logging residues for bioenergy production, and (2) estimate this emission at a typical target of harvest residue removal, i.e. boreal Norway spruce forest in Finland. The removal of stumps caused a larger indirect emission per unit of energy produced than the removal of branches because of a lower decomposition rate of the stumps. The indirect emission per unit of energy produced decreased with time since starting to collect the harvest residues as a result of decomposition at older harvest sites. During the 100 years of conducting this practice, the indirect emission from average-sized branches (diameter 2 cm) decreased from 340 to 70 kg CO_2 eq. MWh^{-1} and that from stumps (diameter 26 cm) from 340 to 160 kg CO_2 eq. MWh^{-1}. These emissions are an order of magnitude larger than the other emissions (collecting, transporting, etc.) from the bioenergy production chain. When the bioenergy production was started, the total emissions were comparable to fossil fuels. The practice had to be carried out for 22 (stumps) or four (branches) years until the total emissions dropped below the emissions of natural gas. Our results emphasize the importance of accounting for land-use-related indirect emissions to correctly estimate the efficiency of bioenergy in reducing CO_2 emission into the atmosphere.

Keywords: bioenergy, forest harvest residue, indirect emissions, land use, soil carbon, Yasso07

Received 14 May 2010 and accepted 30 June 2010

Introduction

Bioenergy, i.e. energy derived from renewable biomass, is used to replace fossil fuels in energy production in order to decrease greenhouse gas emissions into the atmosphere. The rationale behind this practice is that bioenergy does not cause any net carbon dioxide (CO_2) emissions since the amount of CO_2 released into the atmosphere in combustion is taken up again by the next generation of growing plants (Wihersaari, 2005; Stupak *et al.*, 2007; Lattimore *et al.*, 2009).

Following this idea, as a means to cut down greenhouse gas emissions, the Council of the European Union (EU) adopted a directive on the promotion of renewable energy, including bioenergy. This directive set targets to produce 20% of the final energy consumption using renewable energy sources in the EU by the year 2020. This target is higher for member states already producing a lot of renewable energy, for example as a by-product of pulping industry. Consequently, the national commitment is 38% for Finland and 49% for Sweden (Directive 2009/28/EC). During the reference year of the directive 2005, renewable sources represented already 28% of the total energy production in Finland and 39% in Sweden, while the EU-average was 11%.

These high targets for renewable energy are increasing the focus on biomass for energy production. Worldwide, this growing interest in bioenergy puts pressure

Correspondence: Anna Repo, tel. +358 400 148 652, e-mail: anna.repo@ymparisto.fi

© 2010 Blackwell Publishing Ltd

on land use changes, including deforestation and consequent conversion of the forest land to energy crop cultivation (Melillo *et al.*, 2009).

Recently, indirect CO_2 emissions from bioenergy production associated with these land use changes have caused concern (Searchinger *et al.*, 2008, 2009; Melillo *et al.*, 2009). These indirect emissions occur when bioenergy production reduces the carbon stocks of biomass or soil. These carbon losses may be remarkable, and it is even possible that replacing fossil fuels with bioenergy increases net greenhouse gas emissions into the atmosphere as a consequence of large indirect emissions. The assumed CO_2 neutrality of biofuels like ethanol and their actual potential to mitigate climate change have already been questioned because of large negative impacts on the carbon stock of soil (Fargione *et al.*, 2008; Searchinger *et al.*, 2008, 2009; Melillo *et al.*, 2009).

It is important to realize that the indirect emissions of bioenergy production are not limited to the cases of land use change but may also be caused by new practices of ecosystem management within the same land use. In countries with extensive forest cover and an already high share of renewable energy, an appealing way to produce bioenergy is to intensify biomass removals from forests. Forested countries Finland and Sweden are pioneers in the field of using forest residues for energy production (Mälkki & Virtanen, 2003). Still, in order to meet the EU commitment of renewable energy, Finland plans to increase the use of logging residues for energy production from $3.6\,Mm^3\,yr^{-1}$ in 2006 to $12\,Mm^3\,yr^{-1}$ by 2020 (Ministry of Employment and the Economy of Finland, 2008).

Until now, research on the effects of logging residue removal has focused on nutrient balances (e.g. Wall, 2008; Luiro *et al.*, 2009), socioeconomic impacts (e.g. Börjesson, 2000), profitability (e.g. Heikkilä *et al.*, 2007), forest productivity (e.g. Peng *et al.*, 2002) and properties of wood fuel (e.g. Alakangas, 2005), whereas the indirect emissions have received little attention. Lattimore *et al.* (2009) dealt with the indirect emissions to some extent in their recent review. They concluded that, in order to be sustainable, bioenergy production from forest residues must not have adverse effects on soil quality, hydrology and water quality, site productivity, or forest biodiversity but also not on greenhouse gas balances.

The indirect emissions from removing forest harvest residues, and using them for energy production, result from combusting the residues and releasing CO_2 into the atmosphere soon after harvesting instead of letting them decompose slowly at the harvested site. As a consequence of such practice, the amount of carbon stored at the forest site decreases, possibly to a remarkable degree.

There are some field studies (Johnson *et al.*, 2002; Jones *et al.*, 2008) and model-based calculations (Palosuo *et al.*, 2001; Peng *et al.*, 2002; Ågren & Hyvönen, 2003; Eriksson *et al.*, 2007) regarding the effect of logging residue removal on the carbon stock of soil. Some of these studies show clearly that intensified removal of harvest residues reduces the soil carbon stock (Johnson & Curtis, 2001; Ågren & Hyvönen, 2003; Eriksson *et al.*, 2007). Palosuo *et al.* (2001) estimated that the indirect emissions from decreasing carbon stock are an order of magnitude larger than the other emissions from an energy production chain utilizing forest harvest residues. Despite the significant contribution of indirect emissions to the estimate of total emissions per unit of produced energy, Palosuo *et al.* (2001) calculate emissions of approximately $50\,kg\,CO_2\,eq.\,MWh^{-1}$, which is 80–90% less than the emissions from various fossil fuels.

The indirect emission of using logging residues for energy production depend critically on the decomposition rate of the residues if they were left at the site. Studies based on extensive sets of measurements have been published recently making it possible to estimate the decomposition rate of the harvest residues more reliably than before (e.g. Tarasov & Birdsey, 2001; Palviainen *et al.*, 2004; Mäkinen *et al.*, 2006; Vávřová *et al.*, 2009). We have used these measurements plus other measurements related to decomposition and carbon cycling in soil and developed a new soil carbon model Yasso07 (Tuomi *et al.*, 2008, 2009). The large datasets used and advanced mathematical methods applied make the Yasso07 model particularly suitable for estimating the decomposition rate of woody litter in boreal forests.

In this study, we used this model to estimate the indirect emissions from using logging residues for bioenergy production. The objectives of the current study were to (1) introduce an approach to estimate the indirect CO_2 emissions associated with bioenergy production from forest harvest residues, (2) estimate these emissions in a forested boreal landscape during the first 100 years after starting to produce bioenergy from harvest residues, and (3) compare the total CO_2 emissions per unit of bioenergy produced to the emissions caused by using other fuels.

Materials and methods

Modelling decomposition of forest harvest residues

To estimate the indirect CO_2 emissions from producing bioenergy from forest harvest residues in boreal conditions, we simulated the decomposition of logging residues using a user-interface of the dynamic soil carbon

model Yasso07 (Tuomi *et al.*, 2008, 2009, http://www.environment.fi/syke/yasso). The measurements of the decomposition of woody litter used to develop the model were taken in Finland and neighboring regions in Estonia and Russia (M. Tuomi, R. Laiho, A. Repo & J. Liski, unpublished results). These measurements used represent the majority of data on woody litter decomposition in this region. The data sets includes branches and stems ranging from 0.5 to 60 cm in diameter, and the mass loss of these woody biomass components has been followed for 1–70 years since the start of decomposition. In addition to these data, the Yasso07 model is based on an extensive data set on decomposition of nonwoody litter across Europe and North and Central America (Tuomi *et al.*, 2009) plus data sets on the accumulation and stock of soil organic carbon (Liski & Westman, 1995, 1997; Liski *et al.*, 1998). These additional measurements specially provide information on the cycling of recalcitrant organic carbon compounds in soil that are relevant for the long-term carbon balance of decomposing woody litter.

The parameter values of Yasso07 have been sampled using a Markov chain Monte Carlo method (Tuomi *et al.*, 2009). This method has been used to make sure that, first, the model is not over-parameterized given the data and, second, there are unequivocal maximum likelihood values for each parameter combination. This mathematical approach and the data available in the development process of Yasso07 make this model suitable for this study because the uncertainty estimates of the model predictions are available and because the data covers the simulated scenarios well without extrapolation.

Model simulations

Using Yasso07, we simulated the decomposition of harvest residues at a typical site of harvest residue removal in Finland, namely an even-aged mature 81–100-year-old Norway spruce (*Picea abies* L.) forest stand located in the Pirkanmaa region of Southern Finland. Spruce stands cover some 40% of forest area in this region (Korhonen *et al.*, 2000). Clear-cut spruce stands are favorable targets of harvest residue removals because there are more logging residues than in clear-cut Scots pine stands, which are also common in the region. Spruce stumps are also preferred over pine stumps because they are easier to extract from the soil because of a shallower root structure (Alakangas, 2005; Wihersaari, 2005).

To illustrate differences in decomposition rate between different harvest residues, we simulated decomposition of spruce branches varying from 1 to 5 cm in diameter and stumps varying from 10 to 35 cm in diameter for a 100-year period after the start of decomposition. The mean diameters of spruce branches and stems in the study region, 2 and 26 cm, respectively (Korhonen *et al.*, 2000; Kantola *et al.*, 2007), were chosen for more detailed analyses of the indirect emissions caused by using the logging residues for bioenergy production. The other input variables of the Yasso07 model used in the simulations are shown in Table 1. When estimating the indirect emissions we assumed that needles were left at the site and only branches or stumps were removed. We assumed also that there was little or no delay in combusting the harvest residues at a power plant and thus CO_2 was released to the atmosphere at once.

Energy production estimation

The indirect CO_2 emissions from using the harvest residues for bioenergy production were taken to be equal to amount of carbon remaining in the harvest residues if the residues were left to decompose at the site harvested. These emissions were also related to the amount of bioenergy produced. The cumulative indirect emissions caused by combusting the harvest residues until year i were calculated by summing up the amounts of carbon left in the harvest residues until this year (i) and relating these emissions to the cumulative amount of bioenergy produced. In other words, we

Table 1 The values of input variables used in the Yasso07 model

Climate variables	
Mean annual temperature	3.2 °C
Temperature amplitude	11.6 °C
Precipitation	681 mm
Chemical composition of woody litter	**Branch ± SD/stump ± SD (%)**
Acid hydrolysable compounds	59 ± 4.3/70 ± 5.0
Water soluble compounds	1 ± 0.3/1 ± 0.2
Ethanol soluble compounds	1 ± 0.3/1 ± 0.2
Klason lignin (neither hydrolysable nor soluble compounds)	37 ± 1.0/28 ± 0.8

The climate values represent averages for southern Finland between 1971 and 2000 (Drebs *et al.*, 2002) and the chemical composition averages of several individual studies (Hakkila, 1989). The standard deviation (SD) values of the chemical composition are based on coefficients of variation calculated from a data base of foliage litter (Berg *et al.*, 1991). The temperature amplitude means a half of the difference between the mean temperatures of the warmest and the coldest month of the year.

© 2010 Blackwell Publishing Ltd,

simulated a case where the practice of removing the harvest residues and using them for bioenergy production was started and continued on a harvest area of similar size year after year. We applied biomass-compartment-specific net calorific heating values to estimate the amount of energy obtained by combusting the harvest residues, i.e. 19.30 MJ kg^{-1} for dry Norway spruce branches and 19.18 MJ kg^{-1} for dry stumps (Nurmi, 1997). These values of dry logging residues range commonly from 18 to 20 MJ kg^{-1} (Alakangas, 2005). The carbon content of the harvest residues was assumed to be equal to 50% of dry wood (m/m).

In order to estimate the full fuel cycle emissions from using the logging residues for energy production, we added other emissions from a typical wood chip fuel production chain using harvest residues to the calculated indirect emissions. These emissions result from (1) collecting, chipping, and transporting the harvest residues, (2) emitting methane (CH_4) and nitrous oxide (N_2O) from combustion, (3) fertilizing the forest to compensate for nutrient loss, and (4) recycling ash, and they range typically from 5 to 18 kg CO_2 eq. MWh^{-1} produced (Palosuo *et al.*, 2001; Wihersaari, 2005). We used a central value of this range, 12 kg CO_2 eq. MWh^{-1} produced, in our calculations. Other estimates for direct emissions from wood fuel chain range from 5 to 20 kg CO_2 eq. MWh^{-1} (Korpilahti, 1998; Mälkki & Virtanen, 2003; Berg, 2010) depending on background information and included operations in the estimates. Fossil fuel comparison values 280, 306, and 395 kg CO_2 eq. MWh^{-1} were estimates of entire fuel cycle emissions of natural gas, oil, and diesel, and coal (Statistics Finland, 2006; Ecoinvent Centre, 2007).

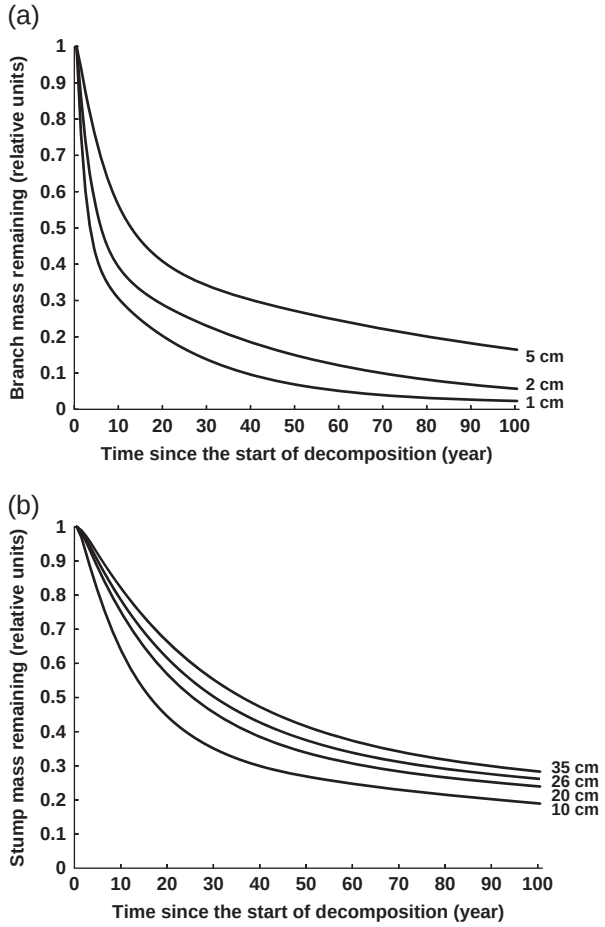

Fig. 1 Mass remaining of decomposing Norway spruce branches (diameter 1–5 cm) and stumps (diameter 10–35 cm) over a 100-year period after the start of decomposition in southern boreal conditions as simulated using the Yasso07 model (model input values in Table 1).

Results

Branches lost mass at a remarkably higher rate than stumps because the simulated decomposition rate of woody litter was dependent on the initial diameter (Fig. 1). For example, after 10 years of decomposition, the branches 1–5 cm in diameter had 30–55% of the initial mass still remaining (Fig. 1a) while stumps 10–35 cm in diameter had 63–81% (Fig. 1b). The simulated rate of mass loss decreased over time, and after 100 years of decomposition there was still 2–16% of the initial branch mass remaining and 19–28% of the initial stump mass remaining.

The indirect CO_2 emissions, caused by combusting logging residues after harvesting instead of letting them decompose at the harvested site, were equal to the CO_2 emissions from combustion, 340 kg CO_2 MWh^{-1}, when the practice was started but these emissions decreased over time as a result of decomposition of the harvest residues (Fig. 2). The indirect emissions of using branches for bioenergy decreased faster than the emissions of using stumps because the branches decomposed faster (Figs 1 and 2). After the first 10 years of conducting this practice, the indirect emissions from branches were equal to 200 kg CO_2 MWh^{-1} and those from stumps 310 kg CO_2 MWh^{-1} (Fig. 2). After the first 100 years, these emissions from the branches and stumps were equal to 70 and 160 kg CO_2 MWh^{-1}, respectively.

The estimated greenhouse gas emissions from the rest of the bioenergy production chain, i.e. the emissions from collecting, transporting, chipping, and combusting the harvest residues plus the emissions from fertilizing the forest and recycling the ash, were equal to 12 kg CO_2 eq. MWh^{-1} (Fig. 3). At the time of starting this practice, these direct emissions represented only 3% of the total emissions caused by using the harvest residues

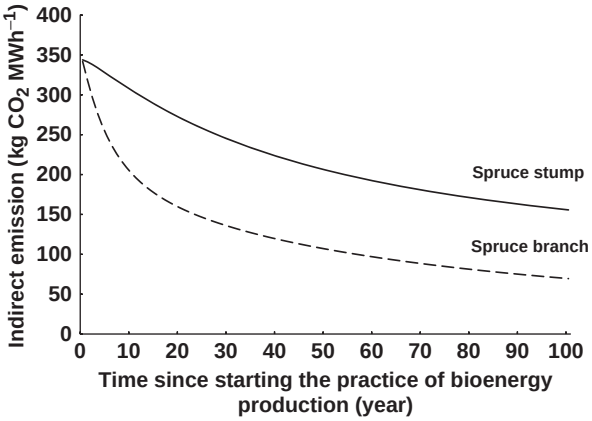

Fig. 2 Indirect CO_2 emission per unit of energy produced from using Norway spruce stumps (diameter 26 cm) or branches (diameter 2 cm) for bioenergy over a 100-year period after starting this practice. This indirect emission is equal to the carbon stock of woody litter lost in combustion per energy obtained until each year.

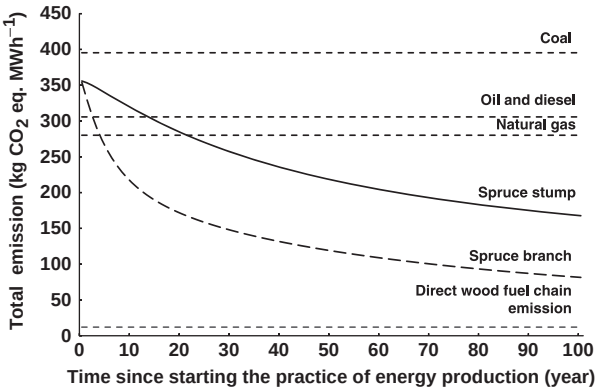

Fig. 3 The total greenhouse gas emission per unit of energy produced from using Norway spruce branches (diameter 2 cm) or stumps (diameter 26 cm) for bioenergy over a 100-year period after starting this practice and the total emissions from various fossil fuels. The emission estimates of bioenergy production include both an indirect (see Fig. 2) emission resulting from decreasing carbon stock and a direct wood fuel chain emission (equal to 12 kg CO_2 eq. MW h^{-1}) resulting from collecting, chipping and transporting the harvest residues, CH_4 and N_2O emissions from combusting the residues, fertilizing the forest to compensate for nutrient loss, and recycling of ash. The estimates of the fossil fuels represent entire fuel cycle emissions (Statistics Finland, 2006; Ecoinvent Centre, 2007).

for bioenergy. After the 100-year period of conducting this practice, this share increased to 15% if bioenergy was produced from branches and to 7% if bioenergy was produced from stumps (Fig. 3). The increased contribution of the direct emissions was a result of the decreased indirect emissions (Fig. 2).

At the time of starting to use the harvest residues for energy production, the total emissions were comparable to the emissions caused by using fossil fuels (Fig. 3). After 10 years of producing bioenergy from branches, the total emissions caused were 210 kg CO_2 eq. MWh^{-1}. These emissions are 24%, 30%, or 46% lower than the emissions caused by producing the energy from natural gas, oil, or coal, respectively. If bioenergy was produced from stumps, it took 22 years for the average emissions to decrease below the emissions of producing the energy from natural gas or 14 years for the emissions to decrease below the emissions of oil. After 100 years of producing energy by combusting branches, the emissions were lower by 71%, 74%, or 79% than the emissions caused by producing the energy from natural gas, oil, or coal, respectively. For bioenergy produced by combusting stumps, these percentages of emission reductions were 40%, 46%, or 58%, over 100 years, compared with the emissions of natural gas, oil, or coal, respectively.

Discussion

Using logging residues for energy production decreases the amount of carbon stored in forest and causes thus indirect CO_2 emissions into the atmosphere. These indirect emissions occur because combustion releases carbon of logging residues to the atmosphere at once, otherwise the residues would form a slowly decomposing carbon stock at the harvest site. The indirect emissions are an order of magnitude larger than the direct emissions from the rest of this bioenergy production chain (Fig. 3), not accounting for the CO_2 emissions of combusting the harvest residues. The indirect emissions depend on the decomposition rate of the harvest residues, with the decomposition rate being lower with an increasing size of woody litter (Fig. 1, Harmon *et al.*, 1986; Janisch *et al.*, 2009; M. Tuomi, R. Laiho, A. Repo & J. Liski, unpublished results). The use of bigger-sized stumps for energy production causes therefore larger indirect emissions than the use of smaller-sized branches (Fig. 2). The average indirect emissions per unit of energy produced decrease over time since the start of this form of bioenergy production (Fig. 2) but during the first few years, or a couple of decades in the case of stumps, the total emissions caused by energy production from harvest residues are comparable to the emissions of fossil fuels (Fig. 3).

The reliability of the current results depends critically on the decomposition estimates of the harvest residues. The Yasso07 decomposition and soil carbon model used in this study is based on a large collection of mass loss measurements taken on woody litter in boreal forests across Finland and neighboring countries plus large

sets of other relevant measurements from across the world (see 'Materials and methods'). This model has been shown to give unbiased estimates for the decomposition of woody (M. Tuomi, R. Laiho, A. Repo & J. Liski, unpublished results) and nonwoody litter (Tuomi *et al.*, 2009). Compared with other studies on the decomposition of woody litter carried out under comparable conditions, the estimates of this study are similar except for the end of the 100-year study period; for this late phase of decomposition, the current estimates of mass remaining are higher. Mäkinen *et al.* (2006) estimated that Norway spruce stems lost about 20% of their initial mass during the first 10 years of decomposition and the stems disappeared completely in some 60–80 years of time. On the other hand, according to the residuals reported by Mäkinen *et al.* (2006), their model seems to underestimate the mass remaining after 30 years of decomposition. Melin *et al.* (2009) compared several decomposition models developed for Norway spruce logs, snags, and stumps. They concluded that after 10 years of decomposition some 60–75% of the initial mass was still remaining whereas after 100 years of decomposition practically none or $<10\%$ of the initial mass was still left. Our higher estimates of mass remaining during the late phases of decomposition can be explained by a difference between the methods used. The two earlier studies were based on measurements of woody litter mass remaining. These measurements may not capture the formation and translocation of well-decayed soil organic matter originating from woody litter. The Yasso07 model, on the other hand, is additionally based on measurements of formation of soil organic matter (Tuomi *et al.*, 2009). For this reason, we think that the estimates of Yasso07 model are probably more realistic for the late phases of woody litter decomposition.

In addition to the decomposition estimates, the reliability of the current results depends also on the other parameters of our calculations such as the reference energy systems or combustion techniques chosen as well as variation in the chemical composition of litter (affecting the decomposition rate estimates of the harvest residues) and calorific values. Furthermore, the simulations were done for climate conditions prevailing in Southern Finland today. The results do not thus account for the effects of climate change or those of increased atmospheric CO_2 concentration on forest growth. In addition, forest soil disruption associated with stump removal may release additional CO_2 into the atmosphere. Currently, empirical research on the magnitude of these emissions is few in number (Jandl *et al.*, 2007; Walmsley & Godbold, 2010). Hope (2007) found that stump removal together with forest floor scarification reduced soil carbon stocks in the first year of stump harvesting and 9 years later. This conclusion is apparent only if during stump removal the forest soil is completely scarified by removal or mixing with mineral soil. Although the quantitative data on stump extraction and emissions associated with this practice is scarce, generally it is known that soil disturbance can change the microclimate and stimulate the decomposition of litter (Johansson, 1994). In a Finnish study site preparation after a clear-cut with mixing organic matter with mineral soil increased CO_2 efflux from soil but this effect leveled off rapidly (Pumpanen *et al.*, 2004). Despite of these uncertainties, we think that the current estimates are reliable enough to demonstrate the magnitude of indirect emissions associated with producing bioenergy from harvest residues in boreal coniferous forest.

The indirect emissions, caused by the reduced carbon stock of decomposing harvest residues, represented 85–97% of the total emissions of this bioenergy production chain, not accounting for the CO_2 emissions from combusting the harvest residues. These emissions are thus highly significant for the full fuel cycle emissions of logging residues. When comparing the present results to earlier ones it is important to acknowledge differences in system boundaries, energy use-technology, reference energy system, conversion technology and type and management of raw material (Cherubini *et al.*, 2009). Still, it is possible to conclude that a common outcome of the earlier studies is that the greenhouse gas emissions from logging, collecting, chipping, and transporting harvest residues are relatively low (Börjesson, 1996; Palosuo *et al.*, 2001; Mälkki & Virtanen, 2003; Wihersaari, 2005). These estimates have ranged from 4 to $20\,kg\,CO_2\,MWh^{-1}$ depending on the details of the bioenergy production chains studied. The current study shows that if indirect CO_2 emissions are accounted for, the total CO_2 emissions are at least an order of magnitude higher than these emissions which have been considered to represent the total emissions (cf. Mälkki & Virtanen, 2003).

The decreasing effect of logging residue removal on soil carbon stock has been demonstrated earlier but this has not been considered to be problematic as long as this removal practice does not jeopardize the carbon sink of soil (Börjesson, 2000; Ågren & Hyvönen, 2003; Mälkki & Virtanen, 2003; Petersen Raymer, 2006; Eriksson *et al.*, 2007; Sievänen *et al.*, 2007; Eriksson & Gustavsson, 2008). Sievänen *et al.* (2007) calculated that increasing the removals of logging residues from 4 to $15\,Mm^3\,yr^{-1}$ in Finland will not turn the Finnish forests from net carbon sinks to net sources. However, the intensified removals of the logging residues would decrease the annual carbon sink of these forest soils by 3.1 million tons of CO_2 eq. (Sievänen *et al.*, 2007). Assuming that $1\,m^3$ of harvest residues gives 2 MWh of

energy (Alakangas, 2005), the indirect emission from the decreasing carbon stock of soil is equal to about 100 kg CO_2 eq. MWh^{-1}. This estimate is somewhat lower than the estimates of the present study because Sievänen *et al*. (2007) applied an earlier version of Yasso soil carbon and decomposition model in their study (Liski *et al*., 2005). This earlier model version gave less reliable, higher estimates for the decomposition rate of woody litter because it was based on a substantially smaller number of measurements. Nevertheless, these figures demonstrate that it is important to relate the indirect and direct emissions of bioenergy production to the amount of energy obtained in order to get a correct picture on the efficiency of using different energy sources in decreasing greenhouse gas emissions to the atmosphere. The current results demonstrate that if the indirect CO_2 emissions are counted in, the total fuel chain emissions from using spruce branches or stumps for energy production may cause even bigger CO_2 emissions during the first years or decades of starting this practice than producing energy from oil or natural gas.

The indirect greenhouse gas emissions resulting from using logging residue for bioenergy production are highest per unit of energy produced immediately when the practice is started. The average emissions per energy unit decrease, however, over time. As a result of this temporal pattern, this form of bioenergy production is not efficient in decreasing emissions to the atmosphere in the near future. Our results stress the importance of considering time perspective when assessing the potential of different bioenergy options to mitigate climate change (Schlamadinger & Marland, 1996; Petersen Raymer, 2006). The issue of which temporal approach is appropriate depends on the management and policy strategies and whether the selection of energy systems is made to meet long-term or short-term greenhouse gas reduction objectives (Schlamadinger *et al*., 1997).

It is possible to reduce the indirect emissions of logging residue removals by collecting quickly decomposing harvest residues for bioenergy production, for example branches instead of stumps. However, it may be still tempting to extract stumps from harvest sites because the gain of primary energy per hectare may be twice that compared with collecting branches (Eriksson & Gustavsson, 2008). Leaving the needles at the harvest site, which helps to avoid nutrient loss, has a marginal effect on the carbon balance at clear-cut sites, although needle and fine root litter produce more than two-thirds of the soil carbon stock in growing forests (Ågren & Hyvönen, 2003).

The indirect emissions have a remarkable effect on the total greenhouse gas emissions from some systems of bioenergy production, as demonstrated in this study for harvest residues of boreal forests, and emphasized for several other systems by Johnson (2009) and Searchinger *et al*. (2009). For this reason, to account for the actual greenhouse gas effect of various alternative bioenergy options, it would be essential to include the indirect emissions adequately in guidelines of greenhouse gas inventorying and reporting. Currently, the rules of carbon accounting applied under the Kyoto Protocol do not count all indirect emissions, which among other things distorts the accounting of net emissions (Johnson, 2009; Searchinger *et al*., 2009). A particular shortcoming of the accounting rules under the Kyoto Protocol is that a party to this protocol may choose not to account for changes in one or several of the agreed carbon pools (aboveground biomass, belowground biomass, litter, dead wood, and soil organic carbon) as long as it can reliably show that the pool is not decreasing. Owing to this threshold, some of the indirect emissions caused by using logging residues for bioenergy production may be excluded from the inventory figures. On the other hand, in inventory reports of greenhouse gases under the United Nations Framework Convention on Climate Change, the carbon release resulting from forest harvesting must be counted and reported as a land-use emission or as a energy emission but not both (IPCC, 2000). Today, the land-use-related greenhouse gas emissions from bioenergy production systems are recognized and investigated (IPCC, 2000; Melillo *et al*., 2009) but one of the practical problems is that measuring methods for the indirect effects and feasible means to bring these impacts to regulatory policies are still lacking (Mathews & Tan, 2009).

Conclusions

Using logging residues as a source of bioenergy causes net CO_2 emissions into the atmosphere and a great majority (85–97%) of these emissions are indirect emissions resulting from a decline in the carbon stock of harvest residues in forest. The amount of the indirect emissions increases with a decreasing decomposition rate of the harvest residues. Norway spruce stumps decay at slower rate than branches and consequently the energy use of the stumps causes 1.5–2 times larger indirect emissions than the use of branches. Production of bioenergy from forest harvest residues causes emissions that are comparable to the emissions of fossil fuel over the first few years (branches) or first few decades (stumps) of the practice. After 50 years, bioenergy produced of Norway spruce stumps decreases average emissions per unit of energy produced by some 20% and bioenergy from branches by some 60% compared with entire fuel cycle emissions of natural gas.

© 2010 Blackwell Publishing Ltd,

Acknowledgements

This study was partially funded by the European Commisson through research project 'Greenhouse gas management in European land use systems' (grant agreement no. 244122). We thank two anonymous reviewers for their comments and suggestions.

References

Ågren G, Hyvönen R (2003) Changes in carbon stores in Swedish forest soils due to increased biomass harvest and increased temperatures analysed with a semi-empirical model. *Forest Ecology and Management*, **174**, 25–37.

Alakangas E (2005) *Properties of wood fuels used in Finland*. VTT Processes, Project report PRO2/P2030/05 (Project C5SU00800), Technical Research Centre of Finland, Jyväskylä.

Berg B, Booltink H, Breymeyer A *et al*. (1991) *Data on needle litter decomposition and soil climate as well as site characteristics for some coniferous forest sites. Part 2. Decomposition data*. Swedish University of Agricultural Sciences Report, Uppsala, Sweden, **42**.

Berg S (2010) *Calculation of the contribution to GWP from the production of some Swedish forest based fuels chains – according to RES directive*. 20 January 2010, Skogforsk – Forest Research Institute of Sweden, 11 pp.

Börjesson P (1996) Emissions of CO_2 from biomass production and transportation in agriculture and forestry. *Energy Conversion and Management*, **37**, 1235–1240.

Börjesson P (2000) Economic valuation of the environmental impact of logging residue recovery and nutrient compensation. *Biomass and Bioenergy*, **19**, 137–152.

Cherubini F, Bird N, Cowie A, Jungmeier G, Schlamadinger B, Woess-Gallasch S (2009) Energy- and greenhouse gas-based LCA of biofuel and bioenergy systems: key issues, ranges and recommendations. *Resources, Conservation and Recycling*, **53**, 434–447.

Drebs A, Nordlund A, Karlsson P, Helminen J, Rissanen P (2002) *Climatic statistics of Finland No. 2002:1*, Finnish Meteorological Institute, Helsinki, 99 pp.

Directive 2009/28/EC of the European Parliament and of the Council of 23 April 2009 on the promotion of the use of energy from renewable sources. *Official Journal of the European Union*, L 140/16.

Ecoinvent Centre (2007) *Ecoinvent Data v2.0*. Swiss Centre for Life Cycle Inventories, Switzerland.

Eriksson E, Gillespie A, Gustavsson L, Langvall O, Olsson M, Sathre R, Stendahl J (2007) Integrated carbon analysis of forest management practices and wood substitution. *Canadian Journal of Forest Research-Revue Canadienne De Recherche Forestiere*, **37**, 671–681.

Eriksson L, Gustavsson L (2008) Biofuels from stumps and small roundwood – costs and CO_2 benefits. *Biomass and Bioenergy*, **32**, 897–902.

Fargione J, Hill J, Tilman D, Polasky S, Hawthorne P (2008) Land clearing and the biofuel carbon debt. *Science*, **319**, 1235–1238.

Hakkila P (1989) *Utilization of Residual Forest Biomass*. Springer-Verlag, Berlin.

Harmon M, Franklin J, Swanson F *et al*. (1986) Ecology of coarse woody debris in temperate ecosystems. *Advances in Ecological Research*, **15**, 133–302.

Heikkilä J, Sirén M, Äijälä O (2007) Management alternatives of energy wood thinning stands. *Biomass and Bioenergy*, **31**, 255–266.

Hope G (2007) Changes in soil properties, tree growth, and nutrition over a period of 10 years after stump removal and scarification on moderately coarse soils in interior British Columbia. *Forest Ecology and Management*, **242**, 625–635.

IPCC (2000) *Land Use, Land-Use Change and Forestry*. Cambridge University Press, Cambridge.

Jandl R, Lindner M, Vesterdal L *et al*. (2007) How strongly can forest management influence soil carbon sequestration? *Geoderma*, **137**, 253–268.

Janisch J, Harmon M, Chen H, Fasth B, Sexton J (2009) Decomposition of coarse woody debris originating by clearcutting of an old-growth conifer forest. *Ecoscience*, **12**, 151–160.

Johansson M-B (1994) The influence of soil scarification on the turn-over rate of slash needles and nutrient release. *Scandinavian Journal of Forest Research*, **9**, 170–179.

Johnson D, Curtis P (2001) Effects of forest management on soil C and N storage: meta analysis. *Forest Ecology and Management*, **140**, 227–238.

Johnson D, Knoepp J, Swank W, Shan J, Morris L, Van Lear D, Kapeluck P (2002) Effects of forest management on soil carbon: results of some long-term resampling studies. *Environmental Pollution*, **116**, 201–S208.

Johnson E (2009) Goodbye to carbon neutral: getting biomass footprints right. *Environmental Impact Assessment Review*, **29**, 165–168.

Jones H, Garrett L, Beets P, Kimberley M, Oliver G (2008) Impacts of harvest residue management on soil carbon stocks in a plantation forest. *Soil Science Society of America Journal*, **72**, 1621–1627.

Kantola A, Mäkinen H, Mäkelä A (2007) Stem form and branchiness of Norway spruce as a sawn timber – predicted by a process based model. *Forest Ecology and Management*, **241**, 209–222.

Korhonen K, Tomppo E, Henttonen H, Ihalainen A, Tonteri T, Tuomainen T (2000) Forest resources 1965–99 and logging possibilities 1999–2028 in Pirkanmaa region. (In Finnish: Pirkanmaan metsävarat 1965–99 hakkuumahdollisuudet 1999–2028). Metsäntutkimuslaitos. Suomen Metsätieteellinen Seura. *Metsätieteen aikakausikirja*, **4B**, 661–739.

Korpilahti A (1998) Finnish forest energy systems and CO_2 consequences. *Biomass and Bioenergy*, **15**, 293–297.

Lattimore B, Smith C, Titus B, Stupak I, Egnell G (2009) Environmental factors in woodfuel production: opportunities, risks, and criteria and indicators for sustainable practices. *Biomass and Bioenergy*, **33**, 1321–1342.

Liski J, Ilvesniemi H, Mäkelä A, Starr M (1998) Model analysis of the effects of soil age, fires and harvesting on the carbon storage of boreal forest soils. *European Journal of Soil Science*, **49**, 407–416.

Liski J, Palosuo T, Peltoniemi M, Sievänen R (2005) Carbon and decomposition model Yasso for forest soils. *Ecological Modelling*, **189**, 168–182.

Liski J, Westman C (1995) Density of organic-carbon in soil at coniferous forest sites in southern finland. *Biogeochemistry*, **29**, 183–197.

Liski J, Westman C (1997) Carbon storage in forest soil of Finland. 2. Size and regional patterns. *Biogeochemistry*, **36**, 261–274.

Luiro J, Kukkola M, Saarsalmi A, Tamminen P, Helmisaari HS (2009) Logging residue removal after thinning in boreal forests: long-term impact on the nutrient status of Norway spruce and Scots pine needles. *Tree Physiology*, **30**, 78–88.

Mäkinen H, Hynynen J, Siitonen J, Sievänen R (2006) Predicting the decomposition of Scots Pine, Norway spruce, and Birch stems in Finland. *Ecological Applications*, **16**, 1865–1879.

Mälkki H, Virtanen Y (2003) Selected emissions and efficiencies of energy systems based on logging and sawmill residues. *Biomass and Bioenergy*, **24**, 321–327.

Mathews J, Tan H (2009) Biofuels and indirect land use change effects: the debate continues. *Biofuels Bioproducts & Biorefining-Biofpr*, **3**, 305–317.

Melillo J, Reilly J, Kicklighter D *et al*. (2009) Indirect emissions from biofuels: how important? *Science*, **326**, 1397–1399.

Melin Y, Petersson H, Nordfjell T (2009) Decomposition of stump and root systems of Norway spruce in Sweden – A modelling approach. *Forest Ecology and Management*, **257**, 1445–1451.

Ministry of Employment and the Economy of Finland (2008) *National long-term climate and energy strategy of Finland*. Government Report to Parliament, November 6, 2008 (in Finnish).

Nurmi J (1997) Heating values of mature trees. *Acta Forestalia Fennica*, **256**, 28 pp.

Palosuo T, Wihersaari M, Liski J (2001) *Net greenhouse gas emissions due to energy use of forest residues – impact of soil carbon balance*. EFI Proceedings no 39, Wood biomass as an energy source challenge in Europe. European Forest Institute, Joensuu, pp. 115–130.

Palviainen M, Finér L, Kurka A-M, Mannerkoski S, Piirainen S, Starr M (2004) Decomposition and nutrient release from logging residues after clear-cutting of mixed boreal forest. *Plant and Soil*, **263**, 53–67.

Peng C, Jiang H, Apps M, Zhang Y (2002) Effects of harvesting regimes on carbon and nitrogen dynamics of boreal forests in central Canada: a process model simulation. *Ecological Modelling*, **155**, 177–189.

Petersen Raymer A (2006) A comparison of avoided greenhouse gas emissions when using different kinds of wood energy. *Biomass and Bioenergy*, **30**, 605–617.

Pumpanen J, Westman CJ, Ilvesniemi H (2004) Soil CO_2 efflux from a podzolic forest soil before and after forest clear-cutting and site preparation. *Boreal Environment Research*, **9**, 199–212.

Schlamadinger B, Apps M, Bohlin F *et al*. (1997) Towards a standard methodology for greenhouse gas balances of bioenergy systems in comparison with fossil energy systems. *Biomass and Bioenergy*, **13**, 359–375.

Schlamadinger B, Marland G (1996) Full fuel cycle carbon balances of bioenergy and forestry options. *Energy Conversion and Management*, **37**, 813–818.

Searchinger T, Hamburg S, Melillo J *et al*. (2009) Fixing a critical climate accounting error. *Science*, **326**, 527–528.

Searchinger T, Heimlich R, Houghton R *et al*. (2008) Use of US croplands for biofuels increases greenhouse gases through emissions from land-use change. *Science*, **319**, 1238–1240.

Sievänen R, Kareinen T, Hirvelä H, Ilvesniemi H (2007) Hakkuumahdollisuusarvioihin perustuvat metsien kasvihuonekaasutaseet (In Finnish). *Metsätieteen aikakausikirja*, **4/2007**, 329–339.

Statistics Finland (2006) *Fuel Classification 2006*. Statistics Finland, Finland.

Stupak I, Asikainen A, Jonsell M *et al*. (2007) Sustainable utilisation of forest biomass for energy-possibilities and problems: policy, legislation, certification, and recommendations and guidelines in the Nordic, Baltic, and other European countries. *Biomass & Bioenergy*, **31**, 666–684.

Tarasov M, Birdsey R (2001) Decay rate and potential storage of coarse woody debris in the Leningrad Region. *Ecological Bulletin*, **49**, 137–147.

Tuomi M, Thum T, Järvinen H *et al*. (2009) Leaf litter decomposition – estimates of global variability based on Yasso07 model. *Ecological Modelling*, **220**, 3362–3371.

Tuomi M, Vanhala P, Karhu K, Fritze H, Liski J (2008) Heterotrophic soil respiration – comparison of different models describing its temperature dependence. *Ecological Modelling*, **211**, 182–190.

Vávřová P, Penttilä T, Laiho R (2009) Decomposition of Scots pine fine woody debris in boreal conditions: implications for estimating carbon pools and fluxes. *Forest Ecology and Management*, **257**, 401–412.

Wall A (2008) Effect of removal of logging residue on nutrient leaching and nutrient pools in the soil after clearcutting in a Norway spruce stand. *Forest Ecology and Management*, **256**, 1372–1383.

Walmsley JD, Godbold DL (2010) Stump harvesting for bioenergy – a review of the environmental impacts. *Forestry*, **83**, 17–38.

Wihersaari M (2005) Greenhouse gas emissions from final harvest fuel chip production in Finland. *Biomass and Bioenergy*, **28**, 435–443.

per Kelvin of globally averaged surface warming[9]. These values for sea-level rise do not include any contributions from land ice melting, which could make the estimates even higher.

These published results have not been highlighted because of scepticism regarding the ability of early models to realistically simulate deep-ocean mixing, and the intuition of some experts that as long as land ice exists, cold water would be available to keep the deep ocean cold. In the past few years, present-day state-of-the-art climate models have revisited the early results and have found similar responses, confirming many of these results[1,10].

In their paper, Li *et al.*[1] show the various physical response timescales found in the atmosphere–ocean–land–sea-ice system (Fig. 1). As the atmosphere and upper ocean are tightly coupled, the surface air temperature and the near surface ocean temperatures have a very similar response timescale. In the deeper ocean layers, the response timescale lengthens, with the longest response timescales found near the ocean bottom. Again, broadly confirming earlier results, Li and colleagues find that the ocean warms quasi-uniformly at depth on a millennial timescale, and that the long-term warming is a substantial fraction of the equilibrium surface air temperature warming.

The large warming throughout the world ocean leads to a large sea-level rise. In the Li *et al.* model, for a fourfold increase in carbon dioxide concentration, the globally averaged surface air temperature increase is 10.8 Kelvin above pre-industrial temperatures, and the globally averaged sea-level rise due to warming water alone is 5.8 metres. The ratio of the surface warming to sea-level rise falls within the range given in the 2007 Intergovernmental Panel on Climate Change report[9], noted above.

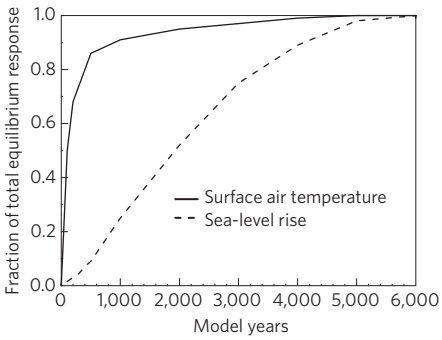

Figure 1 | The response of globally averaged surface air temperature and sea-level rise to an increase of carbon dioxide concentration in the model atmosphere. Li *et al.*[1] modelled carbon dioxide concentrations as increasing at a rate of 1% per year until it reached four times the pre-industrial value and then held it constant. To illustrate the impact of the slow penetration of heat into the ocean on the sea-level response, the fraction of the total equilibrium response is plotted. The timescale of the sea-level response is much slower than that of surface air temperature. Data taken from ref. 1.

Owing to the well-documented uncertainties in the equilibrium climate sensitivity and continuing technical issues with the models used for these studies, readers should take the precise long-term results found in this or any model study cautiously. What matters is that for any equilibrium climate change within the assessed Intergovernmental Panel on Climate Change temperature range of 2.0–4.5 Kelvin for a doubling of carbon dioxide, the equilibrium sea-level rise is quite large — 0.4–2.7 metres (ref. 9). Furthermore, most future projections of carbon dioxide have values that are more than double, which could result in greater sea-level rise. The magnitude of equilibrium sea-level rise from climate sensitivity alone is much larger than that observed over the past century, and larger than many of the projected changes for this century[9]. Again, this emphasizes the slow response of the deep oceanic layers and sea-level rise to forcing changes.

The recent work by Li and colleagues uses a present-day model to confirm earlier results that have so far been de-emphasized. As more climate models obtain similar results, climate modellers will have greater confidence in the long-term projections of deep-ocean warming and sea-level rise.

An important caveat to this discussion is that it is very difficult to predict what technological advances and mitigation strategies will be available in the next 100, 500 or 1,000 years to possibly remove significant amounts of carbon dioxide from the atmosphere. Until such options are available and while there are still significant technical issues surrounding long-term projections from models, it is clear that the decisions we make today, individually and as a society, will impact our planet for a long time. ❐

Ronald J. Stouffer is at the Geophysical Fluid Dynamics Laboratory, National Oceanic and Atmospheric Administration, Princeton, New Jersey 08542, USA.
e-mail: ronald.stouffer@noaa.gov

References

1. Li, C., von Stoch, J-S. & Marotzke, J. *Clim. Dynam.* http://dx.doi.org/10.1007/s00382-012-1350-z (2012).
2. Solomon, S., Plattner, G-K., Knutti, R. & Friedlingstein, P. *Proc. Natl Acad. Sci. USA* **106,** 1704–1709 (2009).
3. Munk, W. H. *Deep-Sea Res.* **13,** 707–730 (1966).
4. Stouffer, R. J. *J. Clim.* **17,** 209–217 (2004).
5. Stouffer, R. J. & Manabe, S. *J. Clim* **12,** 2224–2237 (1999).
6. Stouffer, R. J. & Manabe, S. *Clim. Dynam.* **20,** 759–773 (2003).
7. Voss, R. & Mikolajewicz, U. *Clim. Dynam.* **17,** 45–60 (2001).
8. Gregory, J. M. *et al. Geophys. Res. Lett.* **31,** L03205 (2004).
9. Meehl, G. *et al.* in IPCC *Climate Change 2007: The Physical Science Basis* (eds Solomon, S. *et al.*) 747–845 (Cambridge Univ. Press, 2007).
10. Danabasoglu, G. & Gent, P. R. *J. Clim.* **22,** 2494–2499 (2009).

ENERGY

Analysing fossil-fuel displacement

It is commonly assumed that fossil fuels can be replaced by alternative forms of energy. Now research challenges this assumption, and highlights the role of non-technological solutions to reduce fossil-fuel consumption.

Andrew K. Jorgenson

Much attention is given by both experts and policymakers to the role of non-fossil-fuel energy in the fight against greenhouse-gas emissions. Scientific bodies, including the Intergovernmental Panel on Climate Change[1], as well as non-governmental organizations and sections of the general public, implicitly assume that each unit of alternative energy replaces a given unit of fossil-fuel energy as a form of proportional displacement. Writing in *Nature Climate Change*, Richard York[2] has tested this assumption and suggests that across most nations of the world over the past 50 years, on average, each unit of total national energy use from non-fossil-fuel sources displaced less than one quarter of a unit of fossil-fuel energy use, and the

© 2012 Macmillan Publishers Limited. All rights reserved

amount is even less when focusing on only fuel use for electricity.

Drawing from various areas of multidisciplinary research, including environmental sociology, ecological economics and structural human ecology, York[2] analyses annual data for 132 countries from 1960 to 2009 to assess the extent to which the per capita demand for fossil-fuel energy is affected by the amount of per capita energy produced from non-fossil-fuel sources, while controlling for known driving forces of per capita energy use, including levels of economic development and urbanization. In particular, York[2] estimates a model of per capita fossil-fuel electricity production (dependent variable) including, as explanatory variables, per capita production of non-fossil-fuel energy, gross domestic product (GDP) per capita (adjusted for inflation and in US dollars) and factors unique to each country that do not change through time. He then repeats the estimation exercise by adding other explanatory variables, such as measures of urbanization (percentage of the population living in urban areas), manufacturing (percentage of GDP from the manufacturing sector) and the age-dependency ratio of nations (the ratio of people under 15 and over 64 to those 15 to 64 years of age). Finally, he estimates the same two models again using per capita total energy production from fossil fuels as the dependent variable.

Turning to the results, if the assumption that alternative energy can proportionally displace fossil-fuel energy is indeed valid, one would expect to see an estimated regression coefficient (the 'displacement coefficient') of −1 for the non-fossil-fuel energy production variable, or something close to it. In the first of the per capita fossil-fuel electricity production models, the estimated displacement coefficient is −0.089, and decreases in absolute value to −0.079 in the second model that accounts for a broader range of drivers. These results suggest that each kilowatt hour of non-fossil-fuel electricity that is generated displaces at best only 0.089 kilowatt hours of fossil-fuel-generated electricity — a far cry from proportional displacement. In other words, to displace one kilowatt hour of fossil-fuel electricity requires generating at least 11.326 kilowatt hours of non-fossil-fuel electricity. In the first of the per capita fossil-fuel total energy production models, the estimated displacement coefficient is −0.128, and increases in absolute value to −0.219 in the second, more complete model. Although the results of this second model are closer to proportional displacement, they still suggest that more than 5.5 units of non-fossil-fuel energy are required to displace one unit of fossil-fuel total energy.

© ISTOCKPHOTO/DELECTUS

York's findings contradict the widely held assumption that the expansion of alternative energy production will proportionally suppress fossil-fuel energy production. And the implications are quite clear. For alternative energy sources to adequately displace fossil-fuel sources, non-fossil-fuel energy would need massive global expansions, and such increases would pose unique ecological problems and human health risks[3]. For example, hydropower disrupts aquatic ecosystems, and the recent tragedy at the Fukushima Daiichi nuclear power plant in Japan, as well as the ongoing clean-up efforts at the Hanford Site in the United States, underscore the life-threatening risks associated with nuclear power. And other alternative energy sources, such as wind power, require significant material inputs for their construction as well as large amounts of area to generate nontrivial amounts of energy.

However, all well-executed research has limitations. Some recent studies indicate that forms of economic globalization contribute to national-level fossil-fuel energy consumption and greenhouse-gas emissions[4], whereas other studies suggest that militaries are additional moderate-sized drivers of fossil-fuel energy consumption[5]. Neither economic globalization variables nor national military variables are included in York's analysis. Although such exclusion is unlikely to lessen the validity of the findings, the effects of those variables on York's estimated displacement coefficients would have made his analysis more realistic and potentially increased the overall statistical significance of the models used.

Besides contradicting the proportional displacement assumption, York's research adds to the growing body of environmental social science that highlights how societies cannot only rely on technological solutions to reduce fossil-fuel use and thus anthropogenic carbon dioxide emissions[6–8]. To effectively reduce emissions, societies need to focus on reducing the consumption of energy at both the individual/household level[9] and the system level, with strategies geared towards broader changes in the economic, political and cultural spheres[10]. More broadly, York highlights the importance of integrating research on the human dimensions of climate change — such as the role of individuals and collective human behaviour, the characteristics of social institutions and the complex interrelationships between the world's nations — with research on technological solutions to tackle greenhouse-gas emissions. ❐

Andrew K. Jorgenson is in the Department of Sociology at the University of Utah, 380 South 1530 East, Room 301, Salt Lake City, Utah 84112, USA.
e-mail: andrew.jorgenson@soc.utah.edu

References

1. IPCC *Special Report on Renewable Energy Sources and Climate Change Mitigation* (eds Edenhofer, O. *et al.*) (Cambridge Univ. Press, 2011).
2. York, R. *Nature Clim. Change* **2,** 441–443 (2012).
3. Rosa, E. *et al. Science* **329,** 762–763 (2010).
4. Jorgenson, A. *Soc. Sci. Res.* **41,** 242–252 (2012).
5. Clark, B., Jorgenson, A. & Kentor, J. *Int. J. Sociol.* **40,** 23–43 (2010).
6. Jorgenson, A. & Clark, B. *Soc. Sci. Res.* **40,** 226–244 (2011).
7. Jorgenson, A. & Birkholz, R. *Ecol. Econ.* **69,** 2634–2643 (2010).
8. Roberts, J. T. & Parks, B. *A Climate of Injustice: Global Inequality, North-South Politics, and Climate Policy* (MIT Press, 2007).
9. Dietz, T., Gardner, G., Gilligan, J., Stern, P. & Vandenbergh, M. *Proc. Natl Acad. Sci. USA* **106,** 18452–18456 (2009).
10. Rosa, E., Diekmann, A., Dietz, T. & Jaeger, C. *Human Footprints on the Global Environment: Threats to Sustainability* (MIT Press, 2010).

© 2012 Macmillan Publishers Limited. All rights reserved

nature climate change

LETTERS

PUBLISHED ONLINE: 18 MARCH 2012 | DOI: 10.1038/NCLIMATE1451

Do alternative energy sources displace fossil fuels?

Richard York

A fundamental, generally implicit, assumption of the Intergovernmental Panel on Climate Change reports and many energy analysts is that each unit of energy supplied by non-fossil-fuel sources takes the place of a unit of energy supplied by fossil-fuel sources[1–4]. However, owing to the complexity of economic systems and human behaviour, it is often the case that changes aimed at reducing one type of resource consumption, either through improvements in efficiency of use or by developing substitutes, do not lead to the intended outcome when net effects are considered[5–9]. Here, I show that the average pattern across most nations of the world over the past fifty years is one where each unit of total national energy use from non-fossil-fuel sources displaced less than one-quarter of a unit of fossil-fuel energy use and, focusing specifically on electricity, each unit of electricity generated by non-fossil-fuel sources displaced less than one-tenth of a unit of fossil-fuel-generated electricity. These results challenge conventional thinking in that they indicate that suppressing the use of fossil fuel will require changes other than simply technical ones such as expanding non-fossil-fuel energy production.

The logic of my modelling approach is to control for the principal driving forces of national per capita demand for fossil-fuel energy (coal, oil and gas) and, to test for displacement, include in the models the amount of energy per capita from non-fossil-fuel sources (hydropower, nuclear, geothermal, solar, wind, tidal and wave energy, combustible renewables and waste) measured in the same units as energy from fossil-fuel sources. If, as is the common assumption, non-fossil-fuel energy displaces fossil-fuel energy proportionately, the coefficient for non-fossil-fuel energy should be approximately −1, meaning, controlling for demand, for each unit of non-fossil-fuel energy produced/consumed there should be one unit of fossil-fuel energy that is not produced/consumed. Partial displacement would be indicated by a coefficient between −1 and 0. A coefficient of 0 would indicate that non-fossil-fuel energy sources are simply added on top of fossil-fuel sources, without displacing them.

The displacement coefficients from four models are presented in Table 1 (full results are presented in the Supplementary Information). Models 1 and 2 examine electricity production (in kilowatt hours) per capita from fossil-fuel sources. In model 1, only gross domestic product (GDP) per capita (in inflation-adjusted US dollars) is included to control for demand, as data on it are available for most nations and most time points, giving broad coverage (132 nations, with data for many nations complete from 1960 to 2009), and also because economic production is generally considered the primary force driving energy use. As it is well established that the relationship between GDP per capita and energy use is not necessarily linear, the models are specified to allow for a nonlinear relationship. The displacement coefficient of −0.089 indicates that each kilowatt hour of non-fossil-fuel electricity that is generated displaces only 0.089 kWh of fossil-fuel-generated electricity. Therefore, to displace 1 kWh of fossil-fuel electricity requires generating more than 11 kWh (1/0.089 = 11.236) of non-fossil-fuel electricity.

In model 2, additional independent variables are added to further control for demand: urbanization (percentage of the population living in urban areas), including a specification to allow for a nonlinear relationship, manufacturing (percentage of GDP from the manufacturing sector) and the age-dependency ratio (the ratio of dependent-age people, that is, those under 15 and over 64, to non-dependent age people, that is, those 15–64 years of age)[10]. Including these extra control variables limits the coverage of the models owing to data availability, where 128 nations are included and most nations do not have complete data until the 1980s. Electricity production from non-fossil-fuel sources has a significant coefficient of −0.079, very similar to what was found in model 1. This coefficient indicates that close to 13 kWh (1/0.079 = 12.658) of non-fossil electricity are needed to displace 1 kWh of fossil-fuel electricity.

Models 3 and 4 examine the total national energy use (that is, electricity plus other uses) per capita from fossil-fuel sources (in kilotonnes oil equivalent). In model 3, where only GDP per capita is used to control for demand, the coefficient for energy use from non-fossil-fuel sources is −0.128, indicating that it takes nearly eight units (1/0.128 = 7.813) of non-fossil energy to displace one unit of fossil-fuel energy. Model 4 includes the additional control variables. Energy use from non-fossil-fuel sources has a significant coefficient of −0.219, the strongest coefficient of any model, but, nonetheless, very modest. This coefficient indicates that more than 4.5 units (1/0.219 = 4.566) of non-fossil-fuel energy are required to displace one unit of fossil-fuel energy.

In other versions of the four models I present here, I have tested whether the displacement coefficient varies over time by estimating the coefficient separately for each decade. The coefficients do not differ significantly across decades in any of the four models. I have also estimated models to assess whether the displacement coefficient varies with national affluence by estimating the coefficient separately for cases below the median GDP per capita value and those above it. The coefficients did not differ significantly across the two affluence categories for any of the four models.

I have also estimated models assessing whether the displacement coefficient is different for different types of non-fossil-fuel sources. For total national energy use, data availability limits the potential to disaggregate non-fossil-fuel sources, allowing for separation into only two categories: first, nuclear and non-combustible alternative sources, which represents non-carbohydrate energy sources, which do not emit carbon dioxide when generated (for example, hydropower, geothermal and solar power); and second, combustible renewables and waste, which includes biofuels. In versions of models 3 and 4, I substituted alternative and

Department of Sociology and Environmental Studies Program, University of Oregon, Eugene, Oregon 97403, USA. *e-mail: rfyork@uoregon.edu.

© 2012 Macmillan Publishers Limited. All rights reserved.

Table 1 | Non-fossil-fuel displacement coefficients for models of electricity production and energy use from fossil-fuel sources.

	Fossil-fuel electricity production per capita (kWh)		Fossil-fuel energy use per capita (kilotonnes oil equivalent)	
	Model 1	Model 2	Model 3	Model 4
Displacement coefficient for non-fossil-fuel energy sources per capita	−0.089*	−0.079*	−0.128*	−0.219*
Nations	132	128	132	128
Nation years	4,334	3,267	4,336	3,269

Results are based on statistical analyses of data from most nations of the world for 1960–2009. Each coefficient represents the effect on fossil-fuel use from the addition of one unit of energy from non-fossil-fuel sources. In models 1 and 3, energy demand is controlled for using GDP per capita. In models 2 and 4, energy demand is controlled for using GDP per capita, urbanization, manufacturing and the age-dependency ratio. *Statistically significant at the 0.05 alpha level (two-tailed test).

Table 2 | Nuclear, hydro and non-hydro renewable sources displacement coefficients for models of electricity production from fossil-fuel sources.

	Fossil-fuel electricity production per capita (kWh)	
	Model 5	Model 6
Displacement coefficient for nuclear energy per capita	−0.221*	−0.163*
Displacement coefficient for hydropower per capita	−0.099*	−0.086*
Displacement coefficient for non-hydro renewable sources per capita	0.048	0.018
Nations	132	128
Nation years	4,334	3,267

Results are based on statistical analyses of data from most nations of the world for 1960–2009. Each coefficient represents the effect on fossil-fuel use from the addition of one unit of energy from non-fossil-fuel sources. In model 5, energy demand is controlled for using GDP per capita. In model 6, energy demand is controlled for using GDP per capita, urbanization, manufacturing and the age-dependency ratio. *Statistically significant at the 0.05 alpha level (two-tailed test).

nuclear sources per capita and combustible and renewable sources per capita for the single non-fossil-fuel sources variable. The displacement coefficients for the two categories of energy were not significantly different from each other in either model, indicating that the models presented here with the single combined non-fossil-fuel sources variable are appropriate. Therefore, I do not present the results from the alternative models here.

More fine-grained data are available for sources of electricity, where non-fossil-fuel sources can be broken into three categories: nuclear; hydropower; and non-hydro renewable sources, which include wind, solar, geothermal, tides, biomass and biofuels. The displacement coefficients for these models are presented in Table 2. Model 5 controls only for GDP per capita, whereas model 6 controls for GDP per capita, urbanization, manufacturing and the age-dependency ratio. Model 5 indicates that nuclear power displaces more fossil-fuel electricity than other sources, but still not a substantial amount, with a coefficient of −0.221. Hydropower displaces less, with a coefficient of −0.099. Non-hydro renewable sources have a positive coefficient, indicating the opposite of displacement, but this coefficient is not significantly different from 0, indicating that renewables tend to simply be added to the energy mix without displacing fossil fuels. The differences among all three of these coefficients are statistically significant. Model 6 indicates a similar pattern, where nuclear power displaces the most fossil-fuel electricity, with a coefficient of −0.163, hydropower displaces less, with a coefficient of −0.086, and non-hydro renewables do not displace, with a non-significant coefficient of 0.018. In these models, the coefficient for nuclear power is significantly different from that of non-hydro renewables, but no other coefficients are significantly different from one another.

The lack of a significant displacement effect from non-hydro renewables is not necessarily that surprising, as they are such a small proportion of non-fossil-fuel energy sources (less than 4% of the world total). As they have, in general, been deployed only on a small scale, their potential to displace fossil-fuel use is hard to assess with confidence. Both nuclear and hydropower have significant, if only modest, displacement effects. Nuclear seems to displace somewhat more fossil-fuel use than hydropower does, although the difference between the coefficients for these two electricity sources is statistically significant only in model 5, not in model 6. The lower displacement coefficient for hydro power may stem from the fact that hydroelectric dams are often developed for many reasons, including flood control, irrigation and navigation, with the electrical output being merely one of the purposes. In contrast, nuclear power plants are typically developed primarily for electricity generation. In light of the fact that non-hydro renewables make up such a small proportion of non-fossil-fuel electricity sources, and that the difference in displacement effects between hydro and nuclear sources is ambiguous, the results from models 1 and 2, where all non-fossil-fuel electricity sources are combined, may best represent the general pattern.

Based on all of the results presented above, the answer to the question presented in the title of this paper—do alternative energy sources displace fossil fuels?—is yes, but only very modestly. The common assumption that the expansion of production of alternative energy will suppress fossil-fuel energy production in equal proportion is clearly wrong. The failure of non-fossil energy sources to displace fossil ones is probably in part attributable to the established energy system where there is a lock-in to using fossil fuels as the base energy source because of their long-standing prevalence and existing infrastructure and to the political and economic power of the fossil-fuel industry.

The clear implication of these results is that, if the pattern that has characterized energy use over the past five decades prevails in the future, massive expansion of non-fossil-fuel energy sources will be required to significantly suppress fossil-fuel use. This, of course, has serious environmental implications in light of the fact that non-fossil-fuel energy sources contribute to serious environmental impacts of their own. The recent disaster at the Fukushima Diachi nuclear plant in Japan is enough to highlight the risks associated

© 2012 Macmillan Publishers Limited. All rights reserved.

with expanding nuclear power, without even considering the serious risks stemming from long-term nuclear waste disposal and the environmental damage caused by uranium mining[4]. Hydropower destroys river ecosystems and threatens the survival of anadromous fish and other aquatic species[11]. Solar voltaic power and wind power, although representing less serious environmental threats than nuclear power and hydropower, require large amounts of material, some of it toxic and energy-intensive to produce, as well as large areas of land to produce substantial amounts of energy[12]. In short, all energy sources have environmental costs.

Does this mean that alternative energy sources will be of little help in moving societies away from fossil-fuel use? Not necessarily. Of course all societies need energy. So, obviously, if societies are to stop using fossil fuels they must have other energy sources. However, the results from the analyses presented here indicate that the shift away from fossil fuel does not happen inevitably with the expansion of non-fossil-fuel sources, or at least in the political and economic contexts that have been dominant over the past fifty years around the world. One implication of these results is that direct suppression of fossil-fuel use (for example, by a carbon tax) is likely to be much more effective at reducing fossil-fuel use than simply expanding non-fossil-fuel energy sources. It is possible that non-fossil energy sources could more substantially displace fossil energy sources if they were deployed in a context where there were explicit policies aimed at reducing carbon emissions, such as in California where there is a goal of dramatically reducing carbon emissions over the coming decades[13]. The most effective strategy for curbing carbon emissions is likely to be one that aims to not only develop non-fossil energy sources, but also to find ways to alter political and economic contexts so that fossil-fuel energy is more easily displaced and to curtail the growth in energy consumption as much as possible. A general implication of these findings is that polices aimed at addressing global climate change should not focus principally on developing technological fixes, but should also take into account human behaviour in the context of political, economic and social systems.

Methods

I constructed fixed-effects panel models with the Prais–Winsten correction for first-order autocorrelation, using the nation as the unit of analysis and including dummy variables for each year to control for general period effects. This approach controls for any effects that are constant over the span of time examined for each nation, such as geographic and geological characteristics, and any effects that are constant across nations for a given point in time, such as international energy prices. I used cross-sectional time-series data on all nations for which they are available, for all years for which they are available from 1960–2009, from the World Bank's world development indicators[14]. Note that the data set of the world development indicators records data on Hong Kong separately from China, so Hong Kong is treated as a separate nation in this analysis. All reports of statistical significance or non-significance are based on a 0.05 alpha level with a two-tailed test. The dependent variable in models 1, 2, 5 and 6 was constructed by multiplying electricity production by the proportion of electricity production from oil, gas and coal sources and dividing by total population. The corresponding independent variable is the difference between electricity production from fossil-fuel sources and electricity production from all sources. The dependent variable in models 3 and 4 was constructed by multiplying energy use by the proportion of fossil-fuel energy consumption and dividing by total population. Note that for a small number of observations, the percentage of fossil-fuel energy consumption was recorded as slightly more than 100%. In these cases, it was set at 100%. The corresponding independent variable is the difference between fossil-fuel energy use and overall energy use. All models include linear and polynomial versions of GDP per capita, both a quadratic and a cubic term, so as to control for the nonlinear effects of GDP per capita on fossil-fuel use as precisely as possible. Likewise, models 2 and 6 include a linear and a quadratic version of urbanization. Model 4 was originally estimated with both a linear and a quadratic of urbanization, but as the quadratic version had a non-significant coefficient, the model was re-estimated with only the linear term. To test whether the displacement coefficient varies over time, I included interaction terms for the non-fossil-fuel energy sources variable by decade (that is, 1960–1969, 1970–1979 and so on). To test for whether the displacement coefficient varies with affluence, I included an interaction term for cases below the median from the largest sample (that for model 3) of GDP per capita (US$2,792). To test for whether the displacement coefficient varies across types of non-fossil-fuel sources, I replaced the single non-fossil-fuel variable with the variables described in text and used F-tests to determine whether they were significantly different from one another.

Received 30 August 2011; accepted 15 February 2012; published online 18 March 2012

References

1. IPCC *Climate Change 2007: Mitigation of Climate Change* (eds Metz, B., Davidson, O. R., Bosch, P. R., Dave, R & Meyer, L. A.) (Cambridge Univ. Press, 2007).
2. IPCC *IPCC Special Report on Renewable Energy Sources and Climate Change Mitigation* (Cambridge Univ. Press, 2011).
3. Hoag, H. Low-carbon electricity for 2030. *Nature Clim. Change* **1,** 233–235 (2011).
4. Nuclear fallout. *Nature Clim. Change* **1**, 69 (2011).
5. Sellen, A. J. & Harper, R. H. R. *The Myth of the Paperless Office* (MIT Press, 2002).
6. Polimeni, J. M., Mayumi, K., Giampietro, M. & Alcott, B. *The Jevons Paradox and the Myth of Resource Efficiency Improvements* (Earthscan, 2008).
7. Druckman, A., Chitnis, M., Sorrell, S. & Jackson, T. Missing carbon reductions? Exploring rebound and backfire effects in UK households. *Energ. Policy* **39,** 3572–3581 (2011).
8. Hubacek, K. & Guan, D. The net effect of green lifestyles. *Nature Clim. Change* **1,** 250–251 (2011).
9. York, R. Ecological paradoxes: William Stanley Jevons and the paperless office. *Human Ecol. Rev.* **13,** 143–147 (2006).
10. York, R. Structural influences on energy production in South and East Asia, 1971–2002. *Sociol. Forum* **22,** 532–554 (2007).
11. Stone, R. Mayhem on the Mekong. *Science* **333,** 814–818 (2011).
12. Smil, V. *Energy at the Crossroads: Global Perspectives and Uncertainties* (MIT Press, 2003).
13. Williams, J. H. *et al.* The technology path to deep greenhouse gas emissions cuts by 2050: The pivotal role of electricity. *Science* **335,** 53–59 (2012).
14. World Bank *World Development Indicators.* Available at http://data.worldbank.org/data-catalog/world-development-indicators. Accessed 20 July (2011).

Acknowledgements

I thank T. Koford for helpful comments.

Author contributions

R.Y. designed the research, analysed the data and wrote the manuscript.

Additional information

The author declares no competing financial interests. Supplementary information accompanies this paper on www.nature.com/natureclimatechange. Reprints and permissions information is available online at www.nature.com/reprints.

© 2012 Macmillan Publishers Limited. All rights reserved.

United States
Department of
Agriculture

Forest Service

Pacific Northwest
Research Station

General Technical
Report
PNW-GTR-364
February 1996

Guidelines for Estimating Volume, Biomass, and Smoke Production for Piled Slash

Colin C. Hardy

EXHIBIT 1

Abstract

Hardy, Colin C. 1996. Guidelines for estimating volume, biomass, and smoke production for piled slash. Gen. Tech. Rep. PNW-GTR-364. Portland, OR: U.S. Department of Agriculture, Forest Service, Pacific Northwest Research Station. 17 p.

Guidelines in the form of a six-step approach are provided for estimating volumes, oven-dry mass, consumption, and particulate matter emissions for piled logging debris. Seven stylized pile shapes and their associated geometric volume formulae are used to estimate gross pile volumes. The gross volumes are then reduced to net wood volume by applying an appropriate wood-to-pile volume packing ratio. Next, the oven-dry mass of the pile is determined by using the wood density, or a weighted-average of two wood densities, for any of 14 tree species commonly piled and burned in the Western United States. Finally, the percentage of biomass consumed is multiplied by an appropriate emission factor to determine the mass of PM, PM10, and PM2.5 produced from the burned pile. These estimates can be extended to represent multiple piles, or multiple groups of similar piles, to estimate the particulate emissions from an entire burn project.

Keywords: Fuel, emissions, piled slash, smoke management.

Contents

1 **Introduction**

2 **The Six-Step Process**

3 Step One—Total Gross Volume of the Pile

10 Step Two—Net Volume of the Woody Biomass

10 Step Three—Density or Weighted-Average Density of the Wood

12 Step Four—Consumable (Oven-Dry) Mass of Wood

13 Step Five—Proportion of Mass Consumed

13 Step Six—Mass of Particulate Matter Produced

14 **Recommendations and Guidance**

15 **Literature Cited**

16 **Appendix 1: A Hypothetical Example**

18 **Appendix 2: Full-Sized Copies of the Nomagrams**

Introduction

The guidelines in this document address the critical need to quantify both biomass consumption and the air quality impacts from the burning of piled woody debris. Piling and burning of woody debris from activities such as timber harvesting, road building, and residential or commercial development has been a common practice for as long as these activities have occurred. It is an especially common forestry practice, where logging residue (slash) is piled on the site by bulldozers, and on the terminus (landing) of yarding and skidding trails by bulldozers, cable-yarding equipment, and log loaders. Numerous objectives are met by piling and burning: reduction of on-site woody fuel loading and the resultant reduction in harvest-created fire hazard; scarification of the surface layer and exposure of mineral soil to enhance regeneration of trees; removal of woody and organic material from roadbeds and structure sites to improve the integrity of the construction substrate; and sanitation disposal of stumps and roots infected by disease or pathogens. In some cases, logging slash is piled in anticipation of subsequent use in nonlumber markets such as combustion for energy (hog fuel), pulp chips, and firewood.

On-site burning of piled slash has both negative and positive implications for smoke management. Burning of woody biomass, regardless of its condition and distribution, creates products of incomplete combustion such as carbon monoxide, methane, and particulate matter. A variety of research methods have produced much new knowledge about the quantity and characteristics of smoke emissions from vegetation fires (Ward and Radke 1993) and from piled slash (Ward and others 1989). Piling and burning of slash has positive smoke management implications as well. In contrast with broadcast burning of the same material, piled slash burns more efficiently, with notably less smoke produced per unit mass of fuel consumed (Ward and others 1989). Further, piled slash can be burned under a broad range of weather conditions. This enables the burning of piles to be scheduled for periods of optimal dispersion and also during periods when the conflicts with impacts from other sources are minimized.

Smoke management programs in several Western States now actively encourage the piling and burning of slash, where possible, instead of the more typical practice of broadcast burning. Permitting and fee structures have created incentives for piling and burning. The increased emphasis on the practice demands significant improvements in our ability to quantify preburn fuel loadings, fuel consumption, and emissions production from burning piles.

Several previous efforts have led the way toward the methods and guidelines presented here. Techniques for estimating weights of piles and stumps were developed from a land clearing project in Washington (Mohler 1977). Relations between easy-to-measure dimensions and woody fuel volumes were developed by McNab (1980) for inventorying windrowed forest residues in the Southern United States. Results from these two methods were verified by Johnson (1981) when he compared them to results from destructive sampling. Little developed a method for estimating pile volumes using four stylized shapes and respective volumetric formulae.[1] These shapes, when combined with a ratio estimator for reducing gross pile volume to net wood volume, provide an efficient, simple method for field estimation of woody fuel volumes in piles.

The initial steps in these guidelines use the methodology and generalized shapes presented by Little (see footnote 1). Three additional shapes are included, as are species-specific wood densities, a range of wood-to-pile volume ratios,[2] and several nomagrams intended to reduce the number of manual calculations required to estimate volumes, mass, and smoke emissions.

The Six-Step Process

Six steps are required to estimate particulate emissions from a pile. The product from each step is both relevant in itself and a prerequisite parameter for completion of the next step.

Determine:

1. Total gross volume of the pile.
2. Net volume of the woody biomass.
3. Density or weighted-average density of the wood.
4. Consumable (oven-dry) mass of wood.
5. Proportion of mass consumed.
6. Mass of particulate matter produced (PM, PM10, PM2.5).

[1] Little, S.N. 1980. Estimating the volume of wood in large piles of logging residue. Portland, OR: U.S. Department of Agriculture, Forest Service, Pacific Northwest Forest and Range Experiment Station. 7 p. Administrative Report PNW-1. On file with: Forestry Sciences Laboratory, P.O. Box 3890, Portland, OR 97208-3890.

[2] Hardy, Colin C., Vihnanek, R. Packing ratios for piled woody debris. Manuscript in preparation. USDA Forest Service, Pacific Northwest Research Station, Seattle, WA 98105.

Step One—Total Gross Volume of the Pile

A. Select a representative pile shape—A pile can be categorized into one of the seven generalized shapes shown in figure 1. The number for each shape is its "shape code." The dimensions required to compute volumes are shown in figure 1 for each shape. Choose the shape most similar to your pile(s) from the following descriptions and figures and record the appropriate dimensions.

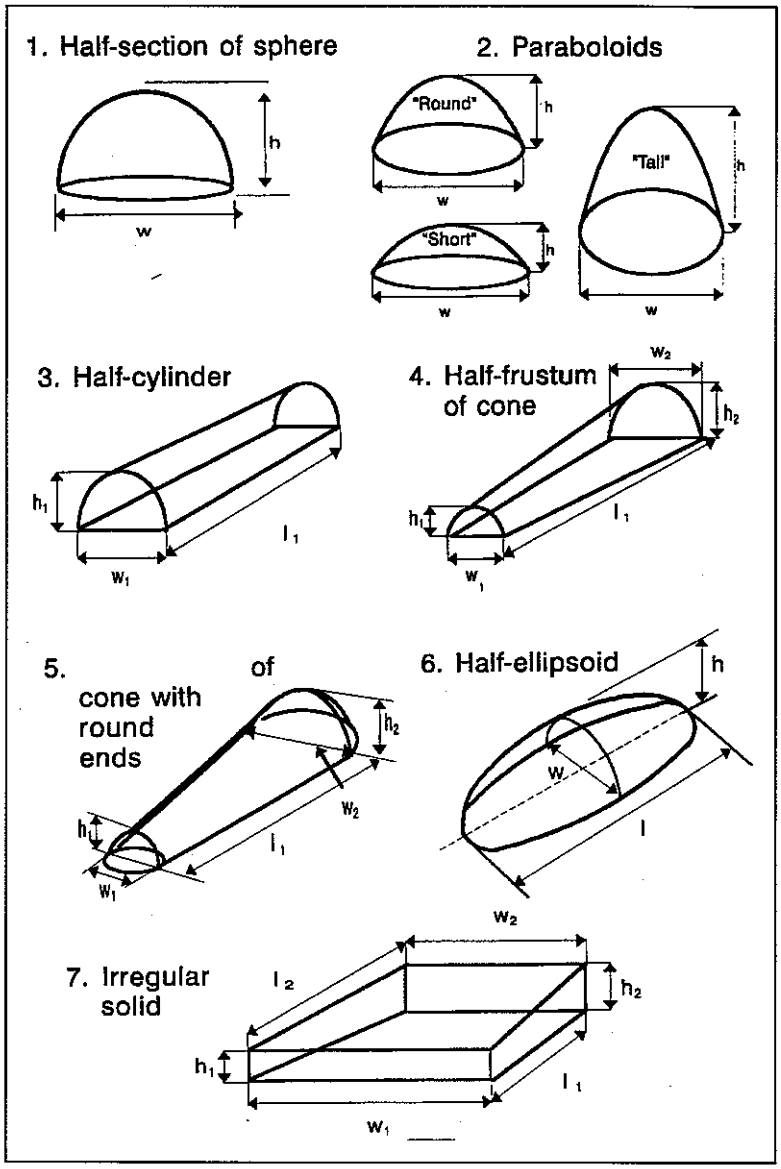

Figure 1—Five generalized pile shapes are used to represent the possible configurations of piled woody debris. Each illustration is numbered by its "shape code" (see text).

Shape code 1: Half-section of a sphere—Truly half of a ball or sphere (fig. 2). The base is round, the width is twice the height, and the sides are well- and evenly-rounded. (Observe and record either height [*h*] or width [*w*].)

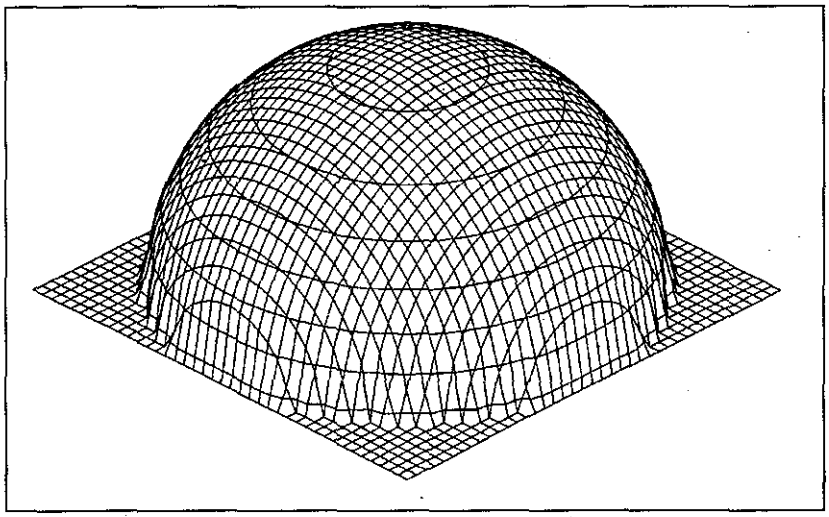

Figure 2—The half-section of a sphere is truly half a ball, with well-rounded sides.

Shape code 2: Half-paraboloid—The base is round, but the sides are parabolic, not round. Three variations of the half-paraboloid shape are shown in figure 3: half-round paraboloid, half-"tall" paraboloid, and half-"short" paraboloid. (Observe and record height [*h*] and width [*w*].)

Shape code 3: Half-cylinder—The pile is generally rounded side-to-side, with both ends of the pile approximately the same height and straight (fig. 1). Logs stacked parallel by a loader or crane can form this shape. (Observe and record width [*w*], height [*h*], and length [*l*].)

Shape code 4: Half-frustum of a cone—This shape is similar to a half-cylinder, but the cylinder tapers lengthwise, so the heights of the ends are different (fig. 1). This shape is seen when logs are stacked parallel, with the tapers oriented in the same direction. (Observe and record length [*l*] and heights or widths of the small and large ends [h_1 or w_1, and h_2 or w_2].)

Shape code 5: Half-frustum of a cone with rounded ends—Similar to shape code 4, but the ends are rounded (fig. 1). In this case, the rounded ends caused by uneven stacking and mixed piece sizes can add considerable volume to the pile. (Observe and record length of straight section of the side [*l*] and width of the small and large end [w_1, w_2].)

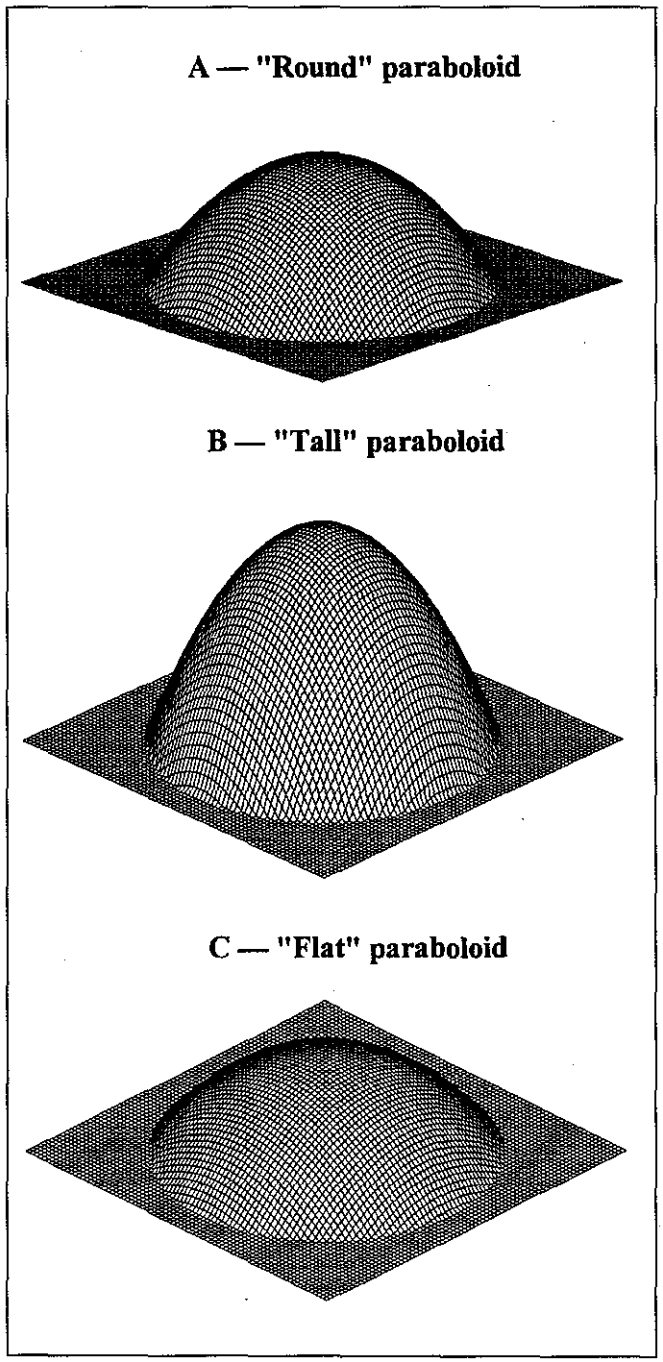

Figure 3—The base of the half-paraboloid is round but the sides are parabolic. Three variations of this shape use the same volumetric formula: (A) "round," (B) "tall," and (C) "flat."

Shape code 6: Half-ellipsoid—This pile is elongated, rounded side-to-side, with well-rounded ends (fig. 4). This shape is typical of windrowed slash. (Observe and record height [h], total length [l], and width at the widest section [w].)

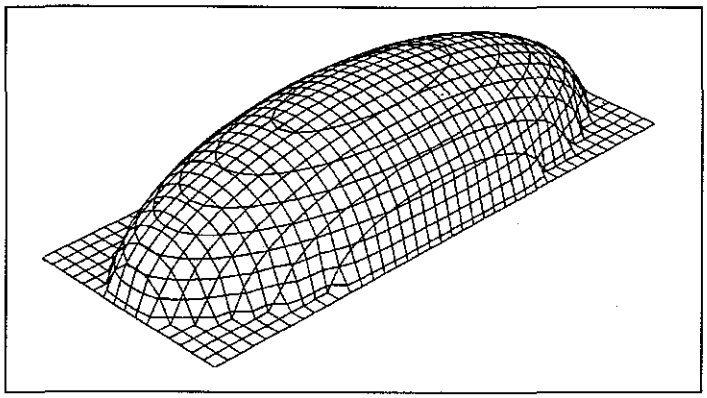

Figure 4—The half-ellipsoid shape represents a long, symmetric, tapering pile with well-rounded ends.

Shape code 7: Irregular solid—This pile is irregularly shaped with straight but uneven sides (fig. 1). The dimensions for opposing sides are not necessarily equal. (Observe and record lengths [l_1, l_2], widths [w_1, w_2], and heights [h_1, h_2].)

B. Calculate the gross volume—The gross volume for a pile represented by any of the seven shape codes can be calculated from the following volumetric formulae,

where: V = gross pile volume (cubic feet),

l, l_1, l_2 = length(s) in feet,

h, h_1, h_2 = height(s) in feet, and

w, w_1, w_1, w_2 = width(s) in feet.

Look-up tables or nomagrams are provided for some of the shapes and are referenced below with the respective formula.

Shape code 1—

$$V = \frac{2\pi h^3}{3} \text{ or } V = \frac{\pi h w^2}{6} \quad .$$

Columns 1-3 of table 1 contain look-up data for this volume. Use either pile height (column 2) or piile height and width (column 1) to determine gross volume (column 3).

Table 1—Gross pile volumes for half-section of a sphere (spheroid) and half-paraboloid pile shapes (shape codes 1 and 2, respectively)[a]

Pile width	Spheroids only		Volume by paraboloid height (in feet)								
	Height	Volume	4	6	8	10	12	14	16	18	20
Feet		*Cubic feet*									
4	2.0	17	25	38	50	63	75	88	101	113	126
5	2.5	33	39	59	79	98	118	137	157	177	196
6	3.0	57	57	85	113	141	170	198	226	254	283
7	3.5	90	77	115	154	192	231	269	308	346	385
8	4.0	134	101	151	201	251	302	352	402	452	503
9	4.5	191	127	191	254	318	382	445	509	573	636
10	5.0	262	157	236	314	393	471	550	628	707	785
11	5.5	348	190	285	380	475	570	665	760	855	950
12	6.0	452	226	339	452	565	679	792	905	1018	1131
13	6.5	575	265	398	531	664	796	929	1062	1195	1327
14	7.0	718	308	462	616	770	924	1078	1232	1385	1539
15	7.5	884	353	530	707	884	1060	1237	1414	1590	1767
16	8.0	1072	402	603	804	1005	1206	1407	1608	1810	2011
17	8.5	1286	454	681	908	1135	1362	1589	1816	2043	2270
18	9.0	1527	509	763	1018	1272	1527	1781	2036	2290	2545
19	9.5	1796	567	851	1134	1418	1701	1985	2268	2552	2835
20	10.0	2094	628	942	1257	1571	1885	2199	2513	2827	3142
21	10.5	2425	693	1039	1385	1732	2078	2425	2771	3117	3464
22	11.0	2788	760	1140	1521	1901	2281	2661	3041	3421	3801
23	11.5	3185	831	1246	1662	2077	2493	2908	3324	3739	4155
24	12.0	3619	905	1357	1810	2262	2714	3167	3619	4072	4524

[a] The volume for a spheroid (column 3) is determined from either the width (column 1) or height (column 2). For a half-paraboloid, find the intersection of width (column 1) and height (columns 4-12).

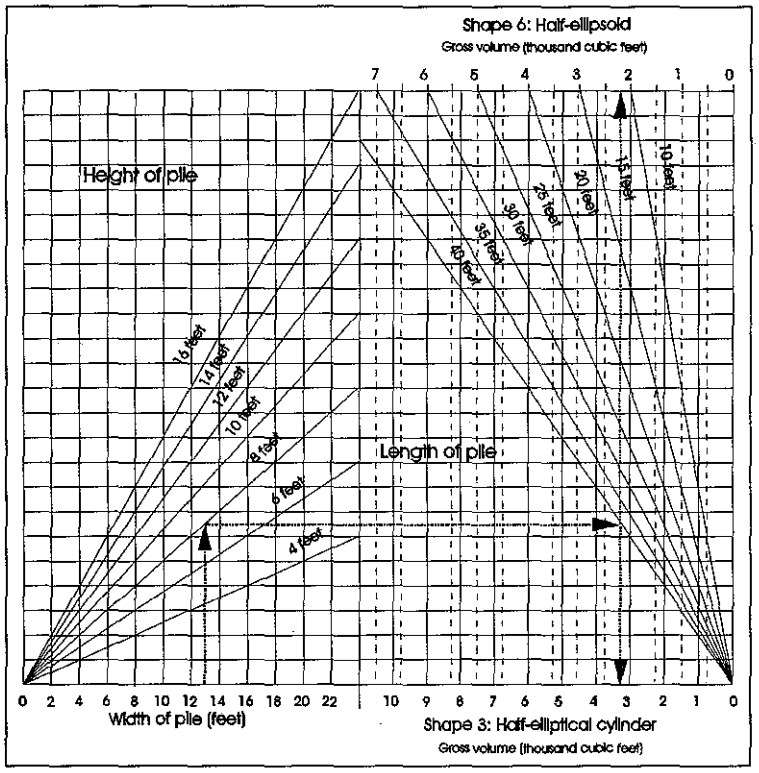

Figure 5—The nomagram assists in determining gross pile volumes (X-axes at upper and lower right) for shape codes 6 and 3, respectively, by width (X-axis at lower left), height (diagonal lines at left), and length (diagonal lines at right).

Shape code 2—

$$V = \frac{\pi h w^2}{8} .$$

The volume for any of the three variations of half-paraboloid is derived from the same equation. Columns 1 and 4-12 of table 1 contain look-up data for this volume, where the intersection of width (column 1) and height (columns 4-12) contains the gross pile volume.

Shape code 3—

$$V = \frac{\pi w l h}{4} .$$

Figure 5 is a nomagram for estimating gross volumes for shape codes 3 and 6 by using width, height, and length.[3]

Begin at the X-axis (horizontal axis) labeled "width of pile"; go up from the correct width to the diagonal line for the correct height; go horizontally to the diagonal line at the right for the correct length; go down to the right-hand X-axis (labeled "gross volume") for shape code 3, half-elliptical cylinder, to determine the gross pile volume.

[3] Full-page versions of all nomagrams are given in appendix 2.

Shape code 4—

$$V = \frac{\pi l_1 \left[h_1^{\,2} + h_2^{\,2} + (h_1 h_2) \right]}{6}$$ if using heights,

or

$$V = \frac{\pi l_1 \left[w_1^{\,2} + w_2^{\,2} + (w_1 w_2) \right]}{24}$$ if using widths.

Shape code 5—

$$V = \frac{\pi \left\{ l_1 \left[w_1^{\,2} + w_2^{\,2} + (w_1 w_2) \right] + w_1^{\,3} + w_2^{\,3} \right\}}{24}$$

Shape code 6—

$$V = \frac{\pi w l h}{6} \; .$$

Figure 5 is a nomagram for estimating gross volumes for shape codes 3 and 6 by using width, height, and length.

Begin at the X-axis (horizontal axis) labeled "width of pile"; go up from the correct width to the diagonal line for the correct height; go horizontally to the diagonal line at the right for the correct length; go up to the top right-hand X-axis (labeled "gross volume") for shape code 6, half-ellipsoid, to determine the gross pile volume.

Shape code 7—

$$V = \frac{(l_1 + l_2)(w_1 + w_2)(h_1 + h_2)}{8} \; .$$

Some piles contain a significant amount of soil, whether entrained among the wood pieces or mounded beneath the pile. The net wood volume must be reduced by an estimate of the percent of the volume occupied by soil.

Step Two—Net Volume of the Woody Biomass

Much of the gross volume of a pile is occupied by air. The ratio of wood volume to total pile volume is called the "packing ratio." The gross pile volume must be multiplied by an appropriate packing ratio to determine the net volume of woody material in a pile. Research on the packing ratio of piled slash has determined that the net wood volume can range from as low as 6 percent to as high as 26 percent (see footnote 2). These values represent extremes from 17 piles studied. The variation in packing ratio is due to numerous factors, including piling specifications, operator and machine performance, species content, and size class distribution. Only expert judgment can be used to ultimately determine a packing ratio for a particular pile or group of similar piles. For the purpose of these guidelines, data from research can be used to suggest the following packing ratios:

Tractor
Hand
Grapple
Landing

- Piles with species content dominated by ponderosa pine, with mean diameters of the large woody fuel of less than 10 inches were found to have a mean packing ratio of 10 percent (0.10).[4]
- Piles dominated by short-needled conifers had packing ratios ranging from 15 percent (0.15) to 20 percent (0.20).
- Highly compacted, clean piles with larger logs (diameters greater than 10 inches), especially those built with a crane or loader, can have packing ratios as high as 25 percent (0.25).

Multiply the gross pile volume determined in step one by an appropriate packing ratio to calculate net wood volume. The nomagram shown on the left side of figure 6 can be used to make this calculation. Begin at the X-axis labeled "gross pile volume"; go up to a diagonal line representing an appropriate packing ratio for the pile(s); go left to the Y-axis to determine the respective net wood volume. This step can be combined with step four if the nomagram is used.

Step Three—Density or Weighted-Average Density of the Wood

The oven-dry density of wood is used to calculate mass of wood for fuel loading, fuel consumption, and smoke production. Table 2 contains oven-dry densities for 14 tree species commonly piled and burned in the Western United States. Use these values if the wood in a pile is predominately one species. If two species are identified, refer to the nomagram in figure 7 to derive a weighted-average density for the pile.

First, find a line in figure 7 connecting the two species. Move from the end of the line representing the dominant species towards the other species until the line interesects the correct percentage content (vertical lines labeled on the X-axis) for the dominant species; then move horizontally either left or right to the Y-axis to determine a weighted-average density for the two species.

[4] Scientific names for tree species are included in table 2.

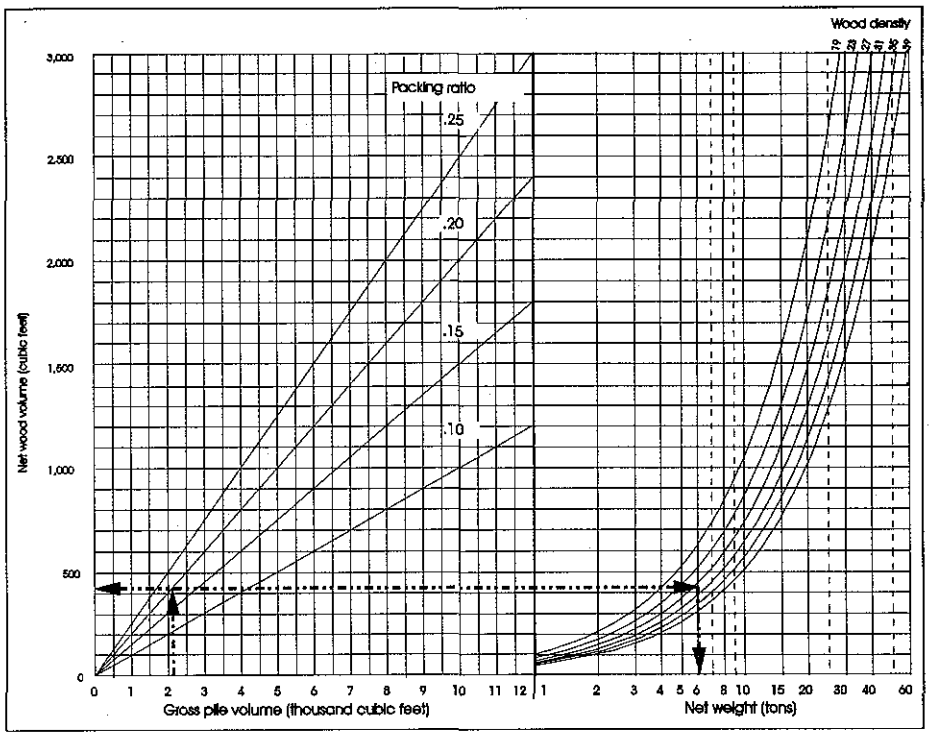

Figure 6—The nomagram assists in determining net mass of the wood (X-axis at right) by using gross pile volume (X-axis at left), packing ratio (diagonal lines at left), net wood volume (Y-axis), and wood density (curves at right).

Table 2—Green specific gravity and oven-dry density for 14 tree species commonly piled and burned in the Western United States

Species	Specific gravity (green)	Density (oven dry)
	Dimensionless	*Lb/ft*^{3}
Rotten wood (not species-specific)	0.30	18.7
Western redcedar (*Thuja plicata* Donn ex D.Don)	.31	19.4
Black cottonwood (*Populus trichocarpa* Torr. & Gray)	.31	19.4
Quaking aspen (*P. tremuloides* Michx.)	.35	21.9
True fir (noble) (*Abies procera* Rehd.)	.37	23.1
Red alder (*Alnus rubra* Bong.)	.37	23.1
Sitka spruce (*Picea sitchensis* (Bong.) Carr.)	.37	23.1
Ponderosa pine (*Pinus ponderosa* Dougl. ex Laws.)	.38	23.7
Lodgepole pine (*P. contorta* Dougl. ex Loud.)	.38	23.7
Western hemlock (*Tsuga heterophylla* (Raf.) Sarg.)	.42	26.2
Bigleaf maple (*Acer macrophyllum* Pursh)	.44	27.5
Vine maple (*Acer circinatum* Pursh)	.44	27.5
Douglas-fir (*Pseudotsuga menziesii* (Mirb.) Franco)	.45	28.1
Western larch (*Larix occidentalis* Nutt.)	.48	30.0
Tanoak (*Lithocarpus densiflorus* (Hook. & Arn.) Rehd.)	.58	36.2

Sources: Panshin and others 1964, USDA Forest Service 1974.

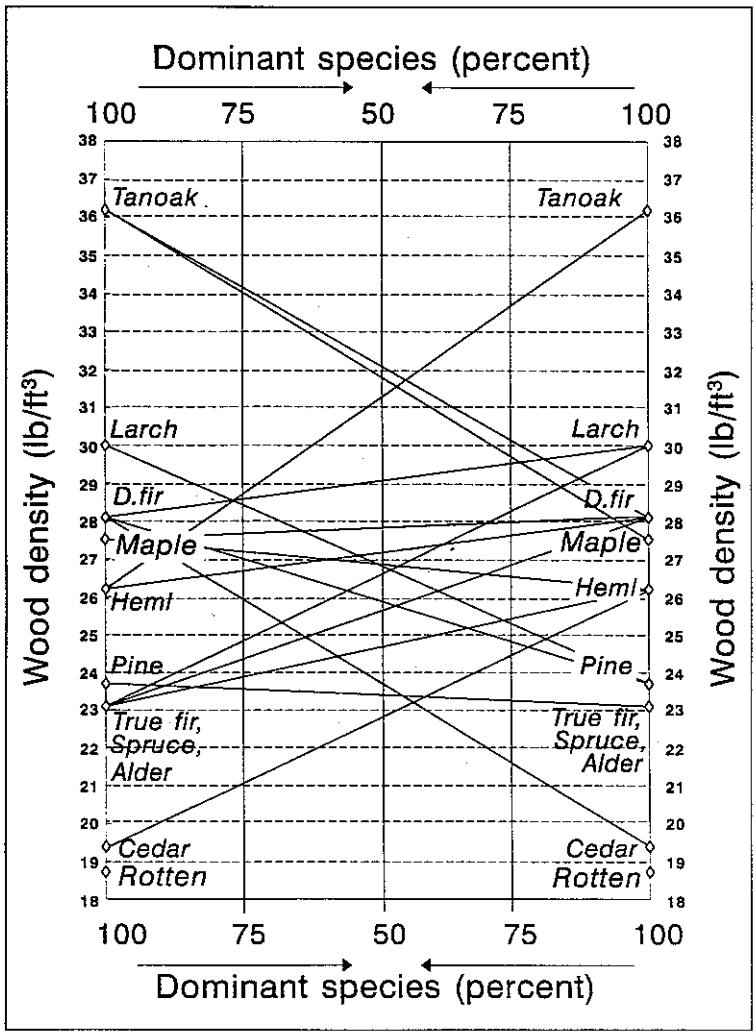

Figure 7—The nomagram can be used to calculate a weighted-average wood density (Y-axes) for two species by finding a point along a diagonal line representing two species that intersects with a vertical line indicating the correct proportion of the two species.

Step Four—Consumable (Oven-Dry) Mass of Wood

Multiply the wood density or weighted-average wood density for the pile by the net wood volume to calculate the oven-dry (consumable) mass of the pile. Divide the result by 2,000 to convert to tons. The nomagram shown on the right side of figure 6 can be used for this step.

Begin with the correct net wood volume shown on the Y-axis at the left side of figure 6; move right, horizontally, to the appropriate wood density curve on the right side of the nomagram; proceed downward (vertically) to determine the net weight of wood in the pile. Note that the X-axis at the right (net weight) is logarithmic, so interpolations must be made only between adjacent numbers on the X-axis.

Step Five—Proportion of Mass Consumed

The percentage of wood mass consumed when piles are burned typically ranges between 75 and 95 percent. Smoke management-reporting programs in several Western States recommend either 85 percent (0.85) or 90 percent (0.90). Experience and expert knowledge must be used to determine the most appropriate value for percentage of consumption. Multiply the percentage by the consumable mass of wood from step four to calculate the total mass of material consumed.

Step Six—Mass of Particulate Matter Produced

The mass of an emission produced by a fire is calculated by multiplying the mass of fuel consumed by an appropriate emission factor for the emission of interest. These guidelines provide emission factors for three size classes of particulate matter: PM (total particulate matter), PM10 (particulate matter smaller than 10 micrometers mean-mass diameter), and PM2.5 (particles smaller than 2.5 micrometers mean-mass diameter). The emission factors for these particle sizes differ with the combustion efficiency of the fire. Cleaner piles burn more efficiently than dirty piles. Consequently, cleaner piles produce less of the products of incomplete combustion, of which particulate matter is a major emission species. Figure 8 provides emission factor curves for PM, PM10, and PM2.5; the relations between the emission factors and combustion efficiency illustrate the impacts of different amounts of soil mixed into a pile. Expert judgment as well as agency policy must be considered when using the curves in figure 8.

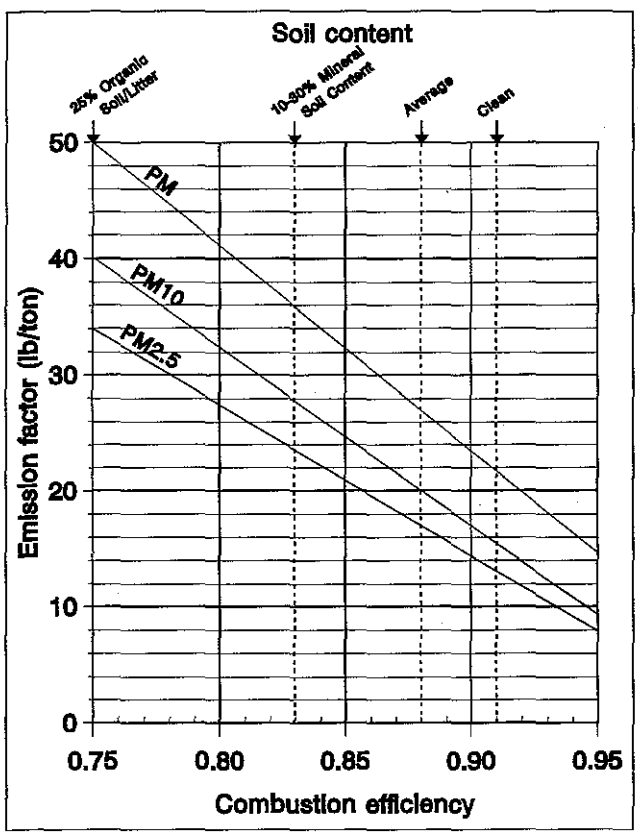

Figure 8—An appropriate emission factor for PM, PM2.5, and PM10 can be determined from knowledge of the relative amount of soil in the pile.

Start in figure 8 from an appropriate combustion efficiency determined from the relative cleanliness of the pile(s); combustion efficiency and soil content are found on the lower and upper X-axes, respectively. Follow the vertical line up from combustion efficiency, or down from soil content, to the intersection of the line for PM, PM10, or PM2.5; from that intersection move horizontally left to determine the emission factor.

Multiply the emission factor by the oven-dry mass of material consumed (from step five) to calculate the total mass of the particulate matter emission produced by the pile(s).

Recommendations and Guidance

The largest errors expected from using these guidelines will occur during the process of determining the gross pile volume(s). The seven stylized pile shapes do not provide an exhaustive choice of geometric shapes for piled slash. These seven are presented because they reflect general shapes observed by the author and other experts, and also because their volumes can be calculated relatively easily from either the formulae or the nomagrams. When the dimensions for a pile are observed, care must be taken to account for irregularities in the pile's surfaces. Try to mentally "smooth" the lobes, ridges, and valleys into an average, smooth surface. Long logs and poles extending from the pile's nominal surface can be accounted for by increasing the dimension(s) of the pile appropriately. If a significant amount of soil is either entrained within the pile or mounded beneath it, the volume of the soil must be estimated and subtracted from the gross pile volume.

The packing ratios presented in these guidelines represent empirical field data from destructive sampling of 17 piles. Even though guidelines are provided to determine an appropriate packing ratio for specific piles, an agency or administrative unit may choose to specify packing ratios for applications under their jurisdiction.

A continuous range of emission factors for PM, PM10, and PM2.5 are presented in these guidelines. The values given for "average" piles are weighted means from eight in situ field tests of emissions from burning of piles of woody debris. Results from many other related tests were used to develop the regression lines (fig. 8), which predict emission factors by using combustion efficiency. The values for PM10 were not derived from actual field observations—only PM2.5 and PM were measured in the field tests from which these data were prepared. PM10 emission factors were estimated by using limited knowledge of the size distribution of particles.

These guidelines provide procedures for estimating volume, biomass, and particulate matter emissions from a single pile. Most applications of these procedures typically will be made for multiple-pile projects. Some or all steps in these guidelines can be extended to represent a group of similar piles. For example, average dimensions can be used for all piles of a similar shape. If possible, it is helpful to map the location, shape, and dimension of each pile on a unit or project. At a minimum, piles of similar shape or size should be tallied; the formulae and nomagrams can then be applied at another time. Each agency or administrative unit may prescribe a specific method for obtaining and aggregating the data for a project.

Literature Cited

Johnson, V.J. 1981. How shape affects the burning of piled debris. Fire Management Notes. 45(3). 4 p.

McNab, H.W. 1980. A technique for inventorying volume and weight of windrowed forest residues. Res. Pap. SE-215. Asheville, NC. U.S. Department of Agriculture, Forest Service, Southeastern Forest Experiment Station. 8 p.

Mohler, J.P. 1977. Estimating weight in piled land clearing debris. Residue Reducer. [Olympia, WA]: State of Washington, Department of Natural Resources; 2(2). 5 p.

Panshin, A.J.; DeZeeuw, C.; Brown, H.P. 1964. Textbook of wood technology—volume 1. New York: McGraw-Hill Book Company. 643 p.

U.S. Department of Agriculture, Forest Service. 1974. Wood handbook: wood as an engineering material. Revised. Agric. Handb. 72. Washington, DC.

Ward, D.E.; Hardy, C.C.; Sandberg, D.V.; Reinhardt, T.E. 1989. Mitigation of prescribed fire atmospheric pollution through increased utilization of hardwoods, piled residues, and long-needled conifers: Part III—emissions characterization. Seattle, WA: U.S. Department of Energy; final report IAG DA-AI179-85BP18509. On file with: Pacific Northwest Research Station, Fire and Environmental Research Applications Group, Seattle, WA.

Ward, D.E.; Radke, L.F. 1993. Emissions measurements from vegetation fires: a comparative evaluation of methods and results. In: Crutzen, P.J.; Goldammer, J.G., eds. Fire in the environment: the ecological, atmospheric, and climatic importance of vegetation fires. New York: John Wiley: 53-76. Chapter 4.

Appendix 1: A Hypothetical Example

- **Shape**–The pile was built with a bulldozer and can be considered a windrow. It is elongated, with an elliptically shaped base, and is rounded side-to-side with well-rounded ends.
- **Dimensions**–Length is 40 feet; width is 13 feet; height is 8 feet.
- **Wood species**–Wood content (by volume) is 75 percent Douglas-fir and 25 percent western hemlock.
- **Packing ratio**–Pile is relatively compact; about 20 percent wood-to-volume ratio (0.20).
- **Fuel consumption**–90 percent of the wood mass will be consumed.
- **Emission factors**–The pile is "average" in soil content and therefore will burn with a combustion efficiency of 0.88.

Step one—Total gross volume of the pile—

A. Select a representative pile shape: Pile shape is half-ellipsoid—shape code 6.

B. Calculate the gross volume:

Formula method: Volume $= \frac{\pi * 13 * 40 * 8}{6} = 2178$ cubic feet.

Nomagram: Refer to figure 5 and follow the arrowed line to the X-axis at the upper right, where the gross volume equals about 2.2 thousand cubic feet.

Step two—Net volume of the woody biomass—

Formula method: Net volume = Gross volume x packing ratio; therefore,

2178*0.20 = 435.6 cubic feet.

Nomagram: Refer to figure 6 and follow the arrowed line to the Y-axis at the left, where the net volume equals about 435 cubic feet.

Step three—Density or weighted-average density of the wood

Formula method: The pile is 75 percent Douglas-fir and 25 percent western hemlock. Refer to table 2 for the densities of Douglas-fir (28.1 lb/ft^3) and western hemlock (26.2 lb/ft^3). Calculate the weighted average:

(0.75*28.1)+(0.25*26.2)=27.63 pounds per cubic foot.

Nomagram: Refer to figure 7, where the diagonal line connecting Douglas-fir and western hemlock intersects the vertical line representing 75 percent Douglas-fir at about 27.7 lb/ft^3 (on the Y-axis).

Step four—Consumable (oven-dry) mass of wood—

Formula method: Net wood mass = net wood volume x wood density

435.6*27.63 = 12,036 pounds or ≅ 6 tons.

Nomagram: Refer to figure 6 and follow the arrowed line to the curves on the right, then down to the X-axis, where the net mass of wood is approximately 6.0 tons.

Step five—Proportion of mass consumed—

Formula method: Mass consumed = net mass x percent consumed

6.0*0.90 = 5.4 tons.

Step six—Mass of particulate matter produced—

Formula: Total emission = mass consumed x emission factor.

Emission factors: Referring to figure 8, for an "average" pile:
PM = 27 lb/ton
PM10 = 20 lb/ton
PM2.5 = 17 lb/ton

Calculate: PM: 5.4 tons*27 lb/ton=145.8 pounds
PM10: 5.4 tons*20 lb/ton=108.0 pounds
PM2.5: 5.4 tons*17 lb/ton=91.8 pounds

Appendix 2: Full-Sized Copies of the Nomagrams

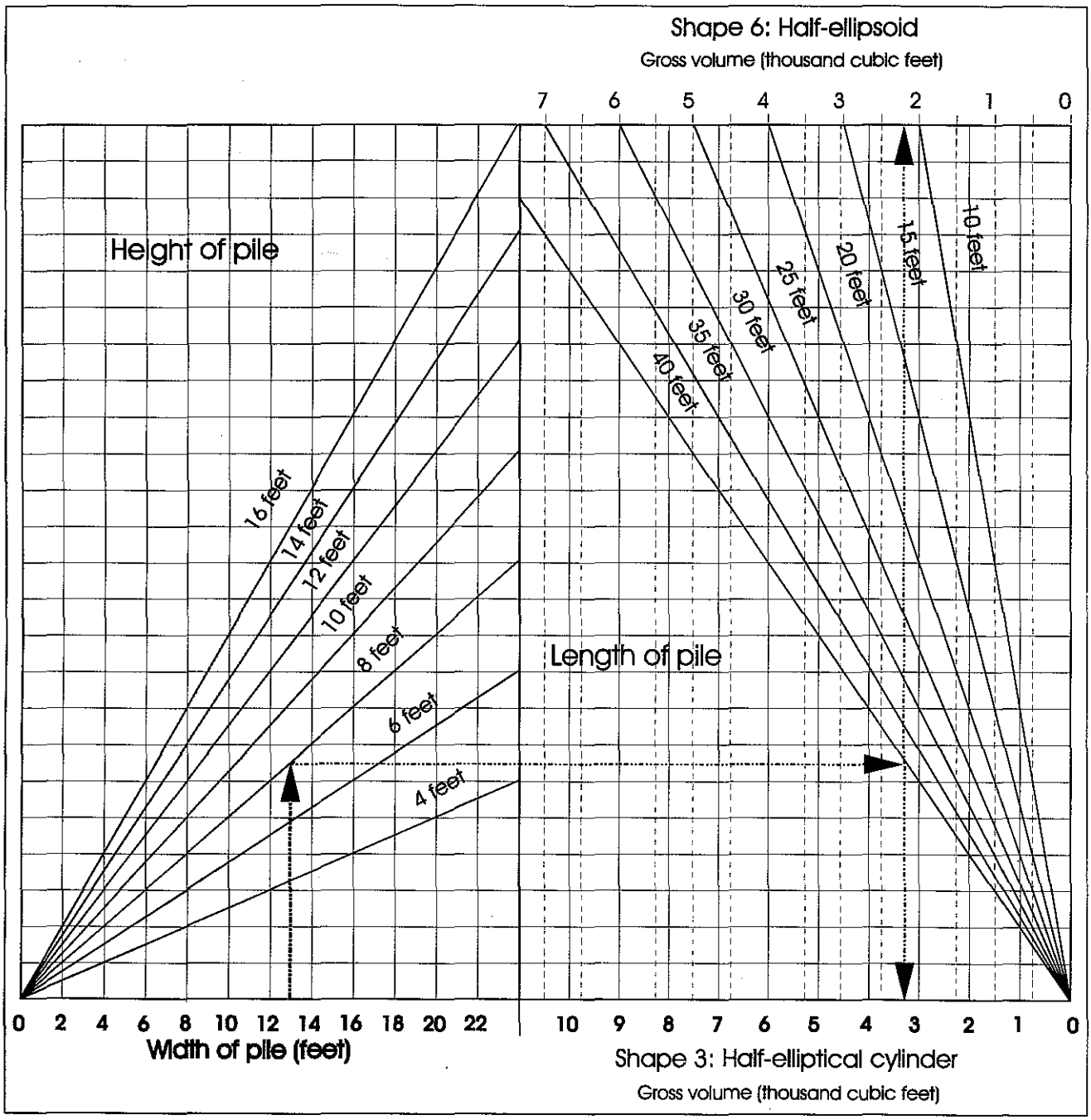

Figure 5—The nomagram assists in determining gross pile volumes (X-axes at upper and lower right) for shape codes 6 and 3, respectively, by width (X-axis at lower left), height (diagonal lines at left), and length (diagonal lines at right).

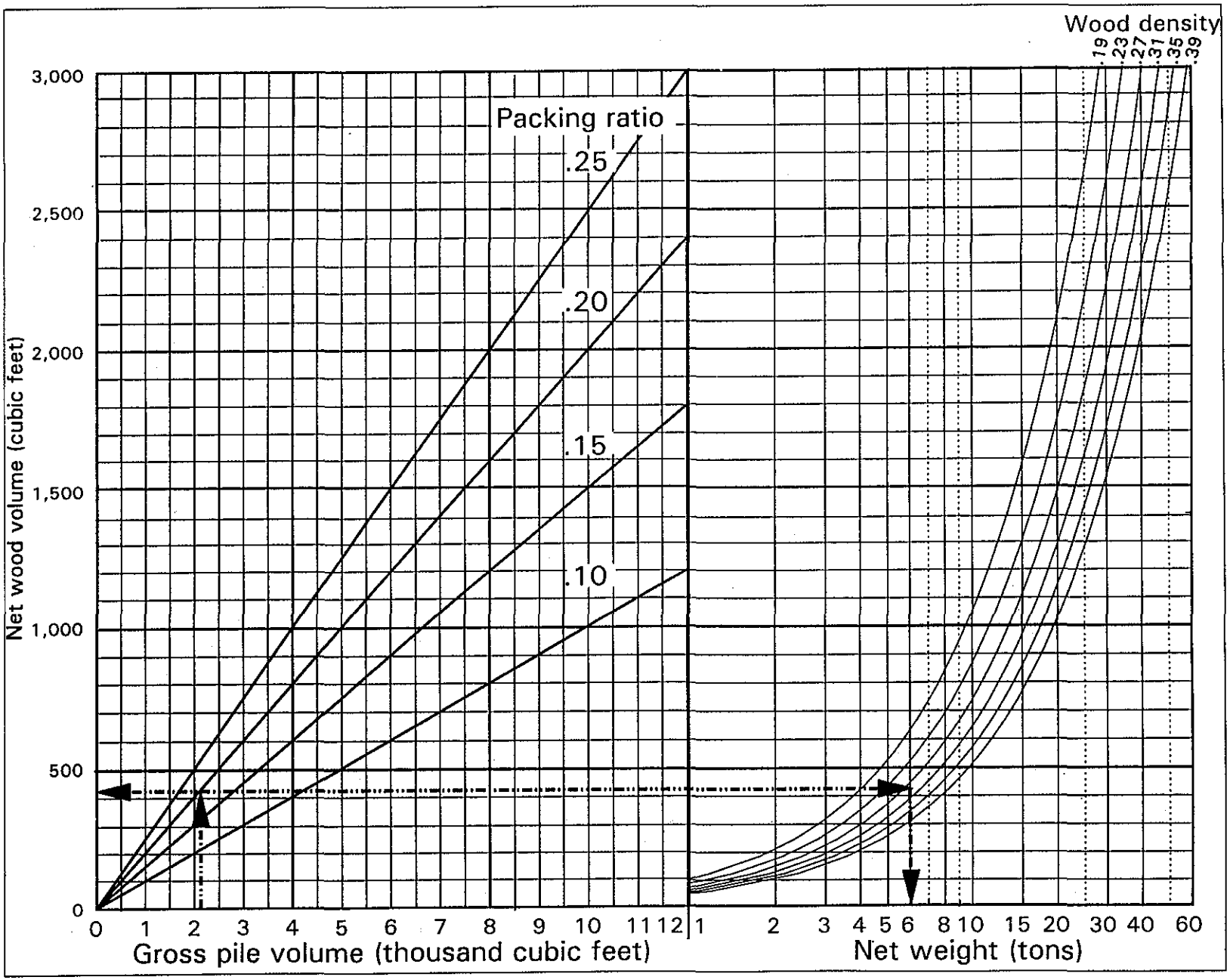

Figure 6—The nomagram assists in determining net mass of the wood (X-axis at right) by using gross pile volume (X-axis at left), packing ratio (diagonal lines at left), net wood volume (Y-axis), and wood density (curves at right).

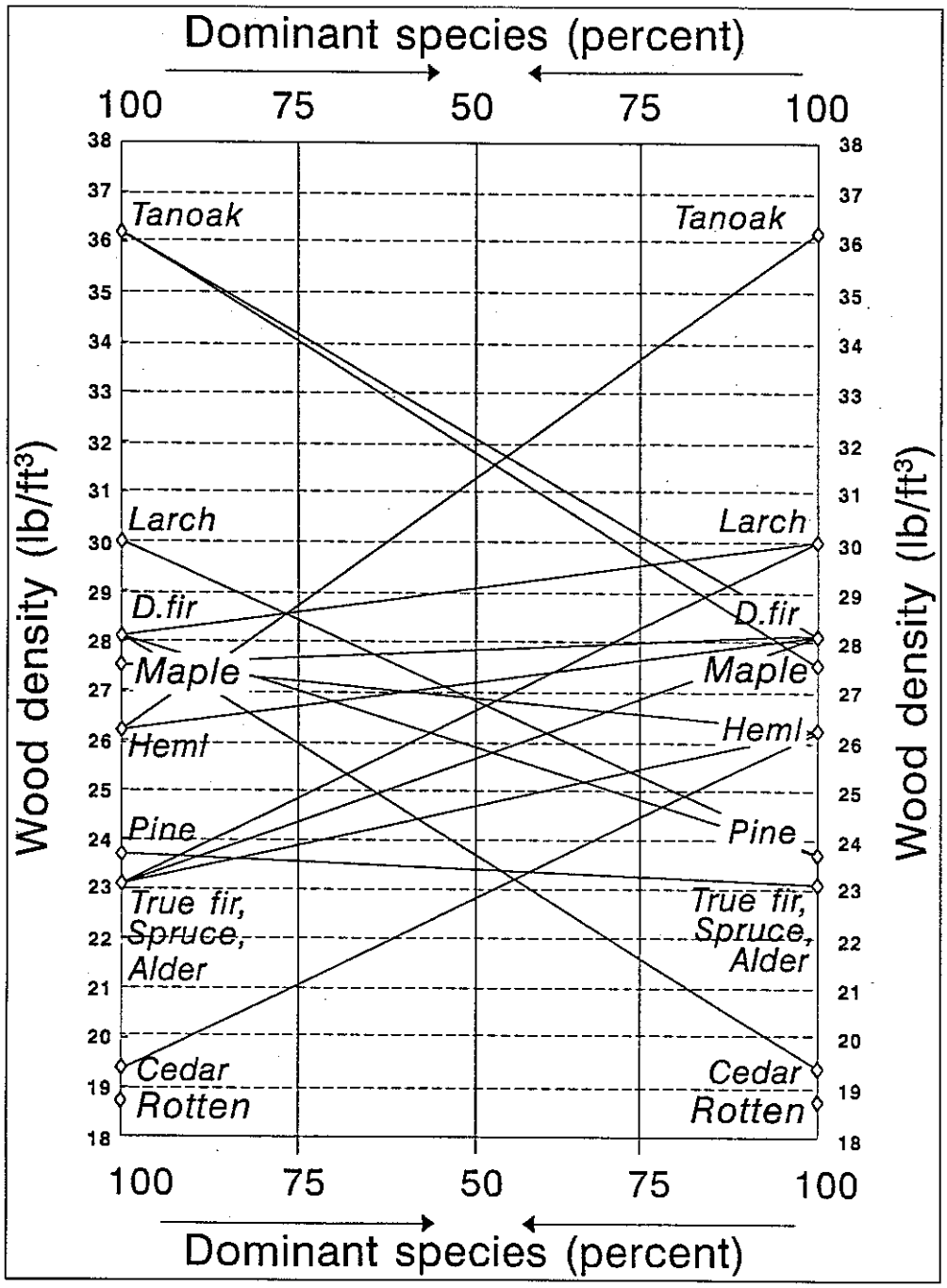

Figure 7—The nomagram can be used to calculate a weighted-average wood density (Y-axes) for two species by finding a point along a diagonal line representing two species that intersects with a vertical line indicating the correct proportion of the two species.

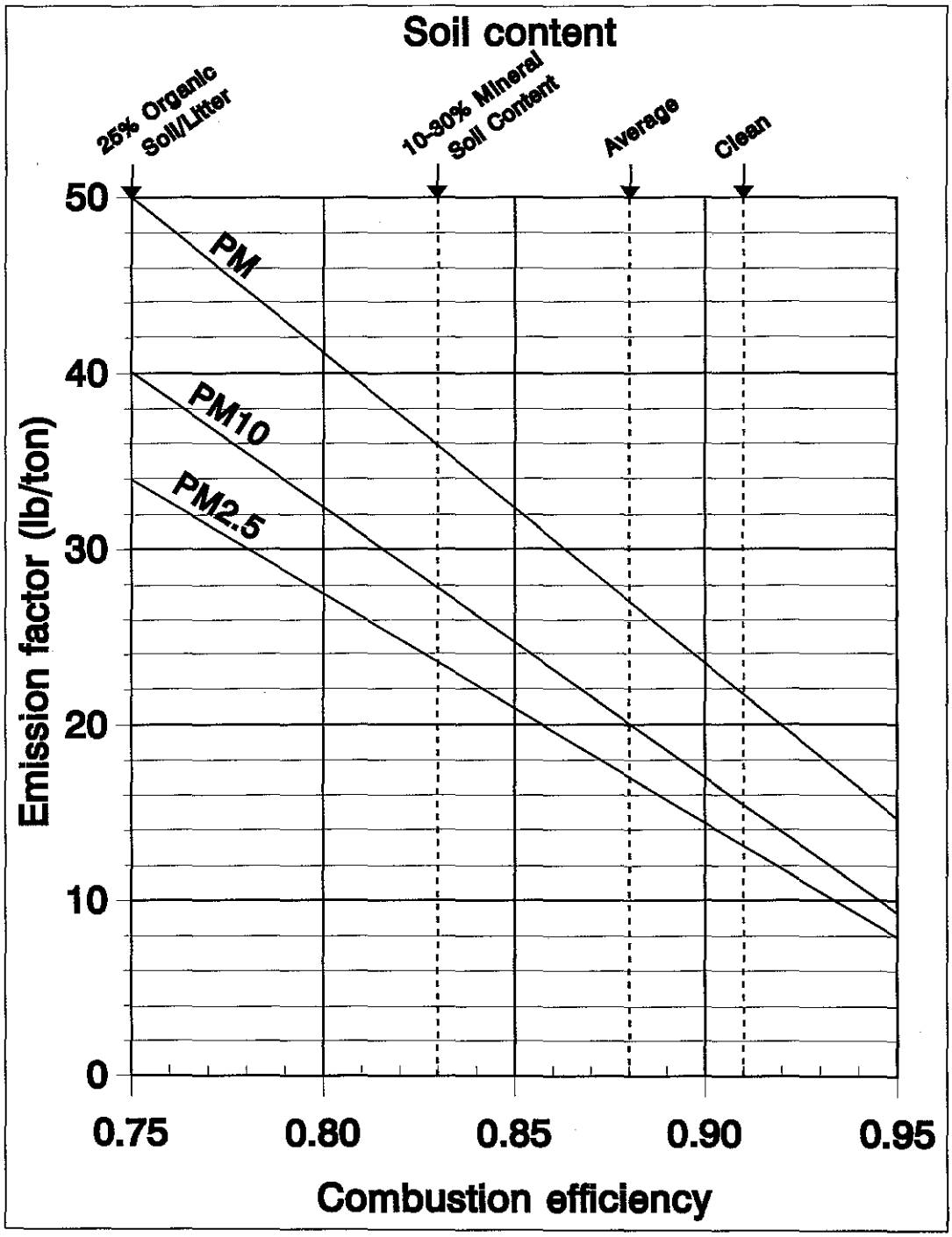

Figure 8—An appropriate emission factor for PM, PM2.5, and PM10 can be determined from knowledge of the relative amount of soil in the pile.

Hardy, Colin C. 1996. Guidelines for estimating volume, biomass, and smoke production for piled slash. Gen. Tech. Rep. PNW-GTR-364. Portland, OR: U.S. Department of Agriculture, Forest Service, Pacific Northwest Research Station. 17 p.

Guidelines in the form of a six-step approach are provided for estimating volumes, oven-dry mass, consumption, and particulate matter emissions for piled logging debris. Seven stylized pile shapes and their associated geometric volume formulae are used to estimate gross pile volumes. The gross volumes are then reduced to net wood volume by applying an appropriate wood-to-pile volume packing ratio. Next, the oven-dry mass of the pile is determined by using the wood density, or a weighted-average of two wood densities, for any of 14 tree species commonly piled and burned in the Western United States. Finally, the percentage of biomass consumed is multiplied by an appropriate emission factor to determine the mass of PM, PM10, and PM2.5 produced from the burned pile. These estimates can be extended to represent multiple piles, or multiple groups of similar piles, to estimate the particulate emissions from an entire burn project.

Keywords: Fuel, emissions, piled slash, smoke management.

The **Forest Service** of the U.S. Department of Agriculture is dedicated to the principle of multiple use management of the Nation's forest resources for sustained yields of wood, water, forage, wildlife, and recreation. Through forestry research, cooperation with the States and private forest owners, and management of the National Forests and National Grasslands, it strives—as directed by Congress—to provide increasingly greater service to a growing Nation.

The United States Department of Agriculture (USDA) prohibits discrimination in its programs on the basis of race, color, national origin, sex, religion, age, disability, political beliefs, and marital or familial status. (Not all prohibited bases apply to all programs.) Persons with disabilities who require alternative means of communication of program information (Braille, large print, audiotape, etc.) should contact the USDA Office of Communications at (202) 720-2791.

To file a complaint, write the Secretary of Agriculture, U.S. Department of Agriculture, Washington, DC 20250, or call (202) 720-7327 (voice), or (202) 720-1127 (TDD). USDA is an equal employment opportunity employer.

Pacific Northwest Research Station
333 S.W. First Avenue
P.O. Box 3890
Portland, Oregon 97208-3890

Available online at www.sciencedirect.com
SCIENCE DIRECT®
Forest Ecology and Management 208 (2005) 383–397
Forest Ecology and Management
www.elsevier.com/locate/foreco

Fuel reduction and coarse woody debris dynamics with early season and late season prescribed fire in a Sierra Nevada mixed conifer forest☆

Eric E. Knapp [a,*], Jon E. Keeley [b], Elizabeth A. Ballenger [b,1], Teresa J. Brennan [b]

[a] *U.S. Forest Service, Pacific Southwest Research Station, 3644 Avtech Parkway, Redding, CA 96002, USA*
[b] *U.S. Geological Survey, Sequoia and Kings Canyon Field Station, HCR 89, Box 4, Three Rivers, CA 93271, USA*

Received 10 November 2004; received in revised form 19 January 2005; accepted 19 January 2005

Abstract

Fire exclusion has led to an unnatural accumulation and greater spatial continuity of organic material on the ground in many forests. This material serves both as potential fuel for forest fires and habitat for a large array of forest species. Managers must balance fuel reduction to reduce wildfire hazard with fuel retention targets to maintain other forest functions. This study reports fuel consumption and changes to coarse woody debris attributes with prescribed burns ignited under different fuel moisture conditions. Replicated early season burn, late season burn, and unburned control plots were established in old-growth mixed conifer forest in Sequoia National Park that had not experienced fire for more than 120 years. Early season burns were ignited during June 2002 when fuels were relatively moist, and late season burns were ignited during September/October 2001 when fuels were dry. Fuel loading and coarse woody debris abundance, cover, volume, and mass were evaluated prior to and after the burns. While both types of burns reduced fuel loading, early season burns consumed significantly less of the total dead and down organic matter than late season burns (67% versus 88%). This difference in fuel consumption between burning treatments was significant for most all woody fuel components evaluated, plus the litter and duff layers. Many logs were not entirely consumed – therefore the number of logs was not significantly changed by fire – but burning did reduce log length, cover, volume, and mass. Log cover, volume, and mass were reduced to a lesser extent by early season burns than late season burns, as a result of higher wood moisture levels. Early season burns also spread over less of the ground surface within the burn perimeter (73%) than late season burns (88%), and were significantly patchier. Organic material remaining after a fire can dam sediments and reduce erosion, while unburned patches may help mitigate the impact of fire on fire-sensitive species by creating refugia from which

☆ This article was written and prepared by U.S. Government employees on official time and is therefore in the public domain and not subject to copyright.

* Corresponding author. Tel.: +1 530 226 2555; fax: +1 530 226 5091.
E-mail address: eknapp@fs.fed.us (E.E. Knapp).
[1] Present address: National Park Service, Southeast Utah Group, 2282 South Resource Blvd., Moab, UT 84532, USA.

0378-1127/$ – see front matter © 2005 Elsevier B.V. All rights reserved.
doi:10.1016/j.foreco.2005.01.016

EXHIBIT 2

these species can recolonize burned areas. Early season burns may be an effective means of moderating potential ecosystem damage when treating heavy and/or continuous fuels resulting from long periods of fire exclusion, if burning during this season is not detrimental to other forest functions.
© 2005 Elsevier B.V. All rights reserved.

Keywords: Burning season; Conifer forest; Duff; Organic matter; Surface fuel; Woody fuel

1. Introduction

Fire exclusion in mixed conifer forests throughout western North America has led to an unnatural accumulation of twigs, branches, logs, litter, and duff, on the forest floor (Parsons and DeBenedetti, 1979; van Wagtendonk, 1985). Due to the lack of fire and increasing tree densities, the spatial continuity of these surface fuels is now also greater (Miller and Urban, 2000). In addition, more of the large downed logs are in a highly decayed state (Skinner, 2002). When ignited, heavy fuels can contribute to extreme wildfire behavior (Arno, 2000; Brown et al., 2003) with potentially detrimental ecosystem consequences (van Wagtendonk, 1985; Stephens, 1998). The heat released by consumption of heavy fuels may cause torching of nearby trees and the embers released by the torching of trees and burning of decayed snags can lead to long-distance spot fires. Rotten logs are readily ignited by embers and are therefore also important in propagating spot fires.

Besides acting as fuel and potentially influencing fire behavior, organic material on the forest floor provides habitat for a large number of forest species, including small mammals (Tallmon and Mills, 1994; Carey and Johnson, 1995; Ucitel et al., 2003; McCay and Komoroski, 2004), reptiles (James and M'Closkey, 2003), amphibians (Bunnell, 1995), and invertebrates (Harmon et al., 1986; Torgersen and Bull, 1995). The presence of organic matter also influences geomorphic processes. Litter and duff aids in water infiltration and reduces the potential for erosion (Agee, 1973). A strong correlation has been found between post-burn watershed sediment yield and the percentage of forest floor exposed by burning (Benevides-Solorio and MacDonald, 2001; Johansen et al., 2001). Logs and other woody debris can dam and retain sediments on slopes and plays an important role in stream channel dynamics (Harmon et al., 1986; Naiman et al., 2002).

With organic matter on the forest floor acting as fuel, habitat, and providing structural integrity to the forest ecosystem, managers are often faced with conflicting considerations (Brown and See, 1981; Brown et al., 2003; Ucitel et al., 2003). Prescription burning is a commonly used method to treat fuels, but fuel reduction targets to reduce wildfire hazard must be balanced with fuel retention targets to maintain habitat and other forest functions. If too much fuel is removed, the heat released may damage trees excessively and the loss of organic matter may lead to erosion and reduced abundance and diversity of fire-sensitive species (Kauffman and Martin, 1989). Conversely, prescribed fires that consume little of the available fuel may not adequately reduce fire hazard. Achieving such a balance can be particularly challenging when fuel loading is high.

The net ecosystem effect of burning, whether by wildfire or prescribed fire, is often closely tied to the amount of heat released. Heat released is in turn proportional to the amount of available fuel (Alexander, 1982; Johnson and Miyanishi, 1995; Whelan, 1995), but fuel moisture, the physical structure of the fuel bed, weather conditions, and a myriad of other factors lead to a high degree of variability in patterns of consumption and subsequent fire effects (Alexander, 1982; Martin and Sapsis, 1992). The excessive litter, duff, and woody debris found in many areas of the Sierra Nevada where fire has been actively suppressed can result in long-duration heating when fire is returned to the system. In the mixed conifer forest, a significant proportion of the "fine fuel" – litter and smaller twigs and stems – is consumed at the flaming front (flaming combustion), leading to a pulse of heat release that has the greatest impact above ground (i.e. canopy scorch on affected trees). The duff layer is typically consumed through smoldering combustion after the flaming front has passed (Kauffman and Martin, 1989). In areas where the duff layer is thick, this smoldering combustion may be

of long duration and generate substantially more heat than flaming combustion (Kauffman and Martin, 1989). Because a significant portion of the heat generated by smoldering combustion is transferred downward (Frandsen and Ryan, 1986; Hartford and Frandsen, 1992), soil and below ground processes are often most strongly impacted. Fire can also persist for long periods in large logs. Decayed logs are more likely to be completely consumed by fire than freshly fallen logs (Brown et al., 1985; Kauffman and Martin, 1989; Skinner, 2002), potentially producing a large amount of heat energy.

Even if extensive crown scorch is avoided with the first burn after a period of fire suppression, the heat produced can injure the cambium, kill roots and lead to the death of even large overstory trees (Ryan and Frandsen, 1991; Swezy and Agee, 1991; Stephens and Finney, 2002). In addition, the greater spatial continuity of fuels may cause fire to burn over a greater proportion of the ground surface. Historically, frequent fires are believed to have kept fuel loads relatively low and the lack of fuel continuity contributed to a highly patchy pattern of fire spread (Swetnam, 1993). The patchiness of fire spread under historical conditions may have been important in reducing the impact of fire on fire-sensitive species by creating abundant refugia from which these species could rapidly recolonize burned areas.

The amount of fuel consumed and percentage of the area burned can be controlled to some extent by varying the fuel moisture and weather conditions that prescription burns are conducted under. In similar mixed conifer forests, Kauffman and Martin (1989) reported that early season burns ignited one month after the last spring precipitation event consumed only 15% of the total available fuel, while early fall burns when fuel moisture was much lower consumed 92% of the total available fuel. Percentage consumption of the litter and duff in early and late season burns was significantly correlated with the moisture content of the lower duff layer. Fuel consumption can also vary by the tree species contributing most of the fuel. Agee et al. (1978) noted that pine litter could be effectively reduced by burning in spring, summer, or fall, but drier summer or fall conditions were required to reduce the more compact white fir (*Abies concolor*) and giant sequoia (*Sequoiadendron giganteum*) litter.

Prior to the policy of fire suppression, fires in the mixed conifer zone of the Sierra Nevada burned a given area approximately every 4–40 years (Kilgore and Taylor, 1979; Swetnam, 1993; Caprio and Swetnam, 1995; Skinner and Chang, 1996). In Sequoia and Kings Canyon National Parks, prescription burning has been used to reduce fuels and restore natural ecosystem processes since the late 1960s (Kilgore, 1973). Most of this burning has been done during the fall months, which is within or after the period when the majority of land area is likely to have burned prior to European settlement (mid-summer to early fall) (Caprio and Swetnam, 1995). Early season (late spring/early summer) burns were historically uncommon and usually associated with dry years. Fires in the fall are desirable from a fire management perspective because they are typically followed by the onset of seasonal rain and snow and therefore require less monitoring. However, fall fires potentially have more impact on air quality in the adjacent Central Valley (Cahill et al., 1996), due to stable atmospheric patterns common at this time of year. A greater proportion of the prescription burning in Sequoia and Kings Canyon National Parks has, in the past few years, been conducted earlier in the season under more favorable smoke dispersal conditions.

The purpose of this study was to evaluate differences in surface fuel consumption, fire coverage (proportion of area burned), and coarse woody debris dynamics with early season and late season prescribed fires, to help managers refine burning prescriptions for this vegetation type. The findings are especially relevant to the first restoration burn after a long period of fire suppression.

2. Materials and methods

2.1. Study site description

Three replicate early season prescribed burn, late season prescribed burn, and unburned control units were established in a completely randomized design in Sequoia National Park (Fig. 1). The study site was located on a northwest-facing bench above the Marble Fork of the Kaweah River, adjacent to the Giant Forest sequoia grove, at elevations ranging from 1900 m to 2150 m above sea level. Each unit was 15–20 ha in

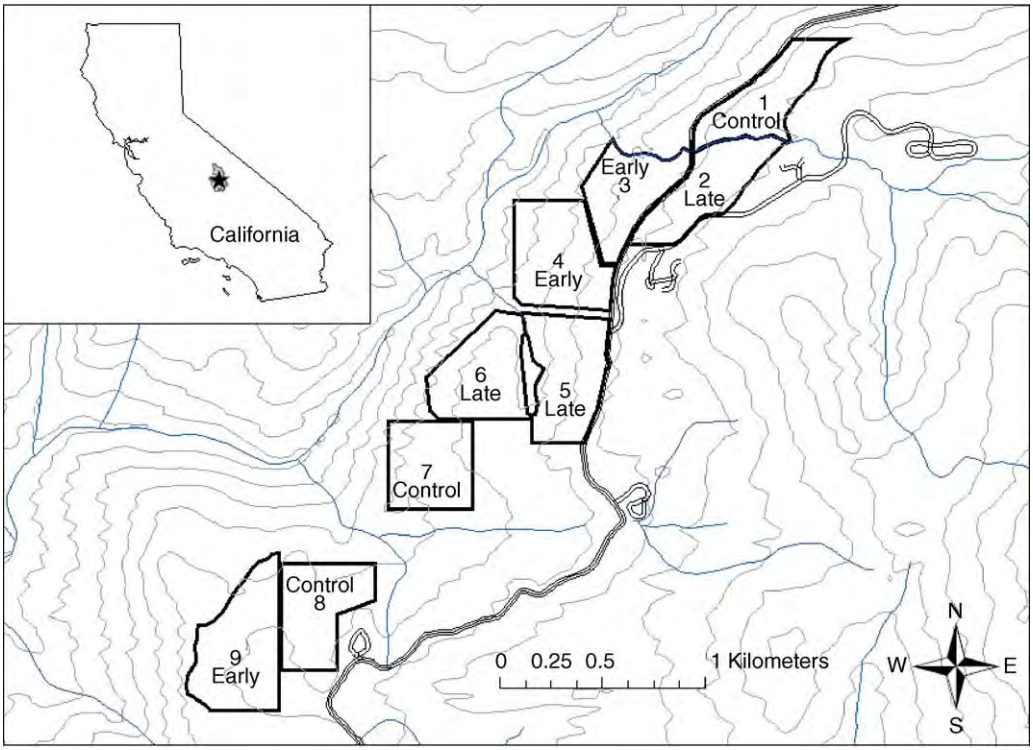

Fig. 1. Map showing location of the early and late season prescribed fire treatment areas in Sequoia National Park, California. The contour interval is 60 m.

size. Tree species in this old-growth mixed conifer forest were, in order of abundance, white fir, sugar pine (*Pinus lambertiana*), incense cedar (*Calocedrus decurrens*), red fir (*A. magnifica* ssp. *shastensis*), Jeffrey pine (*P. jeffreyi*), ponderosa pine (*P. ponderosa*), dogwood (*Cornus nuttallii*), and California black oak (*Quercus kelloggii*). Pre-treatment tree density and basal area averaged 714/ha and 66.5 m^2/ha, respectively. More than half of the trees (370/ha) had a diameter at breast height (dbh) >10 cm and numerous large trees were present (41 trees/ha with a dbh >80 cm). Cross-dating of wood sections containing fire scars collected from snags indicated that the pre-settlement fire return interval in the study area ranged between 15 and 40 years but the last major fire occurred in 1879 (Caprio and Knapp, unpublished data).

Early season burns were conducted 20 and 27 June 2002 and late season burns were conducted 28 September, 17 and 28 October 2001. Weather data (ambient air temperature, relative humidity, wind speed, and wind direction) were taken hourly immediately prior to and during the burns using a belt weather kit. Conditions were similar during burns within burning season treatment. Ambient air temperature was somewhat higher during the early season burns (range = 16–22 °C) than during the late season burns (range = 13–18 °C). Relative humidity and wind speed ranged from 44 to 68% and 0 to 8 km/h, respectively, during the early season burns and 20 to 63% and 0 to 7 km/h, respectively, during the late season burns. The period of relative humidity <40% during the late season burns was confined to the morning of one burn (17 October) and occurred as a temperature inversion dissipated. Relative humidity for much of this burn was within the range experienced during the others.

Ignition was accomplished using drip torches and was initiated at the highest elevation within each burn unit. Three and sometimes four ignition specialists spaced 10–15 m apart walked perpendicular to the slope from higher to lower elevations igniting strips

and spot-igniting fuel ''jackpots''. Burns were mainly strip head fires of low to moderate intensity. With the exception of occasional single small trees that torched, fire was predominantly on the surface.

2.2. Fuel moisture

Fuel moisture measurements were made at the time of ignition for each burn. Woody fuels of different size classes, in addition to litter and duff, were collected in different microenvironments within the burn unit and separately placed into air-tight plastic bags or nalgene bottles. The larger woody fuels were obtained by cutting 1–2 cm wide cross sections out of logs with a chain saw. Samples were returned to the lab, weighed wet, dried in a mechanical convection oven at 85 °C for 48 h, and weighed again. Because several of the duff samples collected prior to one of the early season burns contained a significant amount of mineral soil, separate duff samples were re-collected shortly after the burn in an adjacent unburned forest area with similar aspect, species composition, and canopy cover.

2.3. Surface fuel loading

Mass of surface fuel (dead and down woody fuels plus litter and duff) was estimated both prior to treatment and following treatment using Brown's planar intercept method (Brown, 1974). Two 20 m transects were installed at each of 36 spatially referenced points located on a 50 m grid within each unit. The direction of the first transect was based on a random bearing (n), and the second transect was placed $n + 120^\circ$ from the first. The proximal end of each transect was offset 2 m from the gridpoint to avoid disturbance in the area of the grid point. Number of intercepts of 1-h (hour) (0–6 mm) and 10-h (>6–25 mm) fuels were counted along the first 2 m of the transect, while 100-h (>25–76 mm) fuels were counted along the first 4 m of the transect. The 1000-h fuels (>76 mm) were counted along the entire length of the transect. Diameter, species, and decay class (sound or rotten) of each 1000-h log was noted. A log was considered rotten if it could be dented or broken up with a kick. The maximum height above the ground of elevated dead woody fuel was measured in three adjacent 33 cm long sections in the center of the transect. Litter and duff depth measurements were also taken at three spots along the transect (5 m, 10 m, and 15 m). Depth measurements were made 50 cm to the right of the transect prior to treatment and 50 cm to the left of the transect post-treatment. Because so little of the forest floor was composed of freshly cast leaf and needle material at the time of sampling, we defined litter as both the freshly cast and fermentation layers (fermentation layer = cemented together by fungal growth but the shape and structure of needles, etc. still visible). The duff layer was anything below the fermentation layer down to mineral soil. Fuel loads were calculated using formulas of Brown (1974) with individual tree species constants for bulk density, squared quadratic mean diameter, and non-horizontal correction from van Wagtendonk et al. (1996, 1998). The individual species constants were weighted by the proportional basal area of tree species in the study area. Total litter and duff fuel mass was estimated using fuel depth to weight relationships developed for the study area (described below).

At the time of the second census (post-burn), the total transect length covering areas that burned, did not burn, or were composed of rock were mapped along each Brown's transect. Patchiness of the burn pattern was estimated by calculating the average number and average size of unburned patches. Brown's transects in the early season burn units were surveyed shortly after the burns and in the same growing season, while the late season burns were followed by snowfall and could not be evaluated until the following spring. The fuel reduction estimates for the late season burns were therefore corrected for the amount presumed to have been added over the winter and prior to the fuel survey. Because late season burns consumed nearly the entire litter and duff layers where fire passed over the surface (see duff pin methods, next paragraph), all litter, duff, and small woody fuels on burned ground were assumed to have fallen since the burns and were not considered in the calculation of post-burn fuel estimates. Large woody fuel pieces that obviously fell post-burn (i.e. lying in a burned area but showing no visual evidence of combustion) were also not considered. Few large woody fuel pieces fell over the winter in the unburned controls, and these were identified by comparison with pre-treatment data. Other fuel categories in the unburned controls were not similarly corrected, but their amounts were presumed to have been negligible (far more fuel

was added to the late season burn plots over the winter due to loss of scorched needles and instability of partially consumed snags).

To more accurately evaluate litter and duff consumption in areas where fire burned, duff pins consisting of 30 cm nails or 75 cm sections of rebar were pounded into and flush with the forest floor and extending into the mineral soil. Four duff pins were installed adjacent to each grid point. Shortly after each burn, pins were reexamined and distances from the top of the duff pin to the top of remaining unburned forest floor material as well as the total distance from the top of the pin to mineral soil were measured.

2.4. Litter and duff depth: weight relationships

Forest floor samples were collected across the study area prior to treatment to develop a regression equation relating forest floor depth to forest floor mass. A 30 cm × 30 cm metal frame was pushed into the forest floor 5 m from the end of one fuel transect per gridpoint, at a random bearing. Litter and duff was excavated using a metal cutter and composition of the litter was scored visually as belonging to one of the three following categories; >80% short needle (*Abies* sp. and *Calocedrus decurrens*), >80% long needle (*Pinus* sp.), and mixed. Litter and duff were bagged separately. To ensure collection of all organic material, duff was collected past the mineral soil surface and later washed to remove the soil and rock portion. After the forest floor sample was removed, the depth of each layer was measured at the center of each side of the excavated square and averaged by layer for that sample. All litter and washed duff samples were dried at 85 °C in a mechanical convection oven for 48 h. After weighing the litter samples, all woody fuels with a diameter less than 7.6 cm were removed from the sample and weighed (woody fuels larger than 7.6 cm were not collected—the sampling frame was moved if the sampling point intersected with a section of woody fuel larger than 7.6 cm). Weights of woody fuels were subtracted from the total sample weight in developing the litter and duff depth: weight relationships.

2.5. Other fuels

Estimates of live fuel mass were not taken because the biomass contained within the understory (tree seedlings, grasses, forbs, and shrubs) was minimal relative to mass of dead and downed surface fuel. Although these live fuels did often burn and occasionally resulted in locally more intense fire activity, the overall contribution to fire effects was likely very low.

2.6. Coarse woody debris

Additional measurements were made on larger logs in order to obtain a better understanding of changes in habitat value, such as cover and volume, that could not be gained from Brown's transect data. Course woody debris (CWD) data were collected using methods similar to those described in Bate et al. (2002). A 4 m × 20 m strip plot was established along the second Brown's transects at every other gridpoint, with the transect forming the centerline of the plot. All logs or portions of logs that were at least 1m in total length and with a large end diameter of at least 15 cm (in or out of the plot) were counted and large end and small end diameters measured. If a log extended outside the plot, diameters were measured at the line of intercept with the plot boundary and the CWD piece. Logs were assumed to end when the diameter fell below 7.6 cm. Logs were not measured if more than half of the log was buried within the forest floor material. Two log lengths were measured—the length within the plot area, and total length. Log number was estimated as a count of logs with midpoints falling within the boundaries of the plot.

2.7. Data analysis

Separate fuel depth to weight regression equations were calculated for litter and duff composed primarily of fir, primarily of pine, and mixed species. In all calculations, the y-intercept was assumed to be equal to zero. The hypothesis of no difference between slopes of the lines for the three forest floor categories was tested using equations given in Zar (1999).

Fuel moisture of different classes and the percentage of residual litter and duff remaining in areas that burned were summarized at the experimental unit level and arcsine square root transformed prior to analysis using one-way ANOVAs with treatment (early season burn and late season burn) as the sole factor. Differences among treatments in fuel and CWD

variables were evaluated with analysis of covariance (ANCOVA), using the pre-treatment numbers as a covariate. The treatment × covariate interaction was included in the model as well in cases where it was statistically significant. Linear contrasts, set a priori, were used to estimate the effect of burning (burns versus unburned control), and the effect of season of burning (early versus late). If the treatment × covari-covariate interaction was significant, the contrasts were calculated on the interaction at the level of the mean of the covariate. Differences between burning treatments in percentage of area burned, number of unburned patches per 20 m, and unburned patch size were evaluated using one-way ANOVAs. While both the average number of unburned patches and average unburned patch size variables did not require transformation, average percentage of area burned was arcsine square root transformed prior to analysis. A statistical significance level of $P < 0.05$ was used for all tests. Calculations were made using either SYSTAT v. 10 (SPSS Inc., Chicago, IL) or SAS v. 8 (SAS Institute, Cary, NC).

3. Results

3.1. Fuel moisture

Fuels within all size categories were significantly wetter during the early season burns than during the late season burns (Table 1). The difference in moisture was especially pronounced for large woody fuels and duff. Early season fuel moisture was for most woody fuel categories somewhat higher than the range within which Sequoia and Kings Canyon National Parks usually conducts prescribed burns in this vegetation type (Table 1). While woody fuels in the late season were within the prescription range, the 1000 h fuels were on the dry end of the prescription (Table 1).

3.2. Fuel loading and consumption

Separate regression coefficients for the depth to weight relationship were initially calculated for the three tree overstory categories—short needled, long needled, and mixed. However, neither the slope coefficients for the three litter categories nor the slope coefficients for the three duff categories were found to differ significantly from each other. Therefore, all data were combined and single equations were calculated for the litter and duff layers. A significant linear relationship with high r^2 was found between depth and mass for both litter and duff fuel samples (Fig. 2).

Prior to treatment, total fuel load averaged 191.6 Mg/ha across treatments (Table 2). Over half of this fuel (105.7 Mg/ha) was found in the litter and duff layers. Large logs (>7.6 cm diameter) comprised the majority of the woody fuels (77.5 Mg/ha), and 69% were classified as rotten. All surface fuel categories were significantly reduced by either early or late season burning, relative to the unburned control (Table 3). However, significantly less total fuel was consumed by early season burns (Table 3). The early season and late season burns consumed 67% and 88% of the available surface fuel, respectively. When broken down into individual surface fuel categories, significantly less was consumed for most with early

Table 1
Percentage moisture of fuels at the time of early season and late season prescribed burns in Sequoia National Park

Fuel type (fuel diameter)	Fuel moisture (%)		*P*-value	Fuel moisture prescription range (%)
	Early season (June 2002)	Late season (September/October 2001)		
1 h (0–0.6 cm)	13.5	8.9	0.018	5–12
10 h (0.6–2.5 cm)	12.7	8.8	0.001	6–13
100 h (2.5–7.6 cm)	16.9	10.4	0.032	7–14
1000 h (>7.6 cm)	26.4	10.6	0.020	10–20
Litter	22.5	11.3	0.011	–
Duff	37.9	11.7	0.002	–

Litter was considered the freshly cast and fermentation layers, while duff was considered the humus layer. Statistical significance of difference between treatments was tested using analysis of variance after arcsine square root transformation.

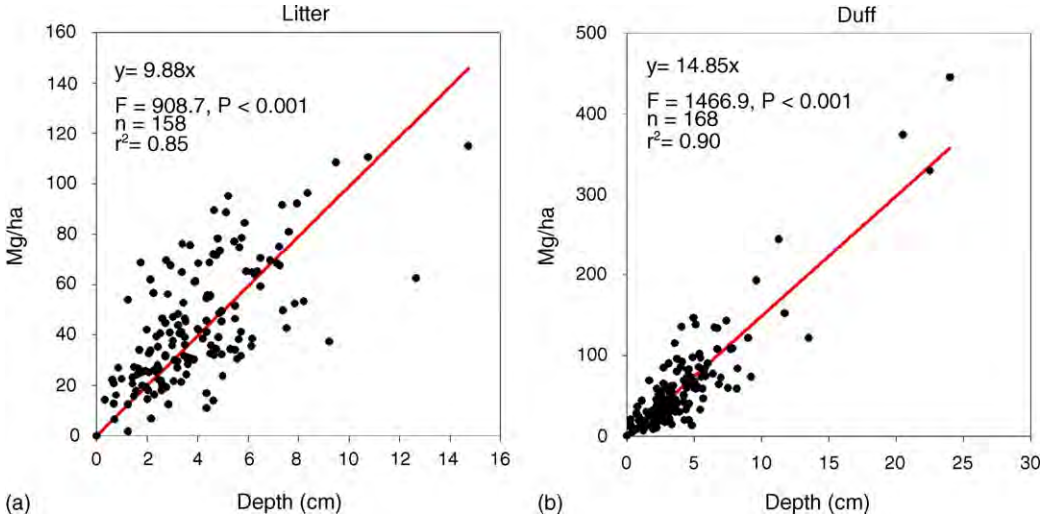

Fig. 2. Depth to mass regressions for (a) litter (freshly cast and fermentation layers) and (b) duff (humus layer) from systematic collections of litter and duff made throughout the study area. Samples were dried at 85 °C for two days before weighing.

season burns, and differences in the 10 h and 1000 h categories were nearly statistically significant. Average height of woody surface fuel above the forest floor was significantly reduced by fire, but there was no difference between the early and late season prescribed fire treatments (Table 3).

Less fuel consumption by early season burns was due to both a significantly greater amount of residual fuel remaining in areas that burned (Fig. 3a), and significantly less area burned within the fire perimeter (Fig. 3b). Early season burns left approximately five times more litter and duff unconsumed in areas where fire passed over the forest floor than late season burns. Early season burns were also significantly patchier (Fig. 3c) and the size of these unburned patches tended to be smaller (Fig. 3d).

3.3. Coarse woody debris

Large quantities of coarse woody debris were found in the study area. Prior to the prescribed burns, number of downed logs averaged 173/ha (91 with a diameter <30 cm and 82 with a diameter ≥30 cm) and covered an average of 4.3% of the ground surface area (Table 4). The total length of logs averaged 1064 m/ha, with a total volume of 190 m^3/ha (Table 4). Log mass averaged 61.7 Mg/ha, less than the 78.6 Mg/ha of 1000 h fuel estimated with Brown's transects. The

Table 2
Mean mass (standard error in parenthesis) of different fuel categories and height of woody fuels above the litter surface prior to and after treatment by early season and late season prescribed burns

Treatment	Time of survey	1 h (<0.6 cm) (Mg/ha)	10 h (0.6–2.5 cm) (Mg/ha)	100 h (2.5–7.6 cm) (Mg/ha)	1000 h (>7.6 cm) (Mg/ha)	Litter (L&F layers) (Mg/ha)	Duff (H layer) (Mg/ha)	Fuel total (Mg/ha)	Fuel height (cm)
Unburned	Pre-treatment	1.4 (0.04)	2.8 (0.1)	4.8 (0.3)	95.8 (11.0)	40.5 (4.8)	66.8 (5.6)	212.0 (17.3)	10.6 (1.5)
Early burn	Pre-treatment	1.1 (0.1)	2.7 (0.2)	4.7 (0.3)	70.6 (6.6)	42.8 (0.7)	59.5 (5.9)	181.3 (12.2)	11.3 (1.2)
Late burn	Pre-treatment	1.0 (0.1)	2.4 (0.2)	4.4 (0.3)	66.2 (9.5)	38.0 (1.8)	69.5 (2.9)	181.4 (13.5)	9.4 (0.2)
Unburned	Post-treatment	1.1 (0.02)	2.5 (0.1)	5.0 (0.2)	86.5 (9.8)	37.9 (1.4)	76.5 (0.9)	209.4 (10.2)	12.2 (1.4)
Early burn	Post-treatment	0.3 (0.04)	0.7 (0.1)	1.6 (0.1)	31.0 (4.2)	7.7 (0.3)	18.4 (2.2)	59.7 (5.3)	4.0 (0.6)
Late burn	Post-treatment	0.1 (0.04)	0.2 (0.1)	0.3 (0.1)	15.0 (1.3)	2.0 (0.5)	4.9 (1.8)	22.5 (3.2)	4.0 (1.1)

Table 3
Significance of analysis of covariance results for fuel size categories and fuel height after application of the burning treatments

Effect	d.f.	*P*-value							
		1 h (<0.6 cm)	10 h (0.6–2.5 cm)	100 h (2.5–7.6 cm)	1000 h (>7.6 cm)	Litter (L&F layers)	Duff (H layer)	Fuel total	Fuel height
Covariate	1	0.019	0.031	0.001	0.051	<0.001	0.002	0.007	0.337
Treatment	2	<0.001	<0.001	<0.001	0.002	<0.001	<0.001	<0.001	0.003
Burn vs. unburned	1	<0.001	<0.001	<0.001	0.001	<0.001	<0.001	<0.001	0.001
Early vs. late	1	0.008	0.070	0.001	0.068	0.004	0.004	0.004	0.441
Error	5								

Pre-treatment data were used as a covariate. The treatment × covariate interaction was not significant for any of the dependent variables and was therefore not included.

difference is likely due to the more restrictive definition of CWD.

Burning treatments resulted in a significant reduction in all CWD measures except log number (Table 5). Many logs were not completely consumed by fire. While late season burns resulted in significantly greater reduction in log cover, log volume, and log mass compared to early season burns, reduction in log length and log number did not differ between burning season treatments (Table 5). This difference between CWD variables in response to burning season treatment may be related to the tendency of early season burns to consume just the outer layers of many of the larger logs. While the late season burns also often did not consume the entire log, a greater proportion of the wood circumference was typically consumed. The reduction in CWD mass between burning season treatments was similar for the

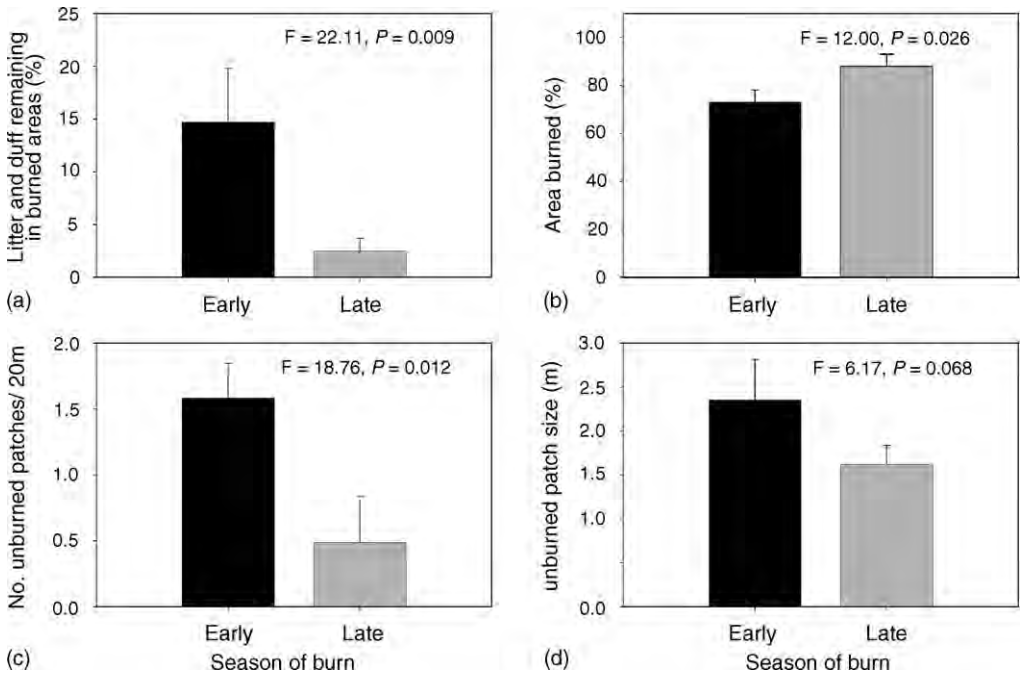

Fig. 3. Average percentage of residual litter and duff remaining in areas that burned (a), average percentage of area burned (b), average number of unburned patches within 20 m long Brown's fuel transects (c), and average size of unburned patches located within 20 m long Brown's fuel transects (d) in early season and late season prescribed fires.

Table 4
Means (standard errors in parentheses) of coarse woody debris attributes prior to and after treatment by early season and late season prescribed burns

Treatment	Time of survey	No. logs/ha, <30 cm diameter	No. logs/ha, ≥30 cm diameter	Log length (m/ha)	Log cover (%)	Log volume (m^3/ha)	Log mass (Mg/ha)
Unburned	Pre-treatment	90.3 (4.0)	108.8 (26.1)	1210.7 (128.3)	5.2 (0.6)	246.1 (19.6)	79.2 (6.4)
Early burn	Pre-treatment	134.3 (4.6)	76.4 (6.9)	1208.2 (51.5)	4.5 (0.7)	184.8 (48.6)	58.8 (14.8)
Late burn	Pre-treatment	48.6 (8.0)	62.5 (13.9)	772.2 (102.9)	3.3 (0.5)	138.5 (19.7)	47.2 (7.0)
Unburned	Post-treatment	111.1 (17.5)	104.2 (28.9)	1155.6 (102.0)	4.6 (0.5)	204.5 (22.8)	69.1 (8.5)
Early burn	Post-treatment	113.4 (11.6)	60.2 (6.1)	708.6 (35.8)	2.2 (0.1)	75.1 (51.3)	26.2 (2.6)
Late burn	Post-treatment	34.7 (10.6)	32.4 (6.1)	302.9 (57.3)	0.8 (0.1)	20.0 (2.1)	7.4 (0.9)

two measurement methods (percentage reduction of these components with early and late season burns averaged 55% and 77%, respectively, when measured using Brown's transects, and 56% and 84%, respectively, when measured using strip plot surveys).

4. Discussion

Fuel moisture was likely the main cause of differences in fuel consumption with early and late season burns. Because energy is necessary to drive off water before combustion is possible, more energy is required to propagate flaming combustion in moist fuels than dry fuels (Frandsen, 1987; Nelson, 2001). Consumption of large woody fuel is often quite high at moisture levels equal to or less than 10–15%, but less than half of these fuels are typically consumed when moisture levels exceed 25–30% (Brown et al., 1985). In this study, some logs were likely drier, while others, particularly partially rotten logs in shady locations, were likely considerably wetter than the average 26% moisture content of large logs (1000 h fuels) at the time of early season burns. Kauffman and Martin (1989) found that moisture content of the lower duff layer was the most important fuel or weather-related variable in multiple regression models of duff consumption. Little duff is consumed when the moisture content exceeds 110%, and the duff layer may burn independently of surface fire at a moisture content of less than 30% (Sandberg, 1980). Between these two values, consumption is related to both moisture content and heat of the surface fire (Reinhardt et al., 1991). Brown et al. (1985) reported an inverse linear relationship between duff moisture and percent duff consumption for mixed conifer forests in the northern Rocky mountains, and suggested that moisture content may become an even stronger predictor of consumption the deeper the duff layer.

Fuel moisture also influences fuel consumption through its effect on the amount of area within the

Table 5
Significance of analysis of covariance results for coarse woody debris attributes after application of the burning treatments

Effect	d.f. (treatment × covariate interaction included)	*P*-value					
		No. logs/ha, <30 cm diameter	No. logs/ha, ≥30 cm diameter	Log length (m/ha)	Log cover (%)	Log volume (m^3/ha)	Log mass (Mg/ha)
Covariate	1	0.132	0.353	0.070	0.009	0.007	0.007
Treatment	2	0.125	0.398	0.008	0.003	0.201	0.134
Treatment × covariate	2	–	–	–	–	0.038	0.024
Burn vs. unburned	1	0.122	0.251	0.003	0.001	0.004	0.003
Early vs. late	1	0.166	0.409	0.184	0.045	0.022	0.011
Error	5 (3)						

Pre-treatment data were used as a covariate. The treatment × covariate interaction was included when significant. In these cases, the contrasts for effect of treatments were calculated on the interaction at a value set to the mean of the covariate.

fire perimeter that burns. In fire simulation studies, Hargrove et al. (2000) reported that modeled fires under high fuel moisture conditions produced dendritic and patchy burn patterns, while at lower fuel moisture conditions, little of the landscape within the fire perimeter remained unburned. The model was based on fire ignition and spread in a gridded landscape where the probability of spread to neighboring fuels was evaluated in eight directions. The probability that fire will propagate to neighboring fuels (I) is reduced at higher fuel moisture levels. Interestingly, the maximum variability in fire burn pattern was predicted to occur near the critical threshold of $I = 0.25$, below which most fires remained small or went out. Using a different model, Miller and Urban (2000) also predicted that the functional connectivity of surface fuels would be reduced under higher fuel moisture conditions. Our findings of significantly reduced amount of area within the fire perimeter burned and greater patchiness of early season burns conducted under higher fuel moisture conditions are consistent with these model predictions. Slocum et al. (2003) similarly found that prescribed burns in Florida conducted under higher fuel moisture conditions were patchier than burns conducted when fuels were drier.

Based on fire scar dendrochronology data collected adjacent to our study area, Swetnam (1993) suggested that a fire-free interval as long as that seen today is likely unprecedented in the last 2000 years. By the time of our prescribed burns, a minimum of three to four cycles of fire had likely been missed. As a result, the fuel mass and CWD attributes reported here (log number, log length, log cover, log volume, and log mass) were likely considerably higher than what might have been present without fire suppression. The average of 191.6 Mg/ha of fuel found prior to the prescribed burns in this study was greater than fuel loadings reported for second growth and old-growth mixed conifer forests in northern portions of the Sierra Nevada by Kauffman and Martin (1989) (range, 74.8–163.9 Mg/ha). Keifer (1998) estimated the amount of pre-burn fuel to be 143.5 Mg/ha in several plots of mixed conifer/giant sequoia forest in Sequoia National Park that hadn't burned in over 40 years. A nearby mixed conifer that had also not experienced fire since pre-settlement times contained 210 Mg/ha of fuel (Mutch and Parsons, 1998), which is comparable to levels found in this study.

Accurate estimates of fuel mass and consumption are essential to predicting fire effects. Slopes of the litter and duff depth to weight regression relationships developed for this study were very similar to the estimates reported by van Wagtendonk et al. (1998) for white fir (litter: 9.88 versus 10.05 for this study and van Wagtendonk et al. (1998), respectively; duff: 14.85 versus 15.18 for this study and van Wagtendonk et al. (1998), respectively), helping to validate the accuracy of both sets of numbers. The 88% reduction in fuel mass recorded in the late season burn treatment was comparable to levels of consumption seen in other fires in mixed conifer forests conducted under dry fall conditions (Kauffman and Martin, 1989; Kilgore, 1972; Mutch and Parsons, 1998), slightly lower than the 91% fuel reduction reported for a dry early fall prescribed fire on a nearby southeast-facing slope in the same watershed (Stephens and Finney, 2002), and somewhat greater than an average consumption of 71% for multiple prescribed fires conducted under a range of fuel moisture conditions in Sequoia National Park (Keifer, 1998). Fuel reduction in the early season burns (67%), while still substantial, was within the range of values reported by Kauffman and Martin (1989) for late spring burns in Sierran mixed conifer forest (61–83%). Our estimate of the percentage of ground surface area within the fire perimeter that burned in the late season prescribed fires (88%) was very close to estimates of Kilgore (1972), who found that 80% of study plots within a late season prescribed fire unit were completely burned, while 14% of plots were partially burned. Similar data has, to our knowledge, not been collected in this vegetation type for early season burns.

With a complete understanding of fire effects often lacking, resource managers may seek to conduct prescription burning operations for restoring the process of fire to these forests that mimic historical fires that the trees and other forest organisms on a site evolved with (Moore et al., 1999; Stephenson, 1999). While the majority of land area historically burned during the dry late summer to early fall period, prescribed fires at the same time of year may now generate fire effects outside of the historical norm, due to the current high fuel loading conditions. These fire effects are potentially a function of not only of

changes in the abundance of fuels, but the changes in the proportion of fuels that are in a highly decayed state. The dominant woody fuels in this system tend to decompose relatively rapidly. Harmon et al. (1987) reported a half life of only 14 years for white fir logs. However, with frequent low to moderate severity fires, large amounts of decomposed wood on the forest floor was likely historically uncommon (Skinner, 2002). Under dry fuel moisture conditions, decomposed logs are more likely to be completely consumed than sound, more recently fallen logs (Kauffman and Martin, 1989; Skinner, 2002; Stephens and Finney, 2002). The cracking and breakage of decomposed wood over time also increases the surface to volume ratio, leading to more rapid consumption and therefore potentially greater heat generation.

In addition to the high surface fuel loadings at the time of the burns, the spatial continuity of these fuels was also likely greater than found historically. Frequent fires are predicted to reduce fuel continuity (Miller and Urban, 2000), and historical fires were therefore likely quite patchy. This same finding can be inferred from Swetnam (1993), who reported a negative relationship between the proportion of trees exhibiting fire scars in any given year and the fire frequency. With more time between fires, the extra fuel buildup apparently aided in fire spread. It is likely that prescribed fires conducted under current levels of fuel continuity and under dry conditions where fire spread is not limited by fuel moisture will result in a greater proportion of the area within the fire perimeter burned, compared to historical fires.

By burning less of the landscape within the fire perimeter, the pattern of consumption of the early season fires was possibly more similar to historical fires. This patchiness may aide in the post-fire recovery of plant and animal populations, as the spatial distribution and size of unburned islands can be important for the recruitment and persistence of species that are sensitive to fire (Turner et al., 1997). Andrew et al. (2000) suggested that refuges provided by unburned logs may allow ant diversity to be maintained, even with frequent fuel-reduction fires. The abundance and distribution of unburned patches may also influence the probability of erosion. From rainfall simulation experiments, Johansen et al. (2001) found that sediment yields resulting from erosion did not change greatly whether 0% or 60–70% of the ground surface was exposed by burning. However, once the threshold of 60–70% of bare ground was exceeded, sedimentation increased sharply, possibly because of the greater probability of the connectedness of bare patches, which made infiltration and sediment capture less likely. The amount of bare ground exposed by early season burns in this study was close to the threshold value reported by Johansen et al. (2001), while the bare ground exposed by late season burns substantially exceeded this threshold. Such erosion simulations may be helpful for better defining target burn area percentages in prescribed fires.

While this study demonstrated that early season burns were not as effective at reducing fuel loading, less fuel consumption and less area within the fire perimeter burned may be beneficial for the recovery rate of important ecosystem components. In addition, more habitat for animal species dependent on CWD was maintained. However, the habitat value of charred but only partially consumed logs, relative to unburned logs, is unknown. Comparisons of these burns with historical fires are not possible, but the early season burns may have produced a landscape closer in many ways to that found after historical fires. The idea of utilizing early season burning as a tool to more gradually get back to the desired forest conditions is not new. Kilgore (1972) described two different strategies for reintroducing fire to the mixed conifer forest after a period of fire exclusion—either a relatively hot ‘‘restoration’’ burn that consumes a large proportion of the total fuel and results in significant mortality of trees, followed by additional burns at longer intervals (necessary because fine fuel accumulation will be slower with fewer remaining overstory trees), or a milder restoration burn followed by additional burns at shorter intervals. Both Arno (2000) and Allen et al. (2002) suggested that fire-induced damage could be reduced by successive burns starting with damp fuels. In the Sierra Nevada, higher fuel moisture conditions can be found both early in the burning season after snow melt, or following the first fall rains but prior to snowfall that persists on the ground. The latter conditions do not occur in all years, and the window of opportunity is typically narrow if it does. Thus, to meet burn area targets with currently available resources and burning strategies will likely

continue to result in substantial burning being conducted during the early season.

Considering burning season as a tool to obtain the desired fire effects needs to also balance other factors that could be influenced by season. For example, earlier burns often occur during the growth or active phase of many organisms, which could potentially result in undesired impacts. Managers have sometimes elected not to conduct burns during bird nesting season, especially for sensitive species that nest in the forest understory (Robbins and Myers, 1992) and early season burns when conditions are moist may coincide with the peak of amphibian surface activity (Pilliod et al., 2003). However, as shown in this study, early season burns conducted under higher fuel moisture conditions also consume less of the forest floor and CWD that provides habitat for these species. Agee (1993) suggested that fires occurring during active growth phase of trees may be more injurious than fires occurring during the dormant season. Early season burns can lead to higher tree mortality by killing more of the fine surface roots of conifers (Swezy and Agee, 1991). In addition, McHugh et al. (2003) found that early season burns result in higher bark beetle activity and greater secondary mortality of some conifer species. All of these factors will need to be considered in decisions about the most appropriate time of year to conduct the first restoration burn after a period of fire suppression. Studies to evaluate potential impacts of burning season on these additional ecosystem components are in progress.

Acknowledgements

We wish to thank Sequoia National Park Fire Management for conducting the prescribed burns, members of the field crews (Anni Ala, Clara Arndt, Todd Erdody, Eric Fabio, Eric Groth, Shauna Hee, Jeffrey Kane, Dan Lieberman, Hanna Mershman, Katie Panichelle, Dorothy Wallace-Senft, and Kelly Wengronowitz) who assisted with data field data collection, Julie Yee and Jim Baldwin for statistical advice, and Tony Caprio for fire history information. The paper benefited from comments by Karen Phillips, Kyle Merriam, Carl Skinner and two anonymous reviewers. This is contribution number 62 of the National Fire and Fire Surrogate (FFS) study, funded by the U.S. Joint Fire Science Program.

References

Agee, J.K., 1973. Prescribed fire effects on physical and hydrologic properties of mixed-conifer forest floor and soil. Ph.D. dissertation, University of California, Berkeley.

Agee, J.K., 1993. Fire Ecology of Pacific Northwest Forests. Island Press, Covelo, CA, USA, p. 493.

Agee, J.K., Wakimoto, R.H., Biswell, H.H., 1978. Fire and fuel dynamics of Sierra Nevada conifers. For. Ecol. Manage. 1, 255–265.

Alexander, M.E., 1982. Calculating and interpreting forest fire intensities. Can. J. Bot. 60, 349–357.

Allen, C.D., Savage, M., Falk, D.A., Suckling, K.F., Swetnam, T.W., Schulke, T., Stacey, P.B., Morgan, P., Hoffman, M., Klingel, J.T., 2002. Ecological restoration of southwestern ponderosa pine ecosystems: a broad perspective. Ecol. Appl. 12, 1418–1433.

Andrew, N., Rodgerson, L., York, A., 2000. Frequent fuel-reduction burning: the role of logs and associated leaf litter in the conservation of ant biodiversity. Aust. Ecol. 25, 99–107.

Arno, S.F., 2000. Fire in western forest ecosystems: effects of fire on flora. In: Brown, J.K., Kapler Smith, J. (Eds.), Wildland Fire in Ecosystems. USDA For. Serv. Gen. Tech. Rep. RMRS-GTR-42, vol. 2. pp. 97–120.

Bate, L.J., Torgersen, T.R., Garton, E.O., Wisdom, M.J., 2002. Accuracy and efficiency of methods to sample logs for wildlife research and management. In: Laudenslayer Jr., W.F., Shea, P.J., Valentine, B.E., Weatherspoon, C.P., Lisle, T.E. (Tech. Coords.), Proceedings of the Symposium on the Ecology and Management of Dead Wood in Western Forests, 2–4 November 1999. Reno, NV. USDA For. Serv. Gen. Tech. Rep. PSW-GTR-181, pp. 811–816.

Benevides-Solorio, J., MacDonald, L.H., 2001. Post-fire runoff and erosion from simulated rainfall on small plots, Colorado Front Range. Hydrol. Processes 15, 2931–2952.

Brown, J.K., 1974. Handbook for Inventorying Downed Woody Material. USDA For. Serv. Gen. Tech. Rep. INT-16.

Brown, J.K., Marsden, M.A., Ryan, K.C., Reinhardt, E.D., 1985. Predicting duff and woody fuel consumed by prescribed fire in the northern Rocky Mountains. USDA For. Serv. Res. Paper INT-337.

Brown, J.K., Reinhardt, E.D., Kramer, K.A., 2003. Coarse woody debris: managing benefits and fire hazard in the recovering forest. USDA For. Serv. Gen. Tech. Rep. RMRS-GTR-105.

Brown, J.K., See, T.E., 1981. Downed dead woody fuel and biomass in the northern Rocky Mountains. USDA For. Serv. Gen. Tech. Rep. INT-117.

Bunnell, F.L., 1995. Forest-dwelling vertebrate faunas and natural fire regimes in British Columbia: patterns and implications for conservation. Conserv. Biol. 9, 636–644.

Cahill, T.A., Carroll, J.J., Campbell, D., Gill, T.E., 1996. Air quality. In: Sierra Nevada Ecosystem Project, Final Report to Congress,

vol. II, Assessments and Scientific Basis for Management Options. University of California Davis, Centers for Water and Wildland Resources, pp. 1227–1260.

Caprio, A.C., Swetnam, T.W., 1995. Historic fire regimes along an elevational gradient on the west slope of the Sierra Nevada, California. In: Brown, J.K., Mutch, R.W., Spoon, C.W., Wakimoto, R.H. (Tech. Coords.), Proceedings of the Symposium on Fire in Wilderness and Park Management, 30 March–1 April 1993. Missoula, MT. USDA For. Serv. Gen. Tech. Rep. INT-320, pp. 173–179.

Carey, A.B., Johnson, M.L., 1995. Small mammals in managed, naturally young, and old-growth forests. Ecol. Appl. 5, 336–352.

Frandsen, W.H., 1987. The influence of moisture and mineral soil on the combustion limits of smoldering forest duff. Can. J. For. Res. 17, 1540–1544.

Frandsen, W.H., Ryan, K.C., 1986. Soil moisture reduces belowground heat flux and soil temperatures under a burning fuel pile. Can. J. For. Res. 16, 244–248.

Hargrove, W.W., Gardner, R.H., Turner, M.G., Romme, W.H., Despain, D.G., 2000. Simulating fire patterns in heterogeneous landscapes. Ecol. Model. 135, 243–263.

Harmon, M.E., Cromack Jr., K., Smith, B.G., 1987. Coarse woody debris in mixed-conifer forests, Sequoia National Park, California. Can. J. For. Res. 17, 1265–1272.

Harmon, M.E., Franklin, J.F., Swanson, F.J., Sollins, P., Gregory, S.V., Lattin, J.D., Anderson, N.H., Cline, S.P., Augmen, N.G., Sedell, J.R., Lienkaemper, G.W., Cromack Jr., K., Cummins, K.W., 1986. Ecology of coarse woody debris in temperate ecosystems. Adv. Ecol. Res. 15, 133–302.

Hartford, R.A., Frandsen, W.H., 1992. When it's hot, it's hot . . . or maybe it's not! (surface flaming may not portend extensive soil heating) Int. J. Wildland Fire 2, 134–144.

James, S.E., M'Closkey, R.T., 2003. Lizard microhabitat and fire fuel management. Biol. Conserv. 114, 293–297.

Johansen, M.P., Hakonson, T.E., Breshears, D.D., 2001. Post-fire runoff and erosion from rainfall simulation: contrasting forests with shrublands and grasslands. Hydrol. Processes 15, 2953–2965.

Johnson, E.A., Miyanishi, K., 1995. The need for consideration of fire behavior and effects in prescribed burning. Rest. Ecol. 3, 271–278.

Kauffman, J.B., Martin, R.E., 1989. Fire behavior, fuel consumption, and forest-floor changes following prescribed understory fires in Sierra Nevada mixed conifer forests. Can. J. For. Res. 19, 455–462.

Keifer, M.B., 1998. Fuel load and tree density changes following prescribed fire in the giant sequoia-mixed conifer forest: the first 14 years of fire effects monitoring. In: Proceedings of the Tall Timbers Fire Ecology Conference, vol. 20. pp. 306–309.

Kilgore, B.M., 1972. Impact of prescribed burning on a sequoia-mixed conifer forest. In: Proceedings of the Tall Timbers Fire Ecology Conference, vol. 12. pp. 345–375.

Kilgore, B.M., 1973. The ecological role of fire in Sierran conifer forests: its application to National Park management. Quaternary Res. 3, 496–513.

Kilgore, B.M., Taylor, D., 1979. Fire history of a sequoia-mixed conifer forest. Ecology 60, 129–141.

Martin, R.E., Sapsis, D.B., 1992. Fires as agents of biodiversity: pyrodiversity promotes biodiversity. In: Harris, R.R., Erman, D.E. (Tech. Coords.), Kerner, H.M. (Ed.), Proceedings of the Symposium on Biodiversity of Northwestern California, Santa Rosa, CA, 28–30 October 1991. University of California, Wildland Resources Center, Berkeley, CA. Report No. 29, pp. 150–157.

McCay, T.S., Komoroski, M.J., 2004. Demographic responses of shrews to removal of coarse woody debris in a managed pine forest. For. Ecol. Manage. 189, 387–395.

McHugh, C.W., Kolb, T.E., Wilson, J.L., 2003. Bark beetle attacks on ponderosa pine following fire in northern Arizona. Environ. Entomol. 32, 510–522.

Miller, C., Urban, D.L., 2000. Connectivity of forest fuels and surface fire regimes. Landscape Ecol. 15, 145–154.

Moore, M.M., Covington, W.W., Fule, P.Z., 1999. Reference conditions and ecological restoration: a southwestern ponderosa pine perspective. Ecol. Appl. 9, 1266–1277.

Mutch, L.S., Parsons, D.J., 1998. Mixed conifer mortality and establishment before and after prescribed fire in Sequoia National Park, California. For. Sci. 44, 341–355.

Naiman, R.J., Balian, E.V., Bartz, K.K., Bilby, R.E., Latterell, J.J., 2002. Dead wood dynamics in stream ecosystems. In: Laudenslayer Jr., W.F., Shea, P.J., Valentine, B.E., Weatherspoon, C.P., Lisle, T.E. (Tech. Coords.), Proceedings of the Symposium on the Ecology and Management of Dead Wood in Western Forests, Reno, NV, 2–4 November 1999. USDA For. Serv. Gen. Tech. Rep. PSW-GTR-181, pp. 23–48.

Nelson Jr., R.M., 2001. Water relations of forest fuels. In: Johnson, E.A., Miyanishi, K. (Eds.), Forest Fires: Behavior and Ecological Effects. Academic Press, San Diego, CA, USA, pp. 79–149.

Parsons, D.J., DeBenedetti, S.H., 1979. Impact of fire suppression on a mixed-conifer forest. For. Ecol. Manage. 2, 21–33.

Pilliod, D.S., Bury, R.B., Hyde, E.J., Pearl, C.A., Corn, P.S., 2003. Fire and amphibians in North America. For. Ecol. Manage. 178, 163–181.

Reinhardt, E.D., Brown, J.K., Fisher, W.C., Graham, R.T., 1991. Woody fuel and duff consumption by prescribed fire in northern Idaho mixed-conifer logging slash. USDA For. Serv. Res. Paper INT-443.

Robbins, L.E., Myers, R.L., 1992. Seasonal Effects of Prescribed Burning in Florida: A Review. Tall Timbers Research Inc., Tallahassee, FL, Misc. Pub. No. 8.

Ryan, K.C., Frandsen, W.F., 1991. Basal injury from smoldering fires in mature *Pinus ponderosa* laws. Int. J. Wildland Fire 1, 107–118.

Sandberg, D.V., 1980. Duff reduction by prescribed underburning in Douglas-fir. USDA For. Serv. Res. Paper PNW-272.

Skinner, C.N., 2002. Influence of fire on the dynamics of dead woody material in forests of California and Southwestern Oregon. In: Laudenslayer Jr., W.F., Shea, P.J., Valentine, B.E., Weatherspoon, C.P., Lisle (Tech. Coords.), Proceedings of the Symposium on the Ecology and Management of Dead Wood in Western Forests, Reno, NV, 2–4 November 1999. USDA For. Serv. Gen. Tech. Rep. PSW-GTR-181, pp. 445–454.

Skinner, C.N., Chang, C., 1996. Fire regimes, past and present. In: Sierra Nevada Ecosystem Project, Final Report to Congress, vol. II, Assessments and Scientific Basis for Management Options.

University of California, Davis, Centers for Water and Wildland Resources, pp. 1041–1069.

Slocum, M.G., Platt, W.J., Cooley, H.C., 2003. Effects of differences in prescribed fire regimes on patchiness and intensity of fires in subtropical savannas of Everglades National Park, Florida. Rest. Ecol. 11, 91–102.

Stephens, S.L., 1998. Evaluation of the effects of silvicultural and fuels treatments on potential fire behavior in Sierra Nevada mixed conifer forests. For. Ecol. Manage. 105, 21–35.

Stephens, S.L., Finney, M.A., 2002. Prescribed fire mortality of Sierra Nevada mixed conifer tree species: effects of crown damage and forest floor combustion. For. Ecol. Manage. 162, 261–271.

Stephenson, N.L., 1999. Reference conditions for giant sequoia forest restoration: structure, process, and precision. Ecol. Appl. 9, 1253–1265.

Swetnam, T.W., 1993. Fire history and climate change in giant sequoia groves. Science 262, 885–889.

Swezy, D.M., Agee, J.K., 1991. Prescribed fire effects on fine root and tree mortality in old growth ponderosa pine. Can. J. For. Res. 21, 626–634.

Tallmon, D., Mills, L.S., 1994. Use of logs within home ranges of California red-backed voles on a remnant of forest. J. Mammol. 75, 97–101.

Torgersen, T., Bull, E., 1995. Down logs as habitat for forest-dwelling ants—the primary prey of pileated woodpeckers in northeastern Oregon. Northwest Sci. 69, 294–303.

Turner, M.G., Romme, W.H., Garder, R.H., Hargrove, W.W., 1997. Effects of fire size and pattern on early succession in Yellowstone National Park. Ecol. Monogr. 67, 411–433.

Ucitel, D., Christian, D.P., Graham, J.M., 2003. Vole use of coarse woody debris and implications for habitat and fuel management. J. Wildlife Manage. 67, 65–72.

van Wagtendonk, J.W., 1985. Fire suppression effects on fuels and succession in short-fire-interval wilderness ecosystems. In: Proceedings of the Wilderness Fire Symposium, Missoula, MT, 15–18 November 1983. USDA For. Serv. Gen. Tech. Rep. INT-182, pp. 119–126.

van Wagtendonk, J.W., Benedict, J.M., Sydoriak, W.M., 1996. Physical properties of woody fuel particles of Sierra Nevada conifers. Int. J. Wildland Fire 6, 117–123.

van Wagtendonk, J.W., Benedict, J.M., Sydoriak, W.M., 1998. Fuel bed characteristics of Sierra Nevada conifers. West. J. Appl. For. 13, 73–84.

Whelan, R.J., 1995. The Ecology of Fire. Cambridge University Press, Melbourne, Australia, p. 356.

Zar, J.H., 1999. Biostatistical Analysis, fourth ed. Prentice Hall, New Jersey, p. 663.

Tipping elements in the Earth's climate system

Timothy M. Lenton*†, Hermann Held‡, Elmar Kriegler‡§, Jim W. Hall¶, Wolfgang Lucht‡, Stefan Rahmstorf‡, and Hans Joachim Schellnhuber†‡‖**

*School of Environmental Sciences, University of East Anglia, and Tyndall Centre for Climate Change Research, Norwich NR4 7TJ, United Kingdom; ‡Potsdam Institute for Climate Impact Research, P.O. Box 60 12 03, 14412 Potsdam, Germany; §Department of Engineering and Public Policy, Carnegie Mellon University, Pittsburgh, PA 15213-3890; ¶School of Civil Engineering and Geosciences, Newcastle University, and Tyndall Centre for Climate Change Research, Newcastle NE1 7RU, United Kingdom; and ‖Environmental Change Institute, Oxford University, and Tyndall Centre for Climate Change Research, Oxford OX1 3QY, United Kingdom

**This contribution is part of the special series of Inaugural Articles by members of the National Academy of Sciences elected on May 3, 2005.

Edited by William C. Clark, Harvard University, Cambridge, MA, and approved November 21, 2007 (received for review June 8, 2007)

The term "tipping point" commonly refers to a critical threshold at which a tiny perturbation can qualitatively alter the state or development of a system. Here we introduce the term "tipping element" to describe large-scale components of the Earth system that may pass a tipping point. We critically evaluate potential policy-relevant tipping elements in the climate system under anthropogenic forcing, drawing on the pertinent literature and a recent international workshop to compile a short list, and we assess where their tipping points lie. An expert elicitation is used to help rank their sensitivity to global warming and the uncertainty about the underlying physical mechanisms. Then we explain how, in principle, early warning systems could be established to detect the proximity of some tipping points.

Earth system | tipping points | climate change | large-scale impacts | climate policy

Human activities may have the potential to push components of the Earth system past critical states into qualitatively different modes of operation, implying large-scale impacts on human and ecological systems. Examples that have received recent attention include the potential collapse of the Atlantic thermohaline circulation (THC) (1), dieback of the Amazon rainforest (2), and decay of the Greenland ice sheet (3). Such phenomena have been described as "tipping points" following the popular notion that, at a particular moment in time, a small change can have large, long-term consequences for a system, i.e., "little things can make a big difference" (4).

In discussions of global change, the term tipping point has been used to describe a variety of phenomena, including the appearance of a positive feedback, reversible phase transitions, phase transitions with hysteresis effects, and bifurcations where the transition is smooth but the future path of the system depends on the noise at a critical point. We offer a formal definition, introducing the term "tipping element" to describe subsystems of the Earth system that are at least subcontinental in scale and can be switched—under certain circumstances—into a qualitatively different state by small perturbations. The tipping point is the corresponding critical point—in forcing and a feature of the system—at which the future state of the system is qualitatively altered.

Many of the systems we consider do not yet have convincingly established tipping points. Nevertheless, increasing political demand to define and justify binding temperature targets, as well as wider societal interest in nonlinear climate changes, makes it timely to review potential tipping elements in the climate system under anthropogenic forcing (5) (Fig. 1). To this end, we organized a workshop entitled "Tipping Points in the Earth System" at the British Embassy, Berlin, which brought together 36 leading experts, and we conducted an expert elicitation that involved 52 members of the international scientific community. Here we combine a critical review of the literature with the results of the workshop to compile a short list of potential policy-relevant future tipping elements in the climate system. Results from the expert elicitation are used to rank a subset of these tipping elements in terms of their sensitivity to global warming and the associated uncertainty. Then we consider the prospects for early warning of an approaching tipping point.

Defining a Tipping Element and Its Tipping Point

Previous reviews (6–10) have defined "abrupt climate change" as occurring "when the climate system is forced to cross some threshold, triggering a transition to a new state at a rate determined by the climate system itself and faster than the cause" (8), which is a case of bifurcation (i.e., one that focuses on equilibrium properties, implying some degree of irreversibility). We have formulated a much broader definition of a tipping element, because (*i*) we wish to include nonclimatic variables; (*ii*) there may be cases where the transition is slower than the anthropogenic forcing causing it; (*iii*) there may be no abruptness, but a slight change in control may have a qualitative impact in the future; and (*iv*) for several important phase changes, state-of-the-art models differ as to whether the transition is reversible or irreversible (in principle).

We consider "components" (Σ) of the Earth system that are associated with a specific region (or collection of regions) of the globe and are at least subcontinental in scale (length scale of order $\approx$1,000 km). A full formal definition of a tipping element is given in supporting information (SI) *Appendix 1*. For the cases considered herein, a system Σ is a tipping element if the following condition is met:

1. The parameters controlling the system can be transparently combined into a single control ρ, and there exists a critical control value ρ_{crit} from which any significant variation by $\delta\rho > 0$ leads to a qualitative change ($\hat{F}$) in a crucial system feature F, after some observation time $T > 0$, measured with respect to a reference feature at the critical value, i.e.,

$$|F(\rho \geq \rho_{\mathrm{crit}} + \delta\rho|T) - F(\rho_{\mathrm{crit}}|T)| \geq \hat{F} > 0. \qquad [1]$$

This inequality applies to forcing trajectories for which a slight deviation above a critical value that continues for some time inevitably induces a qualitative change. This change may oc-

Author contributions: T.M.L., H.H., E.K., J.W.H., and H.J.S. designed research; T.M.L., H.H., E.K., J.W.H., W.L., S.R., and H.J.S. performed research; T.M.L., H.H., E.K., and J.W.H. analyzed data; and T.M.L., H.H., E.K., and H.J.S. wrote the paper.

The authors declare no conflict of interest.

This article is a PNAS Direct Submission.

Freely available online through the PNAS open access option.

†To whom correspondence may be addressed. E-mail: t.lenton@uea.ac.uk or john@pik-potsdam.de.

This article contains supporting information online at www.pnas.org/cgi/content/full/0705414105/DC1.

© 2008 by The National Academy of Sciences of the USA

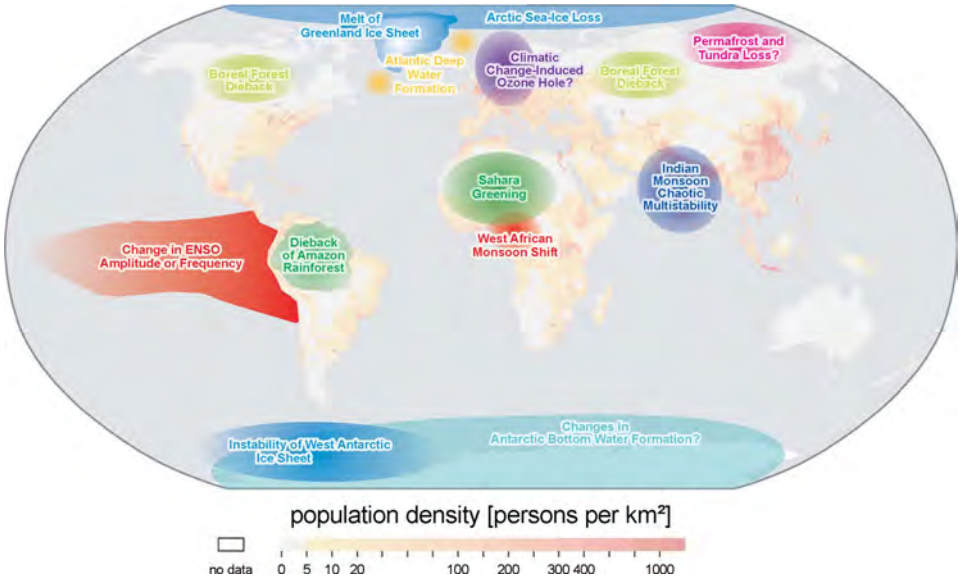

Fig. 1. Map of potential policy-relevant tipping elements in the climate system, updated from ref. 5 and overlain on global population density. Subsystems indicated could exhibit threshold-type behavior in response to anthropogenic climate forcing, where a small perturbation at a critical point qualitatively alters the future fate of the system. They could be triggered this century and would undergo a qualitative change within this millennium. We exclude from the map systems in which any threshold appears inaccessible this century (e.g., East Antarctic Ice Sheet) or the qualitative change would appear beyond this millennium (e.g., marine methane hydrates). Question marks indicate systems whose status as tipping elements is particularly uncertain.

cur immediately after the cause or much later. The definition encompasses equilibrium properties with threshold behavior as well as critical rates of forcing. In its equilibrium application, it includes all orders of phase transition and the most common bifurcations found in nature: saddle-node and Hopf bifurcations. The definition could in principle be applied at any time, e.g., in Earth's history. The feature of the system and the parameter(s) that influence it need not be climate variables. Critical conditions may be reached autonomously (without human interference), and natural variability could trigger a qualitative change.

Here we restrict ourselves to tipping elements that may be accessed by human activities and are potentially relevant to current policy. We define the subset of policy-relevant tipping elements by adding to condition 1 the following conditions:

2. Human activities are interfering with the system Σ such that decisions taken within a "political time horizon" ($T_P > 0$) can determine whether the critical value for the control ρ_{crit} is reached. This occurs at a critical time (t_{crit}) that is usually within T_P but may be later because of a commitment to further change made during T_P.
3. The time to observe a qualitative change plus the time to trigger it lie within an "ethical time horizon" (T_E); $t_{crit} + T \leq T_E$. T_E recognizes that events too far away in the future may not have the power of influencing today's decisions.
4. A significant number of people care about the fate of the component Σ, because it contributes significantly to the overall mode of operation of the Earth system (such that tipping it modifies the qualitative state of the whole system), it contributes significantly to human welfare (such that tipping it impacts on many people), or it has great value in itself as a unique feature of the biosphere. A qualitative change should correspondingly be defined in terms of impacts.

Conditions 2–4 give our definition of a policy-relevant tipping element an ethical dimension, which is inevitable because a focus on policy requires the inclusion of normative judgements. These enter in the choices of the political time horizon (T_P), the ethical time horizon (T_E), and the qualitative change that fulfills condition 4. We suggest a maximum $T_P \sim 100$ years based on the human life span and our (limited) ability to consider the world we are leaving for our grandchildren, noting also the Intergovernmental Panel on Climate Change (IPCC) focus on this timescale. We suggest $T_E \sim 1{,}000$ years based on the lifetime of civilizations, noting that this is longer than the timescale of nation states and current political entities. Thus, we focus on the consequences of decisions enacted within this century that trigger a qualitative change within this millennium, and we exclude tipping elements whose fate is decided after 2100.

In the limit $\delta\rho \to 0$, condition 1 would only include vanishing equilibria and first-order phase transitions. Instead we consider that a "small" perturbation $\delta\rho$ should not exceed the magnitude of natural variability in ρ. Considering global temperature, climate variability on interannual to millennial timescales is 0.1–0.2°C. Alternatively, a popular target is to limit anthropogenic global mean temperature increase to 2°C, and we take a "small" perturbation to be 10% of this. Either way, $\delta\rho \sim 0.2$°C seems reasonable.

One useful way of classifying tipping elements is in terms of the time, T, over which a qualitative change is observed: (*i*) rapid, abrupt, or spasmodic tipping occurs if the observation time is very small compared with T_P (but $T \neq 0$); (*ii*) gradual or episodic tipping occurs if the observation time is intermediate (e.g., of order T_P); and (*iii*) slow or asymptotic tipping occurs if the observation time is very long (in particular, $T \to T_E$).

Several key questions arise. What are the potential policy-relevant tipping elements of the Earth system? And for each: What is the mechanism of tipping? What is the key feature F of interest? What are the parameter(s) projecting onto the control ρ, and their value(s) near ρ_{crit}? How long is the transition time T? What are the associated uncertainties?

Policy-Relevant Tipping Elements in the Climate System

Earth's history provides evidence of nonlinear switches in state or modes of variability of components of the climate system (6–10). Such past transitions may highlight potential tipping elements under anthropogenic forcing, but the boundary conditions under which they occurred were different from today, and anthropogenic forcing is generally more rapid and often different in pattern (11). Therefore, locating potential future tipping points requires some use of predictive models, in combination with paleodata and/or historical data.

Here we focus on policy-relevant potential future tipping elements in the climate system. We considered a long list of candidates (Fig. 1, Table 1), and from literature review and the aforementioned workshop, we identified a short list of candidates that meet conditions 1–4 (top nine rows in Table 1). To meet condition 1, there needed to be some theoretical basis (>1 model study) for expecting a system to exhibit a critical threshold

Table 1. Policy-relevant potential future tipping elements in the climate system and (below the empty line) candidates that we considered but failed to make the short list*

Tipping element	Feature of system, F (direction of change)	Control parameter(s), ρ	Critical value(s),† ρ_{crit}	Global warming†‡	Transition timescale,† T	Key impacts
Arctic summer sea-ice	Areal extent (−)	Local ΔT_{air}, ocean heat transport	Unidentified§	+0.5–2°C	≈10 yr (rapid)	Amplified warming, ecosystem change
Greenland ice sheet (GIS)	Ice volume (−)	Local ΔT_{air}	+≈3°C	+1–2°C	>300 yr (slow)	Sea level +2–7 m
West Antarctic ice sheet (WAIS)	Ice volume (−)	Local ΔT_{air}, or less ΔT_{ocean}	+≈5–8°C	+3–5°C	>300 yr (slow)	Sea level +5 m
Atlantic thermohaline circulation (THC)	Overturning (−)	Freshwater input to N Atlantic	+0.1–0.5 Sv	+3–5°C	≈100 yr (gradual)	Regional cooling, sea level, ITCZ shift
El Niño–Southern Oscillation (ENSO)	Amplitude (+)	Thermocline depth, sharpness in EEP	Unidentified§	+3–6°C	≈100 yr (gradual)	Drought in SE Asia and elsewhere
Indian summer monsoon (ISM)	Rainfall (−)	Planetary albedo over India	0.5	N/A	≈1 yr (rapid)	Drought, decreased carrying capacity
Sahara/Sahel and West African monsoon (WAM)	Vegetation fraction (+)	Precipitation	100 mm/yr	+3–5°C	≈10 yr (rapid)	Increased carrying capacity
Amazon rainforest	Tree fraction (−)	Precipitation, dry season length	1,100 mm/yr	+3–4°C	≈50 yr (gradual)	Biodiversity loss, decreased rainfall
Boreal forest	Tree fraction (−)	Local ΔT_{air}	+≈7°C	+3–5°C	≈50 yr (gradual)	Biome switch
Antarctic Bottom Water (AABW)*	Formation (−)	Precipitation–Evaporation	+100 mm/yr	Unclear¶	≈100 yr (gradual)	Ocean circulation, carbon storage
Tundra*	Tree fraction (+)	Growing degree days above zero	Missing‖	—	≈100 yr (gradual)	Amplified warming, biome switch
Permafrost*	Volume (−)	$\Delta T_{permafrost}$	Missing‖	—	<100 yr (gradual)	CH_4 and CO_2 release
Marine methane hydrates*	Hydrate volume (−)	$\Delta T_{sediment}$	Unidentified§	Unclear¶	10^3 to 10^5 yr ($>T_E$)	Amplified global warming
Ocean anoxia*	Ocean anoxia (+)	Phosphorus input to ocean	+≈20%	Unclear¶	≈10^4 yr ($>T_E$)	Marine mass extinction
Arctic ozone*	Column depth (−)	Polar stratospheric cloud formation	195 K	Unclear¶	<1 yr (rapid)	Increased UV at surface

N, North; ITCZ, Inter-tropical Convergence Zone; EEP, East Equatorial Pacific; SE, Southeast.

*See *SI Appendix 2* for more details about the tipping elements that failed to make the short list.

†Numbers given are preliminary and derive from assessments by the experts at the workshop, aggregation of their opinions at the workshop, and review of the literature.

‡Global mean temperature change above present (1980–1999) that corresponds to critical value of control, where this can be meaningfully related to global temperature.

§Meaning theory, model results, or paleo-data suggest the existence of a critical threshold but a numerical value is lacking in the literature.

¶Meaning either a corresponding global warming range is not established or global warming is not the only or the dominant forcing.

‖Meaning no subcontinental scale critical threshold could be identified, even though a local geographical threshold may exist.

(ρ_{crit}) at a subcontinental scale, and/or past evidence of threshold behavior. Where the proposed ρ_{crit} could be meaningfully related to temperature, condition 2 was evaluated based on an "accessible neighborhood" of global temperatures from the IPCC (12) of 1.1–6.4°C above 1980–1999 that could be committed to over the next $T_P \sim 100$ years, and on recognition that transient warming is generally greater toward the poles and greater on land than in the ocean. Condition 3 was evaluated on the basis of model projections, known shortcomings of the models, and paleodata. Our collective judgement was used to evaluate condition 4.

Our short list differs from that of the IPCC (ref. 12, chapter 10, especially p. 775 ff, p. 818 ff) because our definition and criteria differ from, and are more explicit than, the IPCC notion of abrupt climate change. The evidence base we use is also slightly different because it encompasses some more recent studies. The authors of this paper and the workshop participants are a smaller group of scientists than the IPCC members, the groups are only partially overlapping, and our analysis was undertaken largely in parallel. We seek to add value to the IPCC overview by injecting a more precise definition and undertaking a complementary, in-depth evaluation.

We now discuss the entries that made our short list and seek to explain significant discrepancies from the IPCC where they arise. Those candidates that did not make the short list (and why) are discussed in *SI Appendix 2*.

Arctic Sea-Ice. As sea-ice melts, it exposes a much darker ocean surface, which absorbs more radiation–amplifying the warming. Energy-balance models suggest that this ice-albedo positive feedback can give rise to multiple stable states of sea-ice (and land snow) cover, including finite ice cap and ice-free states, with ice caps smaller than a certain size being unstable (13). This small ice-cap instability is also found in some atmospheric general circulation models (AGCMs), but it can be largely eliminated by noise due to natural variability (14). The instability is not expected to be relevant to Southern Ocean sea-ice because the Antarctic continent covers the region over which it would be expected to arise (15). Different stable states for the flow rate through the narrow outlets that drain parts of the Arctic basin have also been found in a recent model (16). For both summer and winter Arctic sea-ice, the area coverage is declining at present (with summer sea-ice declining more markedly; ref. 17), and the ice has thinned significantly over a large area. Positive ice-albedo feedback dominates external forcing in causing the thinning and shrinkage since 1988, indicating strong nonlinearity and leading some to suggest that this system may already have passed a tipping point (18), although others disagree (19). In IPCC projections with ocean-atmosphere general circulation

models (OAGCMs) (12), half of the models become ice-free in September during this century (19), at a polar temperature of −9°C (9°C above present) (20). The transition has nonlinear steps in many of the models, but a common critical threshold has yet to be identified (19). Thinning of the winter sea-ice increases the efficiency of formation of open water in summer, and abrupt retreat occurs when ocean heat transport to the Arctic increases rapidly (19). Only two IPCC models (12) exhibit a complete loss of annual sea-ice cover under extreme forcing (20). One shows a nonlinear transition to a new stable state in <10 years when polar temperature rises above −5°C (13°C above present), whereas the other shows a more linear transition. We conclude that a critical threshold for summer Arctic sea-ice loss may exist, whereas a further threshold for year-round ice loss is more uncertain and less accessible this century. Given that the IPCC models significantly underestimate the observed rate of Arctic sea-ice decline (17), a summer ice-loss threshold, if not already passed, may be very close and a transition could occur well within this century.

Greenland Ice Sheet (GIS). Ice-sheet models typically exhibit multiple stable states and nonlinear transitions between them (21). In some simulations with the GIS removed, summer melting prevents its reestablishment (22), indicating bistability, although others disagree (23). Regardless of whether there is bistability, in deglaciation, warming at the periphery lowers ice altitude, increasing surface temperature and causing a positive feedback that is expected to exhibit a critical threshold beyond which there is ongoing net mass loss and the GIS shrinks radically or eventually disappears. During the last interglacial (the Eemian), there was a 4- to 6-m higher sea level that must have come from Greenland and/or Antarctica. Increased Arctic summer insolation caused an estimated <3.5°C summertime warming of Greenland, and shrinkage of the GIS contributed an estimated 1.9–3.0 m to sea level, although a widespread ice cap remained (24). Broadly consistent with this, future projections suggest a GIS threshold for negative surface mass balance resides at ≥≈3°C local warming (above preindustrial) (3, 25). Uncertainties are such that IPCC (12) put the threshold at ≈1.9–4.6°C global warming (above preindustrial), which is clearly accessible this century. We give a closer and narrower range (above present) because amplification of warming over Greenland may be greater (26) than assumed (12, 25) because of more rapid sea-ice decline than modeled (17). Also, recent observations show the surface mass balance is declining (12) and contributing to net mass loss from the GIS (27, 28) that is accelerating (28, 29). Finally, existing ice-sheet models are unable to explain the speed of recent changes. These changes include melting and thinning of the coastal margins (30) and surging of outlet glaciers (29, 31), which may be contributed to by the intrusion of warming ocean waters (32). This is partly compensated by some mass gain in the interior (33). There is a lack of knowledge of natural GIS variability, and Greenland temperature changes have differed from the global trend (26), so interpretation of recent observations remains uncertain. If a threshold is passed, the IPCC (12) gives a >1,000-year timescale for GIS collapse. However, given the acknowledged (12) lack of processes that could accelerate collapse in current models, and their inability to simulate the rapid disappearance of continental ice at the end of the last ice age, a lower limit of 300 years is conceivable (34).

West Antarctic Ice Sheet (WAIS). Most of the WAIS is grounded below sea level and has the potential to collapse if grounding-line retreat triggers a strong positive feedback whereby ocean water undercuts the ice sheet and triggers further separation from the bedrock (35–37). The WAIS has retreated at least once during the Pleistocene (38), but the full extent of retreat is not known, nor is whether it occurred in the Eemian or the long, warm interglacial MIS-11 ≈400 ka. Approximately 1–4 m of the Eemian sea-level rise may have come from Antarctica, but some could have been from parts of the East Antarctic Ice Sheet grounded below sea level (and currently thinning at a rapid rate). WAIS collapse may be preceded by the disintegration of ice shelves and the acceleration of ice streams. Ice shelf collapse could be triggered by the intrusion of warming ocean water beneath them or by surface melting. It requires ≈5°C of local warming for surface atmospheric temperatures to exceed the melting point in summer on the major (Ross and Fischner-Ronne) ice shelves (12, 37). The threshold for ocean warming is estimated to be lower (37). The WAIS itself requires ≈8°C of local warming of the surface atmosphere at 75–80°S to reach the melting point in summer (37). Although the IPCC (12) declines to give a threshold, we estimate a range that is clearly accessible this century. Concern is raised by recent inferences from gravity measurements that the WAIS is losing mass (39), and observations that glaciers draining into the Amundsen Sea are losing 60% more ice than they are gaining and hence contributing to sea-level rise (40). They drain a region containing ≈1.3 m of a total ≈5 m of global sea-level rise contained in the WAIS. Although the timescale is highly uncertain, a qualitative WAIS change could occur within this millennium, with collapse within 300 years being a worst-case scenario. Rapid sea-level rise (>1 m per century) is more likely to come from the WAIS than from the GIS.

Atlantic Thermohaline Circulation (THC). A shutoff in North Atlantic Deep Water formation and the associated Atlantic THC can occur if sufficient freshwater (and/or heat) enters the North Atlantic to halt density-driven North Atlantic Deep Water formation (41). Such THC reorganizations play an important part in rapid climate changes recorded in Greenland during the last glacial cycle (42, 43). Hysteresis of the THC has been found in all models that have been systematically tested thus far (44), from conceptual "box" representations of the ocean (45) to OAGCMs (46). The most complex models have yet to be systematically tested because of excessive computational cost. Under sufficient North Atlantic freshwater forcing, all models exhibit a collapse of convection. In some experiments, this collapse is reversible (47) (after the forcing is removed, convection resumes), whereas in others, it is irreversible (48)—indicating bistability. In either case, a tipping point has been passed according to condition 1. The proximity of the present climate to this tipping point varies considerably between models, corresponding to an additional North Atlantic freshwater input of 0.1–0.5 Sv (44). The sensitivity of North Atlantic freshwater input to anthropogenic forcing is also poorly known, but regional precipitation is predicted to increase (12) and the GIS could contribute significantly (e.g., GIS melt over 1,000 years is equivalent to 0.1 Sv). The North Atlantic is observed to be freshening (49), and estimates of recent increases in freshwater input yield 0.014 Sv from melting sea ice (18), 0.007 Sv from Greenland (29), and 0.005 Sv from Eurasian rivers (50), totaling 0.026 Sv, without considering precipitation over the oceans or Canadian river runoff. The IPCC (12) argues that an abrupt transition of the THC is "very unlikely" (probability <10%) to occur before 2100 and that any transition is likely to take a century or more. Our definition encompasses gradual transitions that appear continuous across the tipping point; hence, some of the IPCC runs (ref. 12, p. 773 ff) may yet meet our criteria (but would need to be run for longer to see if they reach a qualitatively different state). Furthermore, the IPCC does not include freshwater runoff from GIS melt. Subsequent OAGCM simulations clearly pass a THC tipping point this century and undergo a qualitative change before the next millennium (48). Both the timescale and the magnitude of forcing are important (51), because a more rapid forcing to a given level can more readily overwhelm the negative feedback

that redistributes salt in a manner that maintains whatever is the current circulation state.

El Niño–Southern Oscillation (ENSO). Gradual anthropogenic forcing is expected, on theoretical grounds, to interact with natural modes of climate variability by altering the relative amount of time that the climate system spends in different states (52). ENSO is the most significant ocean-atmosphere mode, and its variability is controlled by (at least) three factors: zonal mean thermocline depth, thermocline sharpness in the EEP, and the strength of the annual cycle and hence the meridional temperature gradient across the equator (53, 54). Increased ocean heat uptake could cause a permanent deepening of the thermocline in the EEP and a consequent shift from present day ENSO variability to greater amplitude and/or more frequent El Niños (55). However, a contradictory theory postulates sustained La Niña conditions due to stronger warming of the West Equatorial Pacific than the East, causing enhanced easterly winds and reinforcing the up-welling of cold water in the EEP (56). The mid-Holocene had a reduction in ENSO amplitude related to a stronger zonal temperature gradient (57, 58). The globally ≈3°C warmer early Pliocene is characterized by some as having persistent El Niño conditions (59), whereas others disagree (60). Under future forcing, the first OAGCM studies showed a shift from the current ENSO variability to more persistent or frequent El Niño-like conditions. Now that numerous OAGCMs have been intercompared, there is no consistent trend in their transient response and only a small collective probability of a shift toward more persistent or frequent El Niño conditions (61, 62). However, in response to a warmer stabilized climate, the most realistic models simulate increased El Niño amplitude (with no clear change in frequency) (54). This would have large-scale impacts, and even if the transition is smooth and gradual, a tipping point may exist by condition 1. Given also that past climate changes have been accompanied by changes in ENSO, we differ from IPCC (12) and consider there to be a significant probability of a future increase in ENSO amplitude. The required warming can be accessed this century (54) with the transition happening within a millennium, but the existence and location of any threshold is particularly uncertain.

Indian Summer Monsoon (ISM). The land-to-ocean pressure gradient, which drives the monsoon circulation is reinforced by the moisture the monsoon itself carries from the adjacent Indian Ocean (moisture-advection feedback) (63). Consequently, any perturbation that tends to weaken the driving pressure gradient has the potential to destabilize the monsoon circulation. Greenhouse warming that is stronger over land and in the Northern Hemisphere tends to strengthen the monsoon, but increases in planetary albedo over the continent due to aerosol forcing and/or land-use change tend to weaken it. The ISM exhibited rapid changes in variability during the last ice age (64) and the Holocene (65), with an increased strength during recent centuries consistent with Northern Hemisphere warming (66). Recent time series display strongly nonlinear characteristics, from the intraseasonal via the interannual and the decadal to the centennial timescale (67), with the interannual variations lag correlated with the phases of ENSO, although this may be increasingly masked by anthropogenic forcing (68). A simple model (63) predicts collapse of the ISM if regional planetary albedo exceeds ≈0.5, whereas increasing CO_2 stabilizes the monsoon. IPCC projections do not show obvious threshold behavior this century (12), but they do agree that sulfate aerosols would dampen the strength of ISM precipitation, whereas increased greenhouse gases increase the interannual variability of daily precipitation (69). We differ from IPCC (12) on the basis of past apparent threshold behavior of the ISM and because brown haze and land-use-change forcing are poorly captured in the models. Furthermore, conceptual work on the potentially chaotic nature of the ISM (70) has been developed (V. Petoukhov, K. Zickfeld, and H.J.S., unpublished work) to suggest that under some plausible decadal-scale scenarios of land use and greenhouse gas and aerosol forcing, switches occur between two highly nonlinear metastable regimes of the chaotic oscillations corresponding to the "active" and "weak" monsoon phases, on the intraseasonal and interannual timescales. Sporadic bifurcation transitions may also happen from regimes of chaotic oscillations to regimes with highly deterministic oscillations, or to regimes with very weak oscillations.

Sahara/Sahel and West African Monsoon (WAM). Past greening of the Sahara occurred in the mid-Holocene (71–73) and may have happened rapidly in the earlier Bölling-Allerod warming. Collapse of vegetation in the Sahara ≈5,000 years ago occurred more rapidly than orbital forcing (71, 72). The system has been modeled and conceptualized in terms of bistable states that are maintained by vegetation–climate feedback (71, 74). However, it is intimately tied to the WAM circulation, which in turn is affected by sea surface temperatures (SSTs), particularly antisymmetric patterns between the Hemispheres. Greenhouse gas forcing is expected to increase the interhemispheric SST gradient and thereby increase Sahel rainfall; hence, the recent Sahel drought has been attributed to increased aerosol loading cooling the Northern Hemisphere (75). Future 21st century projections differ (75, 76); in two AOGCMs, the WAM collapses, but in one this leads to further drying of the Sahel, whereas in the other it causes wetting due to increased inflow from the West. The latter response is more mechanistically reasonable, but it requires a ≈3°C warming of SSTs in the Gulf of Guinea (76). A third AOGCM with the most realistic present-day WAM predicts no large trend in mean rainfall but a doubling of the number of anomalously dry years by the end of the century (76). If the WAM is disrupted such that there is increased inflow from the West (76), the resulting moisture will wet the Sahel and support greening of the Sahara, as is seen in mid-Holocene simulations (73). Indeed, in an intermediate complexity model, increasing atmospheric CO_2 has been predicted to cause future expansion of grasslands into up to 45% of the Sahara, at a rate of up to 10% of Saharan area per decade (11). In the Sahel, shrub vegetation may also increase due to increased water use efficiency (stomatal closure) under higher atmospheric CO_2 (77). Such greening of the Sahara/Sahel is a rare example of a beneficial potential tipping element.

Amazon Rainforest. A large fraction of precipitation in the Amazon basin is recycled, and, therefore, simulations of Amazon deforestation typically generate ≈20–30% reductions in precipitation (78), lengthening of the dry season, and increases in summer temperatures (79) that would make it difficult for the forest to reestablish, and suggest the system may exhibit bistability. Dieback of the Amazon rainforest has been predicted (2, 80) to occur under ≈3–4°C global warming because of a more persistent El Niño state that leads to drying over much of the Amazon basin (81). Different vegetation models driven with similar climate projections also show Amazon dieback (82), but other global climate models (83) project smaller reductions (or increases) of precipitation and, therefore, do not produce dieback (84). A regional climate model (85) predicts Amazon dieback due to widespread reductions in precipitation and lengthening of the dry season. Changes in fire frequency probably contribute to bistability and will be amplified by forest fragmentation due to human activity. Indeed land-use change alone could potentially bring forest cover to a critical threshold. Thus, the fate of the Amazon may be determined by a complex interplay between direct land-use change and the response of regional precipitation and ENSO to global forcing.

Boreal Forest. The boreal system exhibits a complex interplay between tree physiology, permafrost, and fire. Under climate change, increased water stress, increased peak summer heat stress causing increased mortality, vulnerability to disease and subsequent fire, as well as decreased reproduction rates could lead to large-scale dieback of the boreal forests (77, 86), with transitions to open woodlands or grasslands. In interior boreal regions, temperate tree species will remain excluded from succession due to frost damage in still very cold winters. Continental steppe grasslands will expand at the expense of boreal forest where soil moisture along the arid timberline ecotone declines further (87), amplified through concurrent increases in the frequency of fires. Newly unfrozen soils that regionally drain well, and reductions in the amount of snow, also support drying, more fire and hence less biomass. In contrast, increased thaw depth and increased water-use efficiency under elevated CO_2 will tend to increase available soil moisture, decreasing fire frequency and increasing woody biomass. Studies suggest a threshold for boreal forest dieback of ≈3°C global warming (77, 86), but limitations in existing models and physiological understanding make this highly uncertain.

Others. We remind the reader that we considered other candidate tipping elements, which are not listed here because they did not meet conditions 2–4 for policy relevance. Some are listed in Table 1 and discussed in *SI Appendix 2*.

Ranking the Threat

Given our identification of policy-relevant tipping elements in the climate system, how do we decide which pose the greatest threat to society and, therefore, need the greatest attention? The first step is to asses the sensitivity of each tipping element to global warming and the associated uncertainties, including the confidence of the community in the argument for tipping element status. Our workshop and systematic review of the literature addressed this. In addition, formal elicitations of expert beliefs have frequently been used to bring current understanding of model studies, empirical evidence, and theoretical considerations to bear on policy-relevant variables (88). From a natural science perspective, a general criticism is that expert beliefs carry subjective biases and, moreover, do not add to the body of scientific knowledge unless verified by data or theory. Nonetheless, expert elicitations, based on rigorous protocols from statistics (89–91) and risk analysis (91, 92), have proved to be a very valuable source of information in public policymaking (93). It is increasingly recognized that they can also play a valuable role for informing climate policy decisions (94). In the field of climate change, formal expert elicitations have been conducted, e.g., on climate sensitivity (95), forest ecosystems (96), the WAIS (97), radiative forcing of aerosols (98), and the THC (99).

On the basis of previous experience (99), we used the aforementioned workshop to initiate an elicitation of expert opinions on, among other things, six potential tipping elements listed in Table 1: reorganization of the Atlantic THC, melt of the GIS, disintegration of the WAIS, Amazon rainforest dieback, dieback of boreal forests, and shift of the ENSO regime to an El Niño-like mean state. The elicitation was based on a computer-based interactive questionnaire that was completed individually by participating experts. Following a pilot phase at the workshop, the questionnaire was distributed to 193 international scientists in October and November 2005; 52 experts returned a completed questionnaire (among them 16 workshop participants and 22 contributors to the IPCC Fourth Assessment Report). Although participation inevitably involved a self-selection process, we assembled a heterogeneous group covering a wide range of expertise (see *SI Appendix 3*). The full results will be presented separately (E.K., J.W.H., H.H., R. Dawson, and H.J.S., unpublished work). Here we report a subset that reflect the range of scientific perspectives to supplement our own assessment of the tipping elements.

In the questionnaire, experts were asked for a pairwise comparison of tipping elements in terms of (*i*) their sensitivity to global mean temperature increase and (*ii*) the uncertainty about the underlying physical mechanisms. The exact questions posed to participants and the breakdown of their responses are described in *SI Appendix 3*. We have identified partial rankings of tipping elements from the collection of expert responses. Because the number of experts commenting on individual pairs of tipping elements varied widely, those rankings could not be established with equal credibility. We highlight the difference in expert consensus by using the symbols ≫ and > for strong and weak consensus upon the ordering, respectively, and by providing the number x that agreed with the direction of the ordering compared with the number y of experts who commented on the pair [given as $x(y)$]. For sensitivity to global mean warming, we find

$$\text{GIS} \underset{7(7)\ \text{to THC}}{\overset{8(10)\ \text{to WAIS}}{\gg}} \begin{array}{l} \text{WAIS} \overset{2(3)}{>} \\ \text{Amazon rainforest} \underset{2(2)}{>} \end{array} \text{THC},$$

where the more sensitive tipping element is to the left. Owing to the close link between ENSO and the Amazon rainforest, both were judged of similar sensitivity to warming, but experts were divided as to whether ENSO would be more sensitive than the THC. Boreal forests were only compared with the Amazon rainforest, and three out of five experts judged the former to be more sensitive to global mean warming. Concerning the uncertainty about the physical mechanisms that may give rise to tipping points, we find

$$\begin{array}{l} \text{WAIS} \underset{6(9)\ \text{to GIS}}{\overset{3(4)\ \text{to THC}}{\gg}} \\ \text{Amazon rainforest} \underset{1(1)\ \text{to GIS}}{\overset{2(2)\ \text{to THC}}{>}} \\ \text{ENSO} \underset{2(2)\ \text{to GIS}}{\overset{3+2(6)\ \text{to THC}}{\geq}} \end{array} \text{THC} \overset{6(8)}{\gg} \text{GIS},$$

where the more uncertain tipping element is to the left. We display a greater or equal uncertainty about the ENSO compared with the THC, because three and two out of six experts believed the ENSO to be more and similarly uncertain, respectively. In addition, five out of six experts judged the uncertainty about the response of boreal forests to be larger than for the Amazon rainforest.

Taking into account our own analysis of the literature (summarized in the previous section and Table 1) and the expert elicitation (summarized above), the potential tipping elements in the climate system may be grouped into three clusters: (*i*) high sensitivity with smallest uncertainty: GIS and Arctic sea-ice; (*ii*) intermediate sensitivity with largest uncertainty: WAIS, Boreal forest, Amazon rainforest, ENSO, and WAM; (*iii*) low sensitivity with intermediate uncertainty: THC. ISM is not included in the clustering because its forcing differs, but it clearly has large uncertainty. We conclude that the greatest (and clearest) threat

is to the Arctic with summer sea-ice loss likely to occur long before (and potentially contribute to) GIS melt. Tipping elements in the tropics, the boreal zone, and West Antarctica are surrounded by large uncertainty and, given their potential sensitivity, constitute candidates for surprising society. The archetypal example of a tipping element, the THC appears to be a less immediate threat, but the long-term fate of the THC under significant warming remains a source of concern (99).

The Prospects for Early Warning

Establishing early warning systems for various tipping elements would clearly be desirable, but can ρ_{crit} be anticipated before we reach it? In principle, an incipient bifurcation in a dynamical system could be anticipated (100), by looking at the spectral properties of time series data (101), in particular, extracting the longest system-immanent timescale (τ) from the response of the system to natural variability (102). Systems theory reveals (Fig. 2*A*) (*i*) that those tipping points that represent a bifurcation are universally characterized by $\tau \rightarrow \infty$ at the threshold, and (*ii*) that in principle τ could be reconstructed through methods of time series analysis. Hence a "degenerate fingerprinting" method has been developed for anticipating a threshold in a spatially extended system and applied to the detection of a threshold in the Atlantic THC, by using time series output from a model of intermediate complexity (102) (Fig. 2*B*).

These studies reveal that if a system is forced slowly (keeping it in quasi-equilibrium), proximity to a threshold may be inferred in a model-independent way. However, if the system is forced faster (as is probably the case for the THC today), a dynamical model will also be needed. Even if there is no bifurcation, determining τ is still worthwhile because it determines the system's linear response characteristics to external forcing, and transitions that are not strictly bifurcations are expected to resemble bifurcation-type behavior to a certain degree. For strongly resource-limited ecosystems that show self-organized patchiness, their observable macrostructure may also provide an indication of their proximity to state changes (103).

If a forewarning system for approaching thresholds is to become workable, then real-time observation systems need to be improved (e.g., building on the Atlantic THC monitoring at 26.5°N). For slow transition systems, notably ocean and ice sheets, observation records also need to be extended further back in time (e.g., for the Atlantic beyond the ≈150-year SST record). Analysis of extended time series data could then be used to improve models (104), e.g., an effort to determine the Atlantic's τ and assimilate it into ocean models could reduce the vast intra- and intermodel (44) spread regarding the proximity to a tipping point (102).

Conclusion

Society may be lulled into a false sense of security by smooth projections of global change. Our synthesis of present knowledge suggests that a variety of tipping elements could reach their critical point within this century under anthropogenic climate change. The greatest threats are tipping the Arctic sea-ice and the Greenland ice sheet, and at least five other elements could surprise us by exhibiting a nearby tipping point. This knowledge should influence climate policy, but a full assessment of policy relevance would require that, for each potential tipping element, we answer the following questions: Mitigation: Can we stay clear of ρ_{crit}? Adaptation: Can $\dot{F}$ be tolerated?

The IPCC provides a thorough overview of mitigation (105) and adaptation (106) work upon which such a policy assessment of tipping elements could be built. Given the scale of potential impacts from tipping elements, we anticipate that they will shift the balance toward stronger mitigation and demand adaptation concepts beyond incremental approaches (107, 108). Policy analysis and implementation will be extremely challenging given the nonconvexities in the human-environment system (109) that will be enhanced by tipping elements, as well as the need to handle intergenerational justice and interpersonal equity over long periods and under conditions of uncertainty (110). A rigorous study of potential tipping elements in human socioeconomic systems would also be welcome, especially to address whether and how a rapid societal transition toward sustainability could be triggered, given that some models suggest there exists a tipping point for the transition to a low-carbon-energy system (111).

It seems wise to assume that we have not yet identified all potential policy-relevant tipping elements. Hence, a systematic search for further tipping elements should be undertaken, drawing on both paleodata and multimodel ensemble studies. Given the large uncertainty that remains about tipping ele-

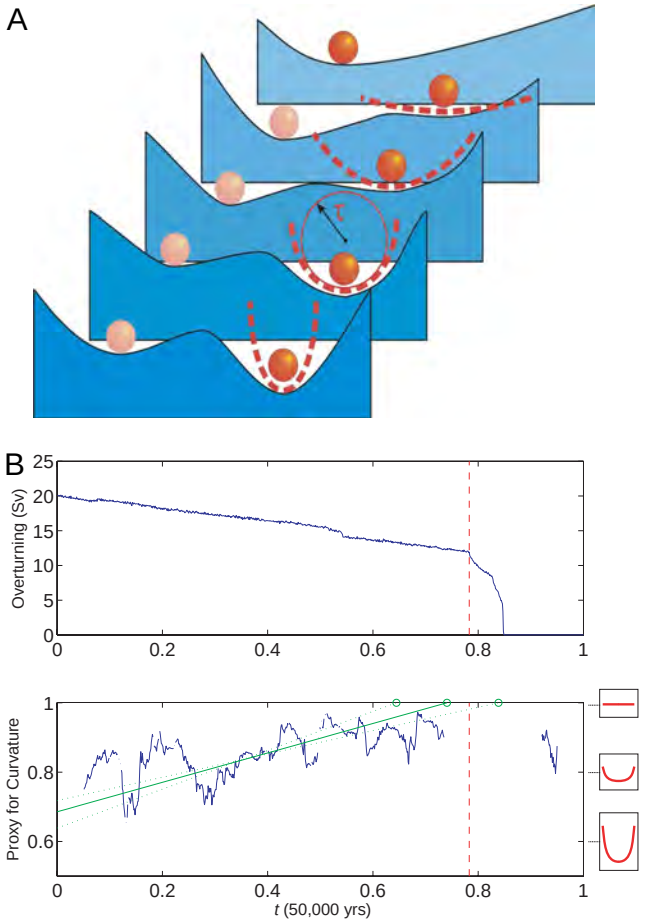

Fig. 2. Method for estimating the proximity to a tipping point. (*A*) Schematic approach: The potential wells represent stable attractors, and the ball, the state of the system. Under gradual anthropogenic forcing (progressing from dark to light blue potential), the right potential well becomes shallower and finally vanishes (threshold), causing the ball to abruptly roll to the left. The curvature of the well is inversely proportional to the system's response time τ to small perturbations. "Degenerate fingerprinting" (102) extracts τ from the system's noisy, multivariate time series and forecasts the vanishing of local curvature. (*B*) Degenerate fingerprinting "in action": Shown is an example for the Atlantic meridional overturning circulation. (*Upper*) Overturning strength under a 4-fold linear increase of atmospheric CO_2 over 50,000 years in the CLIMBER-2 model with weak, stochastic freshwater forcing. Eventually, the circulation collapses without early warning. (*Lower*) Overturning replaced by a proxy of the shape of the potential (as in *A*). Although the signal is noisier in *Lower* than it is in *Upper*, it allows forecasting of the location of the threshold (data taken from ref. 102). The solid green line is a linear fit, and the dashed green lines are 95% error bars.

ments, there is an urgent need to improve our understanding of the underlying physical mechanisms determining their behavior, so that policy makers are able "to avoid the unmanageable, and to manage the unavoidable" (112).

ACKNOWLEDGMENTS. We thank the British Embassy in Berlin for hosting the workshop "Tipping Points in the Earth System" on October 5–6, 2005, and all of the participants of the workshop and the expert elicitation. M. Wodinski prepared Fig. 1. We thank O. Edenhofer, V. Petoukhov, the editor W. C. Clark, and four anonymous referees for their suggestions that improved the paper. T.M.L.'s work is part of the Natural Environment Research Council GENIEfy (NE/C515904), Quaternary QUEST (NE/D001706), and Feedbacks QUEST (NE/F001657) projects. H.H. was supported by the Volkswagen Foundation under Grant II/78470. E.K. is supported by a Marie Curie International Fellowship (MOIF-CT-2005–008758) within the 6th European Community Framework Program, with research infrastructure partly provided by the Climate Decision Making Center (National Science Foundation Grant SES-0345798). W.L.'s work is a contribution to the Leibniz Association's project on the Biosphere, Society and Global Change. H.J.S. is a Senior James Martin Fellow at Oxford University.

1. Rahmstorf S, Ganopolski A (1999) *Clim Change* 43:353–367.
2. Cox PM, Betts RA, Jones CD, Spall SA, Totterdell IJ (2000) *Nature* 408:184–187.
3. Huybrechts P, De Wolde J (1999) *J Clim* 12:2169–2188.
4. Gladwell M (2000) *The Tipping Point*: *How Little Things Can Make a Big Difference* (Little Brown, New York).
5. Schellnhuber H-J, Held H (2002) in *Managing the Earth: The Eleventh Linacre Lectures*, eds Briden J, Downing T (Oxford Univ Press, Oxford), pp 5–34.
6. Rahmstorf S (2001) in *Encyclopedia of Ocean Sciences*, eds Steele J, Thorpe S, Turekian K (Academic, London), pp 1–6.
7. Lockwood JG (2001) *Int J Climatol* 21:1153–1179.
8. National Research Council (2002) *Abrupt Climate Change: Inevitable Surprises* (Natl Acad Press, Washington, DC).
9. Alley RB, Marotzke J, Nordhaus WD, Overpeck JT, Peteet DM, Pielke RA, Pierrehumbert RT, Rhines PB, Stocker TF, Talley LD, Wallace JM (2003) *Science* 299:2005–2010.
10. Rial JA, Pielke RA, Beniston M, Claussen M, Canadel J, Cox P, Held H, De Noblet-Ducoudre N, Prinn R, Reynolds JF, Salas JD (2004) *Clim Change* 65:11–38.
11. Claussen M, Brovkin V, Ganopolski A, Kubatzki C, Petoukhov V (2003) *Clim Change* 57:99–118.
12. IPCC (2007) *Climate Change 2007: The Physical Science Basis. Contribution of Working Group I to the Fourth Assessment Report of the Intergovernmental Panel on Climate Change*, eds Solomon S, Qin D, Manning M, Chen Z, Marquis M, Averyt KB, Tignor M, Miller HL (Cambridge Univ Press, Cambridge, UK).
13. North GR (1984) *J Atmos Sci* 41:3390–3395.
14. Lee W-H, North GR (1995) *Clim Dyn* 11:242–246.
15. Morales Maqueda MA, Willmott AJ, Bamber JL, Darby MS (1998) *Clim Dyn* 14:329–352.
16. Hibler WD, Hutchings JK, Ip CF (2006) *Ann Glaciol* 44:339–344.
17. Stroeve J, Holland MM, Meier W, Scambos T, Serreze M (2007) *Geophys Res Lett* 34:L09501.
18. Lindsay RW, Zhang J (2005) *J Clim* 18:4879–4894.
19. Holland MM (2006) *Geophys Res Lett* 33:L23503.
20. Winton M (2006) *Geophys Res Lett* 33:L23504.
21. Saltzman B (2002) *Dynamical Paleoclimatology* (Academic, London).
22. Toniazzo T, Gregory JM, Huybrechts P (2004) *J Clim* 17:21–33.
23. Lunt DJ, De Noblet-Ducoudre N, Charbit S (2004) *Clim Dyn* 23:679–694.
24. Otto-Bliesner BL, Marshall SJ, Overpeck JT, Miller GH, Hu A, CAPE Last Interglacial Project Members (2006) *Science* 311:1751–1753.
25. Gregory JM, Huybrechts P (2006) *Philos Trans R Soc A* 364:1709–1731.
26. Chylek P, Lohmann U (2005) *Geophys Res Lett* 32:L14705.
27. Mitrovica JX, Tamislea ME, Davis JL, Milne GA (2001) *Nature* 409:1026–1029.
28. Velicogna I, Wahr J (2006) *Nature* 443:329–331.
29. Rignot E, Kanagaratnam P (2006) *Science* 311:986–990.
30. Krabill W, Abdalati W, Frederick E, Manizade S, Martin C, Sonntag J, Swift R, Thomas R, Wright W, Yungel J (2000) *Science* 289:428–430.
31. Joughin I, Abdalati W, Fahnestock M (2004) *Nature* 432:608–610.
32. Bindschadler R (2006) *Science* 311:1720–1721.
33. Johannessen OM, Khvorostovsky K, Miles MW, Bobylev LP (2005) *Science* 310:1013–1016.
34. Hansen JE (2005) *Clim Change* 68:269–279.
35. Mercer JH (1978) *Nature* 271:321–325.
36. Oppenheimer M (1998) *Nature* 393:325–332.
37. Oppenheimer M, Alley RB (2004) *Clim Change* 64:1–10.
38. Scherer RP, Aldahan A, Tulaczyk S, Possnert G, Engelhardt H, Kamb B (1998) *Science* 281:82–85.
39. Velicogna I, Wahr J (2006) *Science* 311:1754–1756.
40. Thomas R, Rignot E, Casassa G, Kanagaratnam P, Acuña C, Akins T, Brecher H, Frederick E, Gogineni P, Krabill W, *et al.* (2004) *Science* 306:255–258.
41. Stocker TF, Wright DG (1991) *Nature* 351:729–732.
42. Rahmstorf S (2002) *Nature* 419:207–214.
43. Ganopolski A, Rahmstorf S (2001) *Nature* 409:153–158.
44. Rahmstorf S, Crucifix M, Ganopolski A, Goosse H, Kamenkovich I, Knutti R, Lohmann G, Marsh R, Mysak LA, Wang Z, Weaver AJ (2005) *Geophys Res Lett* 32:L23605.
45. Stommel H (1961) *Tellus* 13:224–230.
46. Lenton TM, Marsh R, Price AR, Lunt DJ, Aksenov Y, Annan JD, Cooper-Chadwick T, Cox SJ, Edwards NR, Goswami S, *et al.* (2007) *Clim Dyn* 29:591–613.
47. Vellinga M, Wood RA (2002) *Clim Change* 54:251–267.
48. Mikolajewicz U, Gröger M, Maier-Reimer E, Schurgers G, Vizcaíno M, Winguth AME (2007) *Clim Dyn* 28:599–633.
49. Curry R, Dickson B, Yashayaev I (2003) *Nature* 426:826–829.
50. Peterson BJ, Holmes RM, McClelland JW, Vörösmarty CJ, Lammers RB, Shiklomanov AI, Shiklomanov IA, Rahmstorf S (2002) *Science* 298:2171–2173.
51. Stocker TF, Schmittner A (1997) *Nature* 388:862–865.
52. Palmer TN (1999) *J Clim* 12:575–591.
53. Philander SG, Federov A (2003) *Annu Rev Earth Planet Sci* 31:579–594.
54. Guilyardi E (2006) *Clim Dyn* 26:329–348.
55. Timmermann A, Oberhuber J, Bacher A, Esch M, Latif M, Roeckner E (1999) *Nature* 398:694–697.
56. Cane MA, Clement AC, Kaplan A, Kushnir Y, Pozdnyakov D, Seager R, Zebiak SE, Murtugudde R (1997) *Science* 275:957–960.
57. Brown J, Collins M, Tudhope A (2006) *Adv Geosci* 6:29–33.
58. Koutavas A, deMenocal PB, Olive GC, Lynch-Stieglitz J (2006) *Geology* 34:993–996.
59. Wara MW, Ravelo AC, Delaney ML (2005) *Science* 309:758–761.
60. Rickaby REM, Halloran P (2005) *Science* 307:1948–1952.
61. Collins M, Groups TCM (2005) *Clim Dyn* 24:89–104.
62. van Oldenborgh GJ, Philip SY, Collins M (2005) *Ocean Sci* 1:81–95.
63. Zickfeld K, Knopf B, Petoukhov V, Schellnhuber HJ (2005) *Geophys Res Lett* 32:L15707.
64. Burns SJ, Fleitmann D, Matter A, Kramers J, Al-Subbary AA (2003) *Science* 301:1365–1367.
65. Gupta AK, Anderson DM, Overpeck JT (2003) *Nature* 431:354–357.
66. Anderson DM, Overpeck JT, Gupta AK (2002) *Science* 297:596–599.
67. Webster PJ, Magaña VO, Palmer TN, Shukla J, Tomas RA, Yanai M, Yasunari T (1998) *J Geophys Res* 103:14451–14510.
68. Meehl GA, Arblaster JM (2003) *Clim Dyn* 21:659–675.
69. Lal M, Cubasch U, Voss R, Waszkewitz J (1995) *Curr Sci India* 69:752–763.
70. Mittal AK, Dwivedi S, Pandey AC (2003) *Indian J Radio Space Phys* 32:209–216.
71. Claussen M, Kubatzki C, Brovkin V, Ganopolski A, Hoelzmann P, Pachur H-J (1999) *Geophys Res Lett* 26:2037–2040.
72. de Menocal P, Oritz J, Guilderson T, Adkins J, Sarnthein M, Baker L, Yarusinsky M (2000) *Quat Sci Rev* 19:347–361.
73. Patricola CM, Cook KH (2007) *J Clim* 20:694–716.
74. Brovkin V, Claussen M, Petoukhov V, Ganopolski A (1998) *J Geophys Res* 103:31613–31624.
75. Held IM, Delworth TL, Lu J, Findell KL, Knutson TR (2005) *Proc Natl Acad Sci USA* 102:17891–17896.
76. Cook KH, Vizy EK (2006) *J Clim* 19:3681–3703.
77. Lucht W, Schaphoff S, Erbrecht T, Heyder U, Cramer W (2006) *Carbon Balance Manage* 1:6.
78. Zeng N, Dickinson RE, Zeng X (1996) *J Clim* 9:859–883.
79. Kleidon A, Heimann M (2000) *Clim Dyn* 16:183–199.
80. Cox PM, Betts RA, Collins M, Harris PP, Huntingford C, Jones CD (2004) *Theor Appl Climatol* 78:137–156.
81. Betts RA, Cox PN, Collins M, Harris PP, Huntingford C, Jones CD (2004) *Theor Appl Climatol* 78:157–175.
82. White A, Cannell MGR, Friend AD (1999) *Global Environ Change* 9:S21–S30.
83. Li W, Fu R, Dickinson RE (2006) *J Geophys Res* 111:D02111.
84. Schaphoff S, Lucht W, Gerten D, Sitch S, Cramer W, Prentice IC (2006) *Clim Change* 74:97–122.
85. Cook KH, Vizy EK (2008) *J Clim*, in press.
86. Joos F, Prentice IC, Sitch S, Meyer R, Hooss G, Plattner G-K, Gerber S, Hasselmann K (2001) *Global Biogeochem Cycles* 15:891–907.
87. Hogg EH, Schwarz AG (1997) *J Biogeogr* 24:527–534.
88. Morgan MG, Henrion M (1990) *Uncertainty: A Guide to Dealing with Uncertainty in Quantitative Risk and Policy Analysis* (Cambridge Univ Press, New York).
89. Kadane JB, Wolfson LJ (1998) *J R Stat Soc Ser D* 47:3–17.
90. O'Hagan A (1998) *J R Stat Soc Ser D* 47:21–35.
91. Cooke RM (1991) *Experts in Uncertainty* (Oxford Univ Press, Oxford).
92. Apostolakis G (1990) *Science* 250:1359–1364.
93. National Research Council (2002) *Estimating the Public Health Benefits of Proposed Air Pollution Regulations* (Natl Acad Press, Washington, DC).
94. Oppenheimer M, O'Neill BC, Webster M, Agrawala S (2007) *Science* 317:1505–1506.
95. Morgan MG, Keith DW (1995) *Environ Sci Technol* 29:468–476.
96. Morgan MG, Pitelka LF, Shevliakova E (2001) *Clim Change* 49:279–307.
97. Vaughan DG, Spouge JR (2002) *Clim Change* 53:65–91.
98. Morgan MG, Adams PJ, Keith DW (2006) *Clim Change* 75:195–214.
99. Zickfeld K, Levermann A, Morgan MG, Kuhlbrodt T, Rahmstorf S, Keith DW (2007) *Clim Change* 82:235–265.
100. Wiesenfeld K (1985) *Phys Rev A* 32:1744–1751.
101. Kleinen T, Held H, Petschel-Held G (2003) *Ocean Dyn* 53:53–63.
102. Held H, Kleinen T (2004) *Geophys Res Lett* 31:L23207.
103. Rietkerk M, Dekker SC, de Ruiter PC, van de Koppel J (2004) *Science* 305:1926–1929.
104. Schmittner A, Latif M, Schneider B (2005) *Geophys Res Lett* 32:L23710.
105. IPCC (2007) *Climate Change 2007: Mitigation of Climate Change. Contribution of Working Group III to the Fourth Assessment Report of the Intergovernmental Panel on Climate Change*, eds Metz B, Davidson OR, Bosch PR, Dave R, Meyer LA (Cambridge Univ Press, Cambridge, UK).
106. IPCC (2007) *Climate Change 2007: Impacts, Adaptation and Vulnerability. Contribution of Working Group II to the Fourth Assessment Report of the Intergovernmental Panel on Climate Change*, eds Parry ML, Canziani OF, Palutikof JP, van der Linden PJ, Hanson CE (Cambridge Univ Press, Cambridge, UK).
107. Janssen MA, Ostrom E (2006) *Global Environ Change* 16:237–239.
108. Eakin H, Luers AL (2006) *Annu Rev Environ Resour* 31:365–394.
109. Dasgupta P, Mäler K-G (2003) *Environ Resour Econ* 26:499–525.
110. Dasgupta P (2008) *Rev Environ Econ Policy*, in press.
111. Edenhofer O, Lessman K, Kemfert C, Grubb M, Köhler J (2006) *Energy J: Special Issue on Endogenous Technological Change and the Economics of Atmospheric Stabilisation* Special Issue 1:57–108.
112. Scientific Expert Group on Climate Change (2007) *Confronting Climate Change: Avoiding the Unmanageable and Managing the Unavoidable*, Report prepared for the United Nations Commission on Sustainable Development, eds Bierbaum RM, Holdren JP, MacCracken MC, Moss RH, Raven PH (Sigma Xi, Research Triangle Park, NC, and United Nations Foundation, Washington, DC).

**ADMINISTRATIVE CHANGE TO DOE O 451.1B CHG 3,
NATIONAL ENVIRONMENTAL POLICY ACT COMPLIANCE PROGRAM**

LOCATION OF CHANGES:

Page	Paragraph	Changed	To
1	footer	[Update to reflect disestablishment of EH in October 2006] **Delete:** "Office of Environment, Safety and Health"	**Insert:** "Office of the General Counsel"
2	4	[Insertion to reflect policy expressed in 2nd paragraph of Deputy Secretary's memorandum on "Public Involvement in the Environmental Assessment Process" (July 16, 2010)]	**Insert:** "h. Opportunity, whenever possible, for interested parties to review an environmental assessment (concurrent with host state/tribal review under 10 CFR 1021.301) prior to DOE approval."
5	5.d	[Correction of punctuation to accurately reflect regulatory source, 10 CFR 1021.410(e)]	In 5.d(2), line 7, **insert** a comma: "… determination, unless …"
5	5.d	[Insertion of additional paragraph at (3) to reflect provision in 3rd paragraph of DS memorandum; renumbering of subsequent paragraphs, including assigning a number to an unnumbered paragraph following (5) in Change 2 version]	**Insert:** "(3) For an environmental assessment, when an Office makes a draft environmental assessment available for public review, in addition to its usual method of doing so, ensure that the draft is posted on the Department's NEPA website before the start of the public review period."
8	5.g	[Assigning a number to an unnumbered paragraph following (5) in Change 2 version and adjusting the numbers of the 3 subsequent paragraphs]	[Renumbering of (6) through (8)]

Page	Paragraph	Changed	To
9	5.g	[Insertion at (8) in Change 2 version to reflect provision in 3rd paragraph of DS memorandum and renumbering as (9) as noted above] "(8) Maintain DOE's NEPA information resources."	[As renumbered] "(9) Maintain DOE's NEPA information resources, including a public website."

U.S. Department of Energy
Washington, D.C.

ORDER

DOE O 451.1B

Approved: 10-26-00
Review Date: 10-26-02
Chg1: 9-28-01
Chg 2: 6-25-10
Chg 3: 1-19-12

SUBJECT: NATIONAL ENVIRONMENTAL POLICY ACT COMPLIANCE PROGRAM

1. OBJECTIVE. The purpose of this Order is to establish DOE internal requirements and responsibilities for implementing the National Environmental Policy Act of 1969 (NEPA), the Council on Environmental Quality Regulations Implementing the Procedural Provisions of NEPA (40 CFR Parts 1500-1508), and the DOE NEPA Implementing Procedures (10 CFR Part 1021). (Hereinafter, the latter two will be referred to as "the Regulations.") The goal of establishing the requirements and responsibilities presented here is to ensure efficient and effective implementation of DOE's NEPA responsibilities through teamwork. A key responsibility for all participants is to control the cost and time for the NEPA process while maintaining its quality.

2. CANCELLATION. DOE 451.1A, *National Environmental Policy Act Compliance Program*, dated 6-5-97.

3. APPLICABILITY. This Order applies to DOE Elements, including the National Nuclear Security Administration (NNSA). Although contractors may assist in the Department's NEPA implementation, the legal obligation to comply with NEPA belongs to DOE. In accordance with the responsibilities and authorities assigned by Executive Order 12344, codified at 50 USC sections 2406 and 2511, and to ensure consistency throughout the joint Navy/DOE Naval Nuclear Propulsion Program, the Deputy Administrator for Naval Reactors (Director) will implement and oversee requirements and practices pertaining to this Directive for activities under the Director's cognizance, as deemed appropriate. Section 5.a (10), (12), and (14), Section 5.b, and Section 5.f do not apply to NNSA activities, except as provided in Section 6. Section 6 applies only to NNSA activities.

4. REQUIREMENTS.

   In addition to requirements established in NEPA and the Regulations, DOE's NEPA Compliance Program shall include:

   a. A system of DOE NEPA Compliance Officers.

   b. Internal scoping procedures for environmental assessments and environmental impact statements that include development of a schedule. For an environmental impact statement, the schedule, absent extraordinary circumstances, will provide for completion of a final environmental impact statement within 15 months of the issuance of the Notice of Intent.

DISTRIBUTION:
All Departmental Elements

INITIATED BY:
Office of General Counsel

c. NEPA quality assurance plans and public participation plans.

d. Annual NEPA planning summaries. An annual NEPA planning summary will describe briefly: (1) the status of ongoing NEPA compliance activities, (2) any environmental assessments expected to be prepared in the next 12 months, (3) any environmental impact statements expected to be prepared in the next 24 months, and (4) the planned cost and schedule for completion of each NEPA review identified. Every three years starting with 1995, the annual NEPA planning summary for each Field Organization will include an evaluation of whether a site-wide environmental impact statement would facilitate future NEPA compliance efforts.

e. A DOE NEPA Document Manager for each environmental impact statement and environmental assessment.

f. A system for reporting lessons learned and encouraging continuous improvement.

g. Tracking and annually reporting progress in implementing a commitment for environmental impact mitigation that is essential to render the impacts of a proposed action not significant, or that is made in a record of decision.

h. Opportunity, whenever possible, for interested parties to review an environmental assessment (concurrent with host state/tribal review under 10 CFR 1021.301) prior to DOE approval.

5. RESPONSIBILITIES.

a. Each Secretarial Officer and Head of a Field Organization shall, for matters under the office's purview:

(1) Establish a NEPA compliance program and use the NEPA process early in project and program planning to consider environmental factors along with other relevant information.

(2) Maintain a DOE NEPA Compliance Officer for the office and designate a DOE NEPA Document Manager at the start of each environmental assessment and environmental impact statement.

(3) Ensure that internal scoping procedures, a quality assurance plan and a public participation plan are prepared for the office.

(4) Include in new contracts and grants a provision that the awardee may not undertake on DOE's behalf an action that is subject to NEPA until DOE has notified the awardee that DOE has satisfied applicable NEPA requirements.

(5) Incorporate NEPA milestones in project planning documents.

(6) Incorporate NEPA compliance status information in internal budget review documents.

(7) Submit an annual NEPA planning summary to the General Counsel by January 31 of each year and make it available to the public.

(8) Determine that an environmental assessment or an environmental impact statement is appropriate or required.

(9) After an environmental assessment determination, prepare and issue an environmental assessment. Responsibilities for approving and adopting environmental assessments and issuing findings of no significant impact may not be delegated except as provided in this Order. In addition to meeting requirements established in the Regulations, responsibilities include:

(a) When another agency is involved in preparation, determining whether DOE shall be a lead or cooperating agency.

(b) Obtaining concurrence of DOE counsel in the legal adequacy of an environmental assessment before it is approved and in any finding of no significant impact before it is issued.

(c) Determining, based on an environmental assessment, that the impacts of a proposed action are significant and that an environmental impact statement is required, or issuing a finding of no significant impact when appropriate.

(d) Adopting another agency's environmental assessment.

(e) When a commitment to mitigation is essential to render the impacts of a proposed action not significant, preparing a mitigation action plan for any such commitment before issuing the finding of no significant impact.

(f) Tracking and annually reporting progress made in implementing, and the effectiveness of, any commitment for environmental impact mitigation that is essential to render the impacts of a proposed action not significant.

(10) Request from the General Counsel delegation of approval or adoption authority for a specific environmental impact statement when appropriate to expedite the review and approval process.

(11) When required by the Regulations, prepare a supplement analysis and with the concurrence of DOE counsel, determine whether a supplemental or a new environmental impact statement is required for a proposed action, or whether no further documentation is required.

(12) Determine that a proposed action that may be an interim action is clearly allowable under the Regulations. For a proposed action that may be an interim action not clearly allowable under the Regulations, provide the General Counsel with a recommendation for a determination whether the proposed action may proceed.

(13) Incorporate NEPA values, such as analysis of cumulative, off-site, ecological, and socioeconomic impacts, to the extent practicable, in DOE documents prepared under the Comprehensive Environmental Response, Compensation, and Liability Act.

(14) When appropriate, request from the General Counsel a variance from the DOE NEPA Regulations or from this Order.

b. In addition to provisions in paragraph 5.a above, for a proposed action under the office's purview, after an environmental impact statement determination, each Secretarial Officer shall prepare an environmental impact statement and forward it to the General Counsel for approval. Responsibilities for issuing records of decision may not be delegated except as provided in this Order. In addition to meeting requirements established in the Regulations, responsibilities include:

(1) Submitting a notice of intent to prepare an environmental impact statement to the General Counsel for issuance.

(2) [Removed and reserved]

(3) Issuing a record of decision for an environmental impact statement, after obtaining the concurrence of the General Counsel in its environmental content and legal adequacy.

(4) Preparing any mitigation action plan required under the DOE Regulations before taking an action that is the subject of a mitigation commitment made in a record of decision.

(5) Tracking and annually reporting progress made in implementing, and the effectiveness of, any mitigation commitment made in a record of decision.

c. A Head of a Field Organization may delegate environmental assessment responsibilities to a Head of a subsidiary Field Organization (Area or Project Office) after confirming that the subsidiary organization has prepared adequate internal scoping procedures, a quality assurance plan and a public participation plan; has designated a NEPA Compliance Officer; and has adequate DOE legal resources available. (By such delegation, the authority to make categorical exclusion determinations would transfer to the NEPA Compliance Officer of the subsidiary Field Organization.) A Head of a subsidiary Field Organization may not redelegate responsibilities for approving and adopting environmental

assessments and issuing findings of no significant impact except as provided in this Order.

d. A NEPA Compliance Officer shall:

(1) Develop office NEPA procedures and information management requirements, and document the office's compliance with those procedures and requirements.

(2) For actions specifically listed in Appendix A or B to Subpart D of the DOE Regulations, make categorical exclusion determinations and approve and issue any required associated floodplain and wetland documents. These responsibilities may not be delegated except as provided in this Order. Categorical exclusion determinations for actions listed in Appendix B shall be documented and made available to the public by posting online, generally within two weeks of the determination, unless additional time is needed in order to review and protect classified information, "confidential business information" (such as information protected by the Trade Secrets Act or which is otherwise privileged commercial or financial information), or other information that DOE would not disclose pursuant to the Freedom of Information Act (FOIA) (5 U.S.C. Section 552). Posted categorical exclusion determinations shall not disclose classified information, "confidential business information," or other information that DOE would not disclose pursuant to FOIA.

(3) For an environmental assessment, when an Office makes a draft environmental assessment available for public review, in addition to its usual method of doing so, ensure that the draft is posted on the Department's NEPA website before the start of the public review period.

(4) Report to the Office of NEPA Policy and Compliance on lessons learned after completing each environmental impact statement and environmental assessment.

(5) Coordinate NEPA compliance strategies for matters within the office's purview.

(6) Advise on NEPA-related matters, including the provisions of the Regulations, the DOE NEPA Compliance Guide, this Order, and any other related requirements and guidance.

(7) Recommend to the Head of the Office served (i.e., Secretarial Officer, Head of a Field Organization, or Head of a subsidiary Field Organization), whether an environmental assessment or environmental impact statement is appropriate or required.

(8) Assist with the NEPA process and document preparation.

(9) Advise on the adequacy of NEPA documents and other related documents.

(10) Participate in periodic NEPA meetings and workshops conducted by the Office of NEPA Policy and Compliance; provide NEPA training and disseminate NEPA guidance materials and related information.

(11) Notify the Office of NEPA Policy and Compliance promptly—generally, within two weeks of:

(a) The designation of a NEPA Document Manager.

(b) A determination to prepare an environmental assessment.

(c) A transmittal of an environmental assessment to States, Tribes and, when applicable, members of the public, other Federal agencies, and local governments for preapproval review.

(d) A determination to prepare an environmental impact statement.

(12) Provide the Office of NEPA Policy and Compliance promptly—generally, within two weeks of their availability—two copies and one electronic file of:

(a) An approved environmental assessment and any finding of no significant impact.

(b) A proposed finding of no significant impact required under the Council on Environmental Quality Regulations.

(c) [Removed and reserved]

(d) An approved draft or final environmental impact statement.

(e) A record of decision for an environmental impact statement.

(f) A mitigation action plan and corresponding annual mitigation report. The mitigation report may be submitted on the anniversary of a mitigation action plan or in a combined report (for example, as part of the annual NEPA planning summary) for multiple plans until mitigation is completed.

(g) An environmental impact statement supplement analysis and any determination based on it.

e. A NEPA Document Manager shall, for the environmental impact statement or environmental assessment being prepared:

(1) Establish a team, representing all necessary DOE Elements to plan, assist in preparing, and concurrently review documents.

(2) Conduct an early internal scoping process.

(3) Maintain tracking systems to monitor costs of and adherence to the schedule for the NEPA process.

(4) Manage the document preparation process, including reviewing internal drafts for technical adequacy, controlling cost, and maintaining schedule.

(5) Encourage and facilitate public participation through the NEPA process.

(6) [Removed and reserved]

(7) Evaluate, upon completion of the environmental impact statement or environmental assessment, any support contractor's performance for timeliness, quality, cost-effectiveness, responsiveness, and application of requirements and guidance.

(8) Report to the Office of NEPA Policy and Compliance on lessons learned after completing the environmental impact statement or environmental assessment.

f. The General Counsel shall:

(1) Provide DOE policy, guidance, and oversight to ensure adequate and consistent application of NEPA.

(2) For an environmental impact statement:

(a) Issue a notice of intent.

(b) When another agency is involved in preparation, determine whether DOE shall be a lead or cooperating agency.

(c) Evaluate proposed and alternative actions, including alternative mitigation measures, and make any appropriate recommendations to mitigate environmental impacts.

(d) (i) Approve an environmental impact statement, (ii) identify whether it warrants approval by the Secretary of Energy, or (iii) determine that it may be approved by a Secretarial Officer or Head of a Field Organization.

(e) Adopt another agency's environmental impact statement.

(f) Concur in the environmental content and legal adequacy of a record of decision.

(3) For a proposed action that may be an interim action not clearly allowable under the Regulations, determine whether the proposed action may proceed.

(4) When a required NEPA document is not being prepared, direct a Secretarial Officer or Head of a Field Organization to prepare an environmental assessment or environmental impact statement.

(5) Advise the responsible Secretarial Officer and, if appropriate, the Secretary, of a proposed action believed not to conform with DOE policies or applicable environmental laws and regulations.

(6) Resolve disagreements among multiple involved offices concerning the assignment of responsibility for conducting the NEPA process for a proposed action.

(7) Grant appropriate variances from the DOE NEPA Regulations or from this Order.

(8) Coordinate DOE assistance to other Federal agencies throughout their NEPA processes, including DOE's review of documents and submission of comments.

(9) Advise the Secretary of Energy on DOE's NEPA compliance program.

g. The Director, Office of NEPA Policy and Compliance, shall:

(1) Develop policy and guidance documents on NEPA and related environmental review requirements.

(2) Provide NEPA-related technical advice and assistance, on request, to Field and Program organizations.

(3) Perform independent review of proposed actions as appropriate to ensure that NEPA requirements are being met.

(4) Provide workshops and information on NEPA and related requirements and policies.

(5) Provide leadership for continuous improvement of DOE's implementation of NEPA.

(6) Solicit comments from NEPA Compliance Officers, NEPA Document Managers, and other involved persons on lessons learned for each

completed environmental assessment and environmental impact statement and prepare and disseminate a quarterly summary.

(7) File approved draft, final, and supplemental environmental impact statements with the Environmental Protection Agency, pursuant to the Regulations.

(8) Coordinate consultation with the Council on Environmental Quality and the Environmental Protection Agency on matters relating to NEPA.

(9) Maintain DOE's NEPA information resources, including a public website.

6. NNSA PROCEDURES.

a. NNSA shall follow all the applicable procedures set forth in this Order. The Administrator shall ensure that all functions assigned to Secretarial Officers and their subordinates in Section 5 are performed.

b. The Administrator shall approve or adopt environmental impact statements and EIS-related documents for specific NNSA proposals that the Administrator determines, after consultation with the General Counsel, do not warrant Secretarial attention. This authority may not be delegated. In performing these duties, NNSA will consult with the General Counsel to ensure that all NEPA requirements are satisfied. If an unresolvable difference of opinion develops between the offices regarding an EIS or EIS-related matter, the Administrator shall bring the issue to the Secretary [Deputy Secretary] for resolution or direction.

c. For EISs and EIS-related documents for proposals not covered by Section 6.b and for matters described in Section 5.a(14), the Administrator shall submit requests for action or approval to the Secretary (Deputy Secretary). The General Counsel shall provide recommendations to the Secretary (Deputy Secretary) on such requests.

7. CONTACT. Questions regarding this Order and requests for guidance should be addressed to Office of the General Counsel, Office of NEPA Policy and Compliance, at 202-586-4600.

BY ORDER OF THE SECRETARY OF ENERGY:

FRANCIS S. BLAKE
Deputy Secretary

U.S. Department of Energy
Washington, D.C.

PAGE CHANGE

DOE O 451.1B Chg 1

Approved: 10-26-00
Chg 1: 9-28-01

SUBJECT: NATIONAL ENVIRONMENTAL POLICY ACT COMPLIANCE PROGRAM

1. PURPOSE. To transmit revised pages to DOE O 451.1B, *National Environmental Policy Act Compliance Program,* dated 10-26-00.

2. EXPLANATION OF CHANGES. To allow the Under Secretary/Administrator of the National Nuclear Security Administration (NNSA) to approve certain NNSA environmental impact statements.

3. FILING INSTRUCTIONS.

Remove	Dated	Insert	Dated
Page 1	10-26-00	Page 1	9-28-01
Pages 9 and 10	10-26-00	Pages 9 and 10	9-28-01

After filing the attached pages, this transmittal may be discarded.

BY ORDER OF THE SECRETARY OF ENERGY:

FRANCIS S. BLAKE
Deputy Secretary

DISTRIBUTION:
All Departmental Elements

INITIATED BY:
Office of Management, Budget and Evaluation/CFO

U.S. Department of Energy
Washington, D.C.

PAGE CHANGE

DOE O 451.1B Chg 2

Approved: 10-26-00
Chg 2: 6-25-10

SUBJECT: NATIONAL ENVIRONMENTAL POLICY ACT COMPLIANCE PROGRAM

1. PURPOSE. To transmit revised pages to DOE O 451.1B, *National Environmental Policy Act Compliance Program,* dated 10-26-00.

2. EXPLANATION OF CHANGES. The page change reflects changes to Deputy Secretary Policy and DOE organization.

3. LOCATION OF CHANGE.

Pages	Paragraphs
1	3.
3	5.a.(7) and 5.a.(10)
4	5.a.(12) and (14); 5.b.; and 5.b.(1) and (3)
5	5.d.(2)
7	5.f. and 5.f.(2)(d) and (f)
9	6; 6.b.; 6.c.; and 7.

BY ORDER OF THE SECRETARY OF ENERGY:

DANIEL B. PONEMAN
Deputy Secretary